AN EXPERIMENTAL STUDY ON PERFORMANCE OF DIESEL ENGINE OPERATING WITH WASTE TIRE AND WASTE PLASTIC DERIVED FUEL

MOHD. HERZWAN BIN HAMZAH

MASTER OF AUTOMOTIVE ENGINEERING

UNIVERSITI MALAYSIA PAHANG

MOHD. HERZWAN HAMZAH   M. ENG. (AUTOMOTIVE)   2015   UMP

50 mm

50 mm

Top of the cover page

UMP

AN EXPERIMENTAL STUDY ON PERFORMANCE OF DIESEL ENGINE
OPERATING WITH WASTE TIRE AND WASTE PLASTIC DERIVED FUEL

MOHD. HERZWAN BIN HAMZAH

Thesis submitted in fulfilment of the requirements
for the award of the degree of
Master of Engineering in Automotive Engineering

Faculty of Mechanical Engineering
UNIVERSITI MALAYSIA PAHANG

APRIL 2015

UNIVERSITI MALAYSIA PAHANG

DECLARATION OF THESIS AND COPYRIGHT

Author's full name	:	**MOHD. HERZWAN BIN HAMZAH**
Date of birth	:	**21st JANUARY 1988**
Title	:	**AN EXPERIMENTAL STUDY ON PERFORMANCE OF DIESEL ENGINE OPERATING WITH WASTE TIRE AND WASTE PLASTIC DERIVED FUEL**
Academic Session	:	**2014/2015**

I declare that this thesis is classified as:

☐	**CONFIDENTIAL**	(Contains confidential information under the Official Secret Act 1972)
☐	**RESTRICTED**	(Contains restricted information as specified by the organization where research was done)
√	**OPEN ACCESS**	I agree that my thesis to be published as online open access.

I acknowledge that Universiti Malaysia Pahang reserve the right as follows:

1. The Thesis is the Property of University Malaysia Pahang
2. The Library of Universiti Malaysia Pahang has the right to make copies for the purpose of research only.
3. The Library has the right to make copies of the thesis for academic exchange.

Certified by:

_____ _____

(MOHD. HERZWAN BIN HAMZAH)   **(DR. ABDUL ADAM BIN ABDULLAH)**
      880121-13-5453   **711203-06-5359**

   Date: **6th APRIL 2015**   Date: **6th APRIL 2015**

Note: Thesis by means the thesis for Doctor of Philosophy and Master of Engineering (by research) or by any study involved coursework and research or Bachelor Final Year Project.

SUPERVISOR'S DECLARATION

I hereby declare that I have checked this thesis and in my opinion, this thesis is adequate in terms of scope and quality for the award of the degree of Master of Engineering in Automotive Engineering.

Signature   :

Name of Supervisor   : DR. ABDUL ADAM BIN ABDULLAH

Position   : SENIOR LECTURER

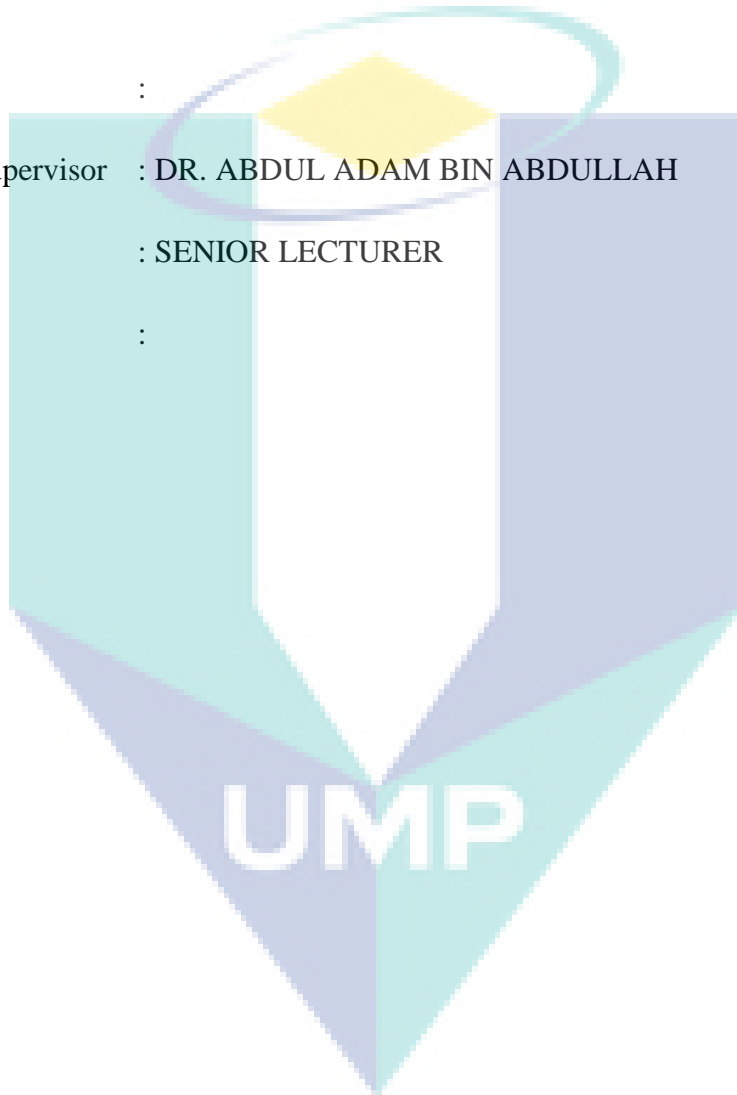Date   :
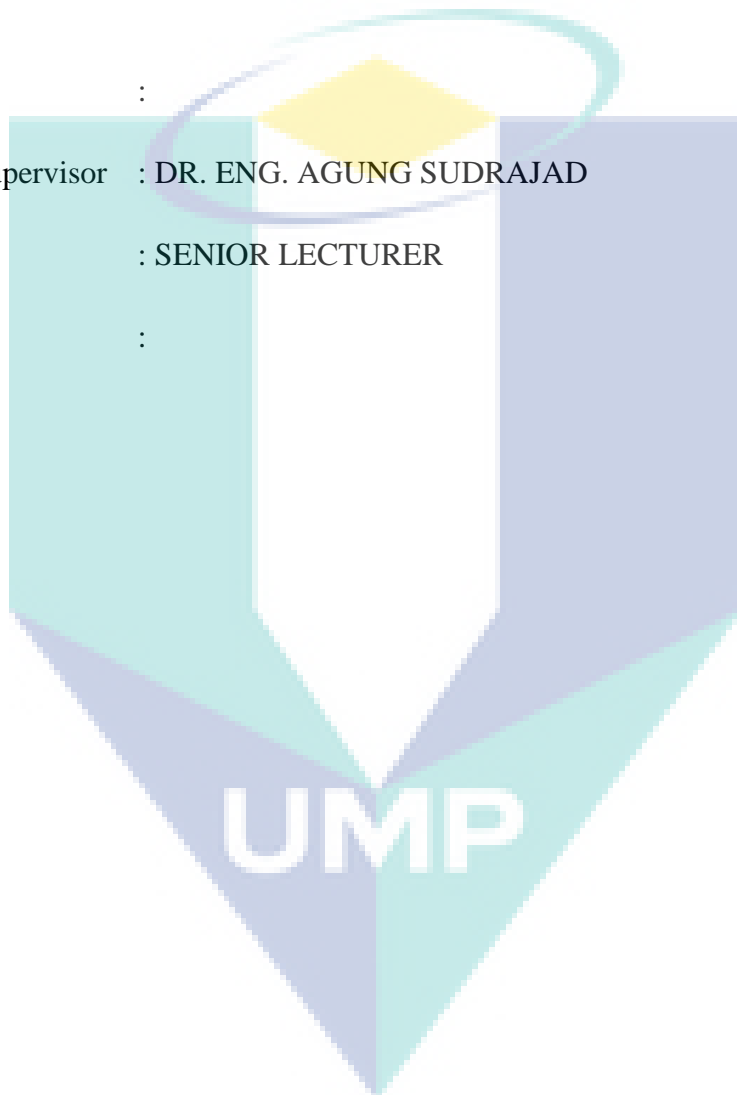
CO-SUPERVISOR'S DECLARATION

I hereby declare that I have checked this thesis and in my opinion, this thesis is adequate in terms of scope and quality for the award of the degree of Master of Engineering in Automotive Engineering.

Signature   :

Name of Supervisor   : DR. ENG. AGUNG SUDRAJAD

Position   : SENIOR LECTURER

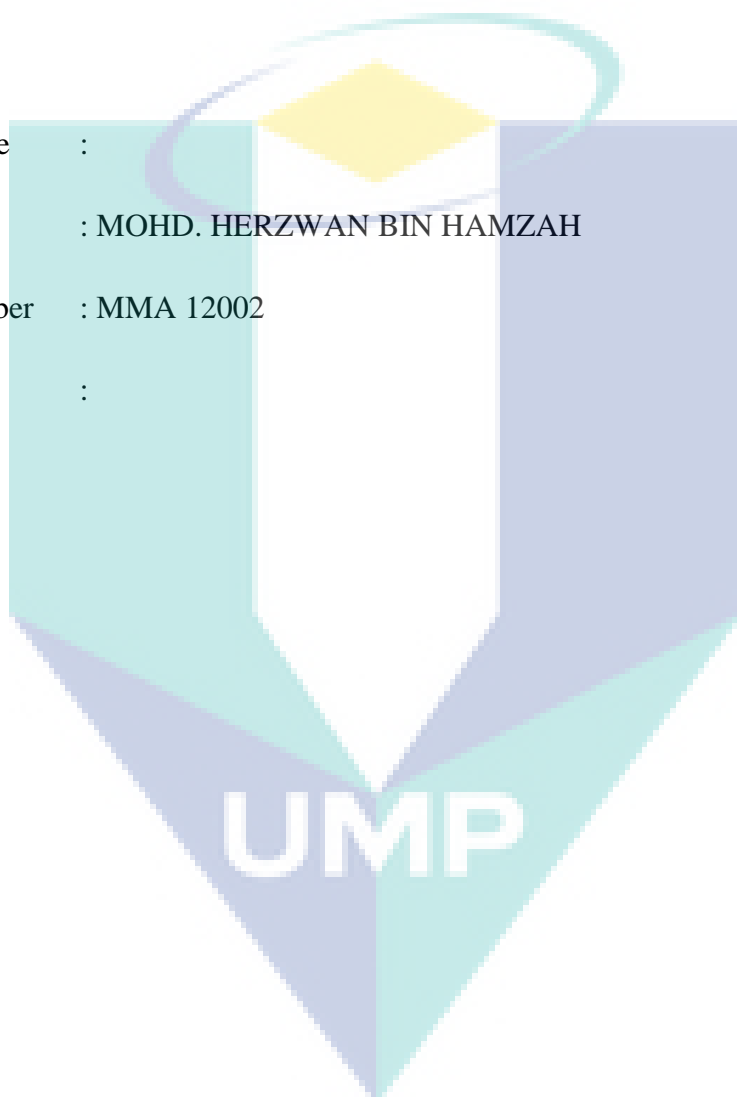Date   :

STUDENT'S DECLARATION

I hereby declare that the work in this thesis is my own except for quotations and summaries which have been duly acknowledged. This thesis has not been accepted for any degree and is not concurrently submitted for award of other degree.

Signature   :

Name   : MOHD. HERZWAN BIN HAMZAH

ID Number   : MMA 12002

Date   :

"**In the name of ALLAH, the Most Beneficent, the Most Merciful**"

This thesis is specially dedicated to:

Beloved father and mother;

HAMZAH BIN MAJID

WAHIDAH BINTI HUSSIN

for your love, trust and support along my journey as a student and as a son. You are my source of inspiration and spirit for me along my study and life.

ACKNOWLEDGEMENT

ABSTRACT

This thesis presents the experimental study on the performance of single cylinder diesel engine operating with tire derived fuel (TDF), TDF-diesel fuel blends and also plastic derived fuel (PDF). The objectives of this project is to determine the fuel properties of TDF, TDF-diesel fuel blends and PDF, evaluating the performance of TDF and PDF when used in diesel engine and also to investigate the effect when several blend ratios between TDF and diesel fuel are used. The performance testing is conducted using a single cylinder engine test rig operating with variable engine speed and constant load exerted to the engine. The diesel engine is equipped with hydraulic dynamometer and necessary sensors to collect and measure the desired data. The parameters that were measured during testing include engine torque, power, combustion pressure and exhaust emissions. The obtained data for all tested fuels are compared to diesel fuel performance data. Then, the properties of all tested fuels are also determined. Six samples of tested fuels are prepared where TDF is blended with diesel fuel at three different ratios which is 10%, 30% and 50% together with 100% unblended TDF, PDF and diesel fuel. The PDF that used is 100% not blended with any other fuel. The comparison between TDF, TDF-diesel fuel blends and diesel fuel shows that TDF-diesel fuel blends produce higher power and torque compared to TDF and diesel fuel. Among tested blend ratio, TDF10% yield highest power and torque compared to other tested fuel. When the TDF blend ratio increases, the power and torque decreases. For cylinder pressure, TDF50% produce highest peak pressure compared to other tested fuels. When the TDF blend ratio decrease, the peak pressure will decrease. For emission, diesel fuel produce lowest CO_x and NO_x emission level compared to other tested fuels while TDF10% produce closest emission level to diesel fuel. PDF produce lowest power, torque and peak pressure compared to TDF and diesel fuel. PDF also produce lowest NO_x and CO emission level compared to TDF and diesel fuel. From the results that were obtained in the experiment, it is concluded that TDF and PDF can be used in diesel engine. However, TDF is not suitable for high speed application since it will cause backfires. Blending process between TDF and diesel fuel enhance the properties of TDF thus producing better performance. From the results obtained, TDF10% produced most optimum performance output compared to the other test fuels.

ABSTRAK

Tesis ini membentangkan hasil kajian berkenaan prestasi enjin diesel silinder tunggal yang beroperasi dengan bahan bakar berasaskan tayar (TDF), campuran antara TDF dan diesel dan bahan bakar berasaskan plastik (PDF). Objektif projek ini adalah untuk menentukan ciri-ciri kimia TDF, campuran antara TDF dan bahan api diesel dan juga PDF, menilai prestasi TDF dan PDF apabila digunakan dalam enjin diesel dan juga untuk mengkaji kesan apabila beberapa nisbah campuran antara TDF dan minyak diesel digunakan terhadap enjin diesel. Ujian prestasi dijalankan menggunakan enjin diesel silinder tunggal yang beroperasi dengan kelajuan enjin yang dimanipulasikan dan beban malar yang dikenakan kepada enjin. Enjin diesel dilengkapi dengan dinamometer hidraulik dan sensor yang diperlukan bagi mengumpul dan mengukur data yang diinginkan. Parameter yang diukur semasa ujian termasuk daya kilas enjin, kuasa enjin, tekanan pembakaran dan kandungan gas ekzos. Data yang diperolehi bagi semua bahan bakar ujian dibandingkan dengan data prestasi bahan api diesel. Kemudian, ciri-ciri kimia semua bahan bakar ujian juga ditentukan. Enam sampel bahan api ujian telah disediakan yang mana TDF dicampur dengan bahan api diesel pada tiga nisbah campuran yang berbeza iaitu 10%, 30% dan 50% bersama-sama dengan 100% TDF yang tidak dicampur, PDF dan bahan api diesel. PDF yang digunakan adalah 100% tidak dicampur dengan apa-apa bahan api lain. Perbandingan antara bahan bakar TDF, campuran bahan bakar TDF-diesel dan bahan api diesel menunjukkan bahawa campuran bahan bakar TDF-diesel menghasilkan kuasa dan daya kilas yang lebih tinggi berbanding TDF dan bahan api diesel. TDF10% menghasilkan kuasa dan daya kilas tertinggi berbanding bahan api ujian yang lain. Apabila nisbah campuran TDF dalam minyak diesel meningkat, kuasa dan daya kilas semakin menurun. Untuk tekanan silinder, TDF50% menghasilkan tekanan puncak paling tinggi berbanding dengan bahan api ujian yang lain. Apabila nisbah campuran TDF menurun, tekanan puncak juga akan menurun. Bagi kadar pelepasan asap ekzos, bahan api diesel menghasilkan COx dan NOx paling rendah berbanding bahan api ujian yang lain. TDF10% menghasilkan tahap pelepasan asap ekzos yang terhampir dengan bahan api diesel. PDF pula menghasilkan kuasa, daya kilas dan tekanan puncak yang paling rendah berbanding TDF dan bahan api diesel. PDF juga menghasilkan kadar NOx dan CO yang paling rendah berbanding TDF dan bahan api diesel. Daripada keputusan yang diperolehi dalam eksperimen, dapat disimpulkan bahawa TDF dan PDF boleh digunakan dalam enjin diesel. Walau bagaimanapun, TDF tidak sesuai untuk kelajuan enjin yang tinggi kerana ia akan menyebabkan 'backfires'. Proses campuran antara TDF dan bahan bakar diesel menambah baik ciri-ciri kimia TDF bagi menghasilkan prestasi enjin yang lebih baik. Nisbah campuran yang memberikan prestasi optimum dalam kajian ini adalah TDF10%.

TABLE OF CONTENTS

LIST OF TABLES

LIST OF FIGURES

LIST OF ABBREVIATONS

AAM	Malaysia Automotive Association
ASTM	American Standard of Testing Methods
BTE	Brake thermal efficiency
CI	Compression ignition
CN	Cetane number
CNC	Computer numerical control
CO	Carbon monoxide
CO_2	Carbon dioxide
DAQ	Data acquisition system
EGR	Exhaust gas recirculation
HC	Hydrocarbon
IMEP	Indicated mean effective pressure
NO_x	Nitrogen oxides
PDF	Plastic derived fuel
PM	Particulate matter
SAE	Society of Automotive Engineers
SI	Spark ignition
SO_2	Sulphur dioxide
TDC	Top dead centre
TDF	Tire derived fuel

LIST OF SYMBOLS

C_d	0.6
d_{pump}	Pump displacement
d	orifice diameter
D	Air density in lb/ft^3
h	100 mm H$_2$O
k	2 (four stroke engine)
n	Maximum engine speed
N_c	Number of cylinder
n_{min}	Minimum engine speed that tested
p	Pressure difference
P_a	1 bar
P_B	Barometric pressure in inches of mercury
$P_{Hydraulic}$	Hydraulic horsepower
P_v	Velocity pressure in inches of water
Q	Flow rate
T_{pump}	Torque absorbed by the pump from the engine flywheel
T_a	293 K (20°C)
V	Air flow rate
V_b	Minimum size of inbox
V_s	Swept volume
η_v	0.8
ω	Engine speed

CHAPTER 1

INTRODUCTION

1.1   BACKGROUND OF STUDY

In the modern world, the emphasis of motor vehicle number becomes significant especially in China, Europe, United States and also including Malaysia. According to a review by Malaysia Automotive Association (MAA) (2012), total of registered vehicle in Malaysia in the first six month in 2012 is 301,224 vehicles, higher than the first six month in 2011, which is 297,203 vehicle. Large amount of scrap tires are produce together with large number of vehicle. According to Chong (2006), Malaysia generates 150,000 tonnes of scrap tires every year. While Budhiarta (2012) stated that waste plastic contribute to 21% from total municipal solid waste (MSW) in Kuala Lumpur in 2010. With the population growth at 6.1%, the production of plastic waste will significantly rise.

Based on this issue, many actions have been taken to overcome the waste problems. One of the steps is to recycle the waste for several purposes. For example, waste tires can be used as racing track and road barriers while waste plastic bottles can be recycled into new plastic product. The other way to utilize the waste tire and waste plastic is through a conversion from solid waste to liquid fuel. The process for the conversion is known as pyrolysis process. In this process, waste tires and plastics will undergo thermal degradation process with the absence of oxygen that can convert the solid waste into useable liquid fuel.

Utilization of the liquid fuel known as tire derived fuel (TDF) and plastic derived fuel (PDF) can overcome the solid tire and plastic waste problem. These liquid fuels are used as fuel in industrial applications such as boilers and cement kilns. In

addition, several researches claimed that TDF and PDF can be used as fuel in internal combustion engine (Murugan et al., 2008, Harshal and Shailendra, 2013). This advantage of liquid fuel from waste tire and waste plastic can solve major global concern problem of reducing the dependence to fossil fuel as energy source.

1.2   PROBLEM STATEMENT

Nowadays, the emphasis on human population around the globe causes an increase of the production of solid waste. This solid waste is commonly disposed through open landfills (Fauziah and Agamuthu, 2012). Open landfills dispose practise will cause problems such as environmental pollution and health issues. Furthermore, a non-biodegradable waste such as plastic and tire will cause space problems since the waste will remain intact at the disposing site for a long period of time. Recycling the waste tires and plastics into useable product such as alternative fuel known as tire derived fuel (TDF) and plastic derived fuel (PDF) can overcome the waste problem. Both fuels are obtained from pyrolysis process. TDF is claimed to have similar calorific value as coal (Abdul-Raouf et al., 2010) while PDF has similar properties as diesel fuel (Mani et al., 2011). Utilization of this alternative fuel can reduce the dependence to fossil fuel.

Aydın and İlkılıç (2012) stated that TDF needed to be blended with diesel fuel to enable it to be used in diesel engine. Diesel engine is unable to operate satisfactorily when 100% pure TDF is used as fuel. Similarly, Bhatt and Patel (2012) suggested further improvement in TDF quality in term of reduction in fuel viscosity and also increase in cetane number. One of the ways to improve the TDF fuel properties is by blending it together with diesel fuel. Therefore, based on the suggestion made by previous research, further investigation is needed to determine the fuel properties of TDF that blended with diesel fuel at several blend ratios. Furthermore, TDF-diesel fuel blend combustion performance on diesel engine need to be further investigated to determine the relationship between the blend ratio and engine performance. As a result, the optimum TDF-diesel blend ratio that possibly can be used in diesel engine can be concluded.

As for the other test fuel, Mani et al. (2011) stated that PDF need further testing in high speed engine since less testing that have been done on this aspect. Diesel engines especially that are used for land transportation operates at high engine speed. Therefore, further investigation on PDF in high speed engine can give further understanding on the performance of PDF that used for high speed applications such as for land transportation.

1.3 OBJECTIVES OF STUDY

The objectives of this study as follows:

1) To determine the fuel properties of TDF, TDF-diesel fuel blends and PDF.
2) To evaluate the engine performance of TDF and PDF when used in diesel engine.
3) To investigate the effect when several blend ratios of TDF and diesel fuel are used to engine performance.

1.4 SCOPES OF STUDY

The scopes of this project are as follows:

1) Single cylinder diesel engine modification for alternative fuel testing.
2) Hydraulic gear pump size calculation and installation to the test rig as dynamometer system.
3) Data acquisition system (DAQ) installation to the engine for performance data collection.
4) Determination of the fuel properties of TDF, PDF and TDF-diesel fuel blends through chemical lab testing
5) Conduct experimental testing to determine the performance and emission of diesel engine operating with TDF, PDF and TDF-diesel fuel blends.

1.5   FLOW CHART
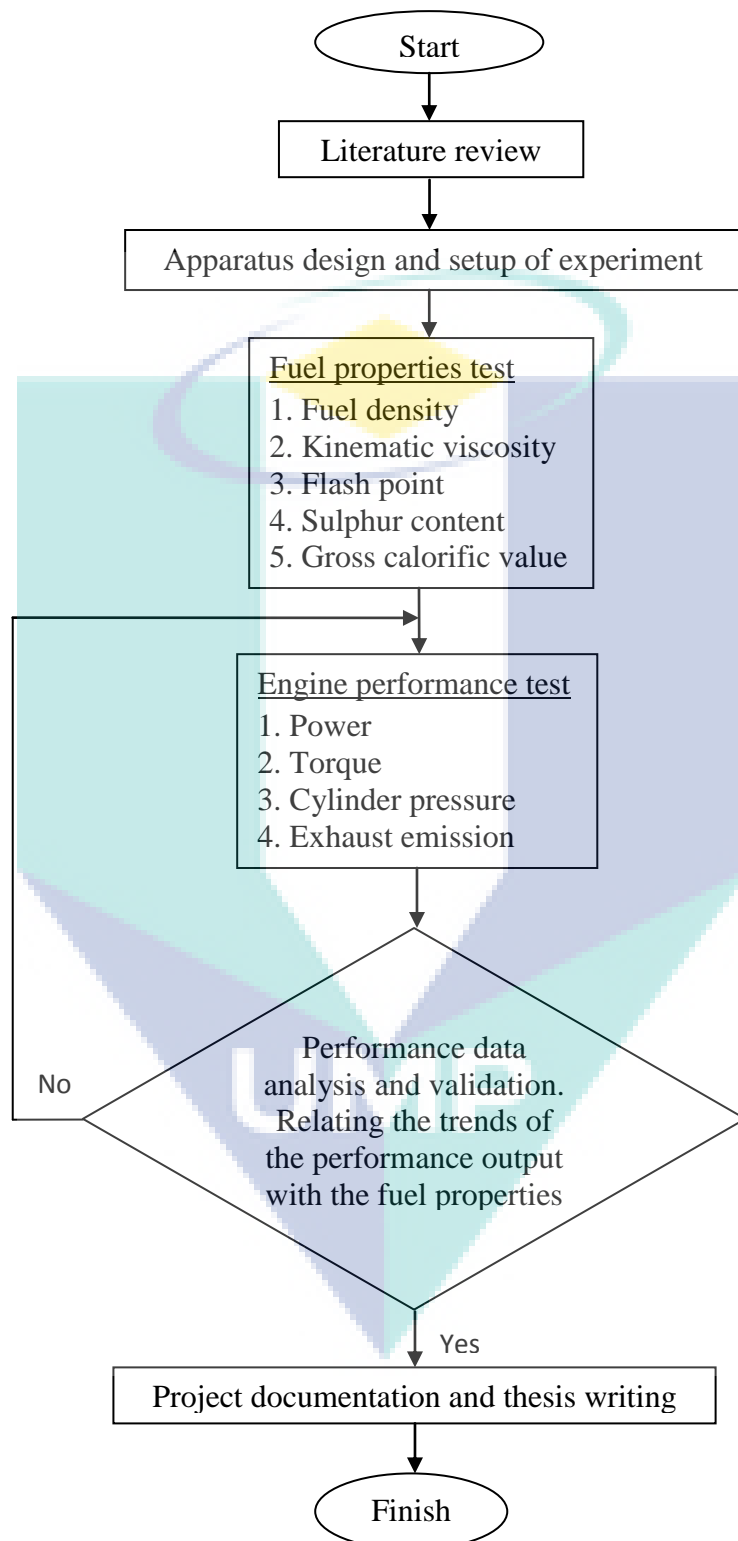
1.6   HYPOTHESIS

The performance of diesel engine operating with TDF blends such as 10%, 30% and 50% blend will decrease when the ratio of TDF in diesel fuel is increased due to the decreasing gross calorific value of the blends. Moreover, the emission gas such as NO, NO_x, CO and CO_2 will increase when the TDF ratio in diesel fuel is increased. The performance of TDF and PDF when used in diesel engine is lower compared to diesel fuel. While for PDF, it will produce lower performance compared to diesel fuel and TDF because it has lower gross calorific value.
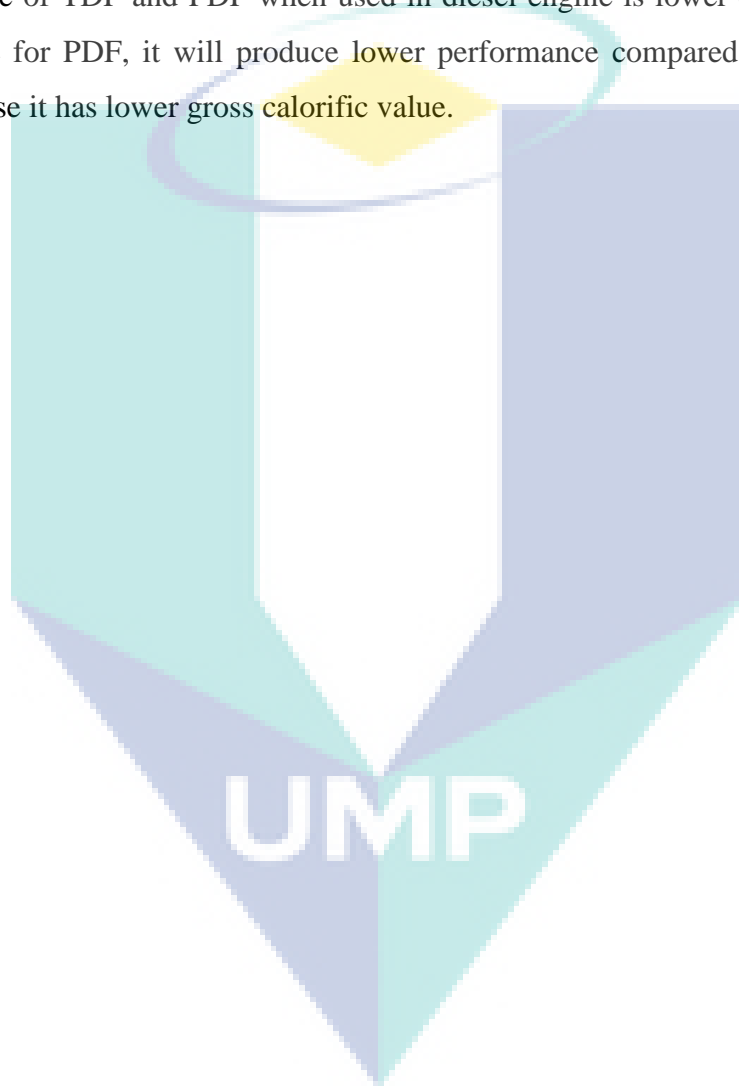
CHAPTER 2

LITERATURE REVIEW

2.1   DIESEL ENGINE

2.1.1   History of Diesel Engine

Diesel engine was invented by Rudolf Diesel in 1897. He was born in Paris, France in 1858. He received his education at Munich Polytechnic and works as refrigerator engineer. He starts working on compression ignition engine in 1893. Rudolf Diesel runs his first model, on 10th August 1893 at Augsburg where the first test was unsuccessful.
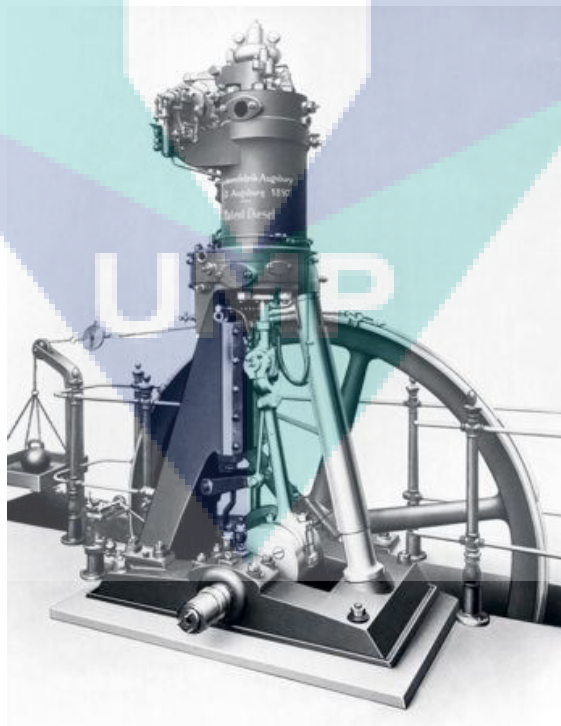
Figure 2.1: Rudolf Diesel's successful engine prototype

Source: Jääskeläinen (2013)

Rudolf Diesel continued working on improvement on his invention for two years and in 1897, he managed to develop successful model that has 26.2% efficiency compared to steam engine which has only 10% efficiency. The successful model consists of single 3.0m (10-foot) iron cylinder with a flywheel at the base as shown in Figure 2.1. The model engine power is about 20 hp (Jääskeläinen, 2013).

2.1.2   Working Principle of Diesel Engine

Diesel engine is a compression ignition engine. This means the fuel is ignited by the high heat produced due to air compression during compression stroke inside the engine. During intake stroke, only air is inducted into a combustion chamber and at near end of the top dead centre (TDC), fuel is injected into the combustion chamber (Ganesan, 2012). The fuel will undergo a vaporization and atomization process, followed by the fuel ignition process. Then the combustion process begins. Compression ratio of diesel engine is ranged from 12 to 24 depends on the engine configuration and application. Engine speed is controlled by varying amount of fuel injected into the combustion chamber. The quantity of air consumed at each speed is essentially constant since diesel engine did not have any throttle valve. Diesel engine operates based on diesel cycle or dual cycle for modern high speed diesel engine.

The earlier diesel engine operates based on diesel cycle. For diesel cycle, injection timing occurs at very end of compression stroke. Due to short time needed to inject the fuel and also ignition delay, the combustion still continue until the expansion stroke. The method maintains the cylinder pressure at maximum level even after TDC. This combustion process is best described as a constant-pressure heat input in an air-standard cycle, also known as Diesel cycle or constant-pressure cycle. Figure 2.2 shows the air standard Diesel cycle.
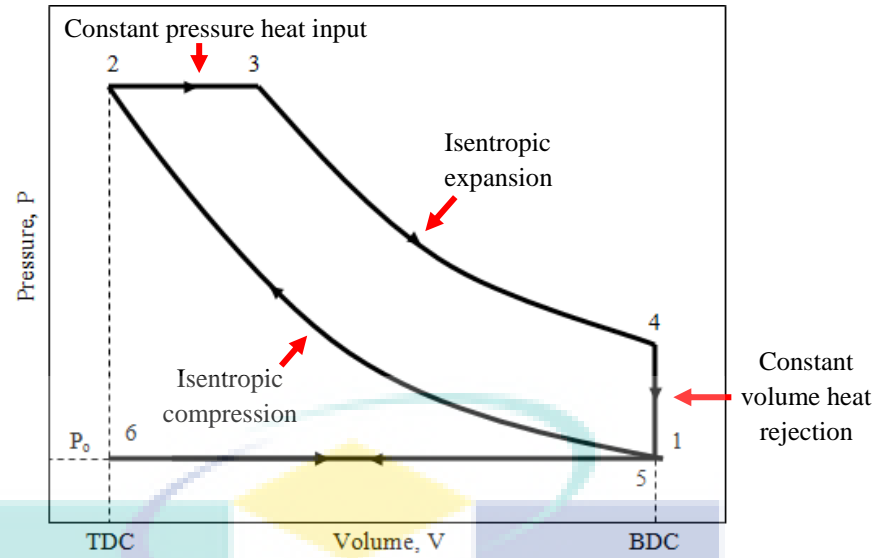
Figure 2.2: Air-standard Diesel cycle

Source: Pulkrabek (2004)

Process 1-2 -- isentropic expansion stroke

    All valves close

$$T_2 = T_1 (V_1/V_2)^{k-1} = T_1 (r_c)^{k-1} \tag{2.1}$$

$$P_2 = P_1 (V_1/V_2)^{k-1} = P_1 (r_c)^{k-1} \tag{2.2}$$

$$V_2 = V_{TDC} \tag{2.3}$$

Process 2-3 -- constant-pressure heat input (combustion)

    All valves close

$$Q_{2\text{-}3} = Q_{in} = m_m c_p (T_3 - T_2) = (m_a + m_f) c_p (T_3 - T_2) \tag{2.4}$$

$$q_{2\text{-}3} = q_{in} = c_p (T_3 - T_2) \tag{2.5}$$

$$T_3 = T_{max} \tag{2.6}$$

Process 3-4 -- isentropic power or expansion stroke

    All valves close

$$q_{3\text{-}4} = 0 \tag{2.7}$$

$$T_4 = T_3 (V_3/V_4)^{k-1} \tag{2.8}$$

$$P_4 = P_3 (V_3/V_4)^{k} \tag{2.9}$$

Process 4-5 -- constant-volume heat rejection (exhaust blowdown)

Exhaust valve open and intake valve close

$q_{4-5} = q_{out} = c_v(T_5 - T_4)$ (2.10)

Thermal efficiency of Diesel cycle

$(\eta_t) = 1 - [c_v (T_4 - T_1) / c_p (T_3 - T_2)]$ (2.11)

In contradiction, the modern diesel engines have simple operating change compare to the early diesel engine. For the modern diesel engine, the injection timing is advanced around 20° before TDC (Pulkrabek, 2004). The first fuel is ignited at the end of compression stroke, and the combustion occurs almost at constant volume at TDC. The fuel injection process is continuing at TDC and the chamber pressure is maintained high until the expansion stroke due to sufficient time available for all fuel to be injected. The air-standard cycle that use to analyse the modern diesel engine is known as Dual cycle (also known as limited pressure cycle) because of heat input process of combustion consists of constant volume and then followed by constant pressure. Figure 2.3 shows the air standard Dual cycle.
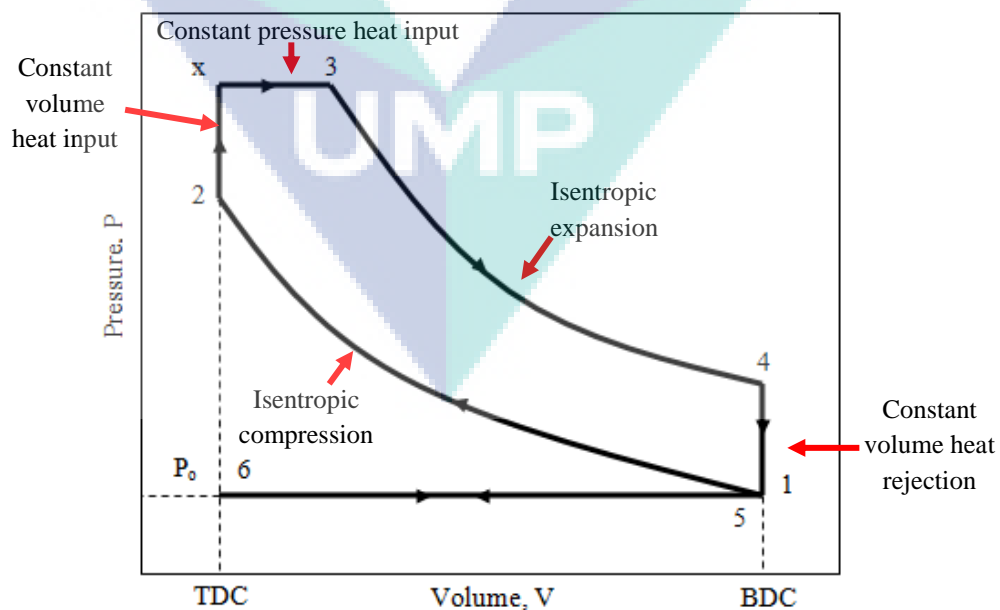
Figure 2.3: Air-standard Dual cycle

Source: Pulkrabek (2004)

Analysis of Dual cycle is same as the Diesel cycle except for heat input process (process 2-x-3).

Process 2-x -- constant-volume heat input (first part of combustion)

All valves close

$$V_x = V_2 = V_{TDC} \tag{2.12}$$

$$w_{2-x} = 0 \tag{2.13}$$

$$Q_{2-x} = (m_a + m_f)\, c_v\, (T_x - T_2) \tag{2.14}$$

$$q_{2-3} = c_v\, (T_x - T_2) \tag{2.15}$$

$$P_x = P_{max} = P_2(T_x/T_2) \tag{2.16}$$

Pressure ratio is defined as the pressure rise during combustion, given as:

$$\alpha = P_x/P_2 = P_3/P_2 = T_x/T_2 = (1/r_c)^k\, (P_3/P_1) \tag{2.17}$$

Process x-3 -- Constant pressure heat input (second part of combustion)

All valves closed

$$P_3 = P_x = P_{max} \tag{2.18}$$

$$Q_{x-3} = m_m c_p\, (T_3 - T_x) = (m_a + m_f)\, c_p\, (T_3 - T_x) \tag{2.19}$$

$$q_{x-3} = c_p\, (T_3 - T_x) \tag{2.20}$$

$$w_{3-4} = P_x\, (v_3 - v_x) = P_3(v_3 - v_x) \tag{2.21}$$

$$T_3 = T_{max} \tag{2.22}$$

Thermal efficiency of Dual cycle is given by:

$$(\eta_t)_{DUAL} = 1 - c_v(T_4 - T_1)/ [\, c_v(T_x - T_2) + c_p(T_3 - T_x)] \tag{2.23}$$

2.1.3 Classification of Diesel Engine

Diesel engine can be divided into several classifications such as basic design, engine cycles, valve locations, positions and number of cylinders, air intake process, fuelling systems, type of cooling and applications. Diesel engine can operates either with four stroke cycle or two stroke cycle. Small and medium size diesel engine commonly operates on four stroke cycle. This is because small and medium diesel engine commonly used for land transportation where the engine size and emission level is concerned. Small and medium engine also operates on higher engine speed compared to large size engine. Large diesel engine especially the one used to power big ships and submarines operates on two stroke cycle since they have higher power-to-weight ratio compared to four stroke diesel engines. In modern world, the diesel engine is commonly fitted with force induction systems to increase the volumetric efficiency thus increase the power output of the diesel engine.
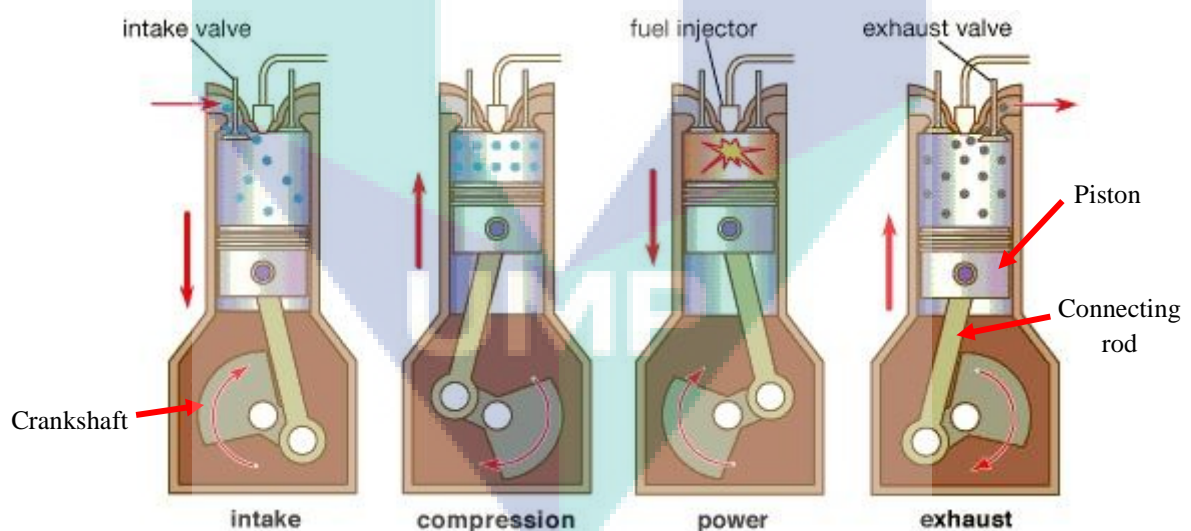
Figure 2.4: Four stroke compression ignition cycle

Source: Pundir (2010)

Figure 2.4 illustrates the compression ignition, four stroke cycle. For the four stroke cycle, the piston completes four separate stroke which is intake stroke, compression stroke, power stroke and exhaust stroke. It takes two crankshaft

revolutions to complete the cycle. One power stroke is produced every two complete crankshaft revolution.

For two stroke cycle, the piston completes two strokes per cycle which is up stroke and down stroke. It takes only one crankshaft revolution to complete the cycle. One power stroke is produced every one crankshaft revolution. Intake process and exhaust happen at same time which also known as scavenging process. The end of combustion stroke and the beginning of compression stroke occurs simultaneously.

Two stroke engines have high power-to-weight ratio because it has less components and lighter compared to four stroke engine. Furthermore, two stroke engines produce one power stroke every one complete crankshaft revolution compared to four stroke cycle that produce one power stroke every two crankshaft revolution. Figure 2.5 shows the two stroke diesel engine.
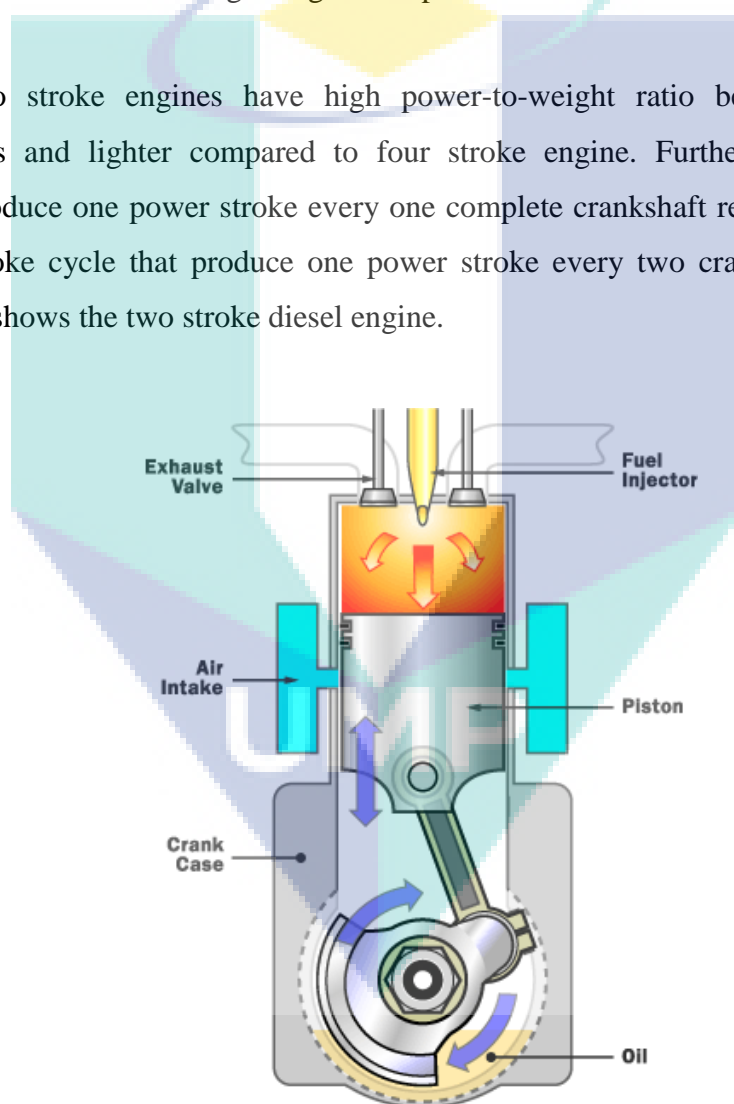
Figure 2.5: Two stroke diesel engine

Source: Brain (2000)

Diesel engines are commonly manufactured as reciprocating engines with different positions and number of cylinders. The numbers of pistons are in range of 1 to 14 cylinders, fitted either in V-engine, in-line engine, opposed cylinder or opposed piston engine configurations.

V-engine consists of two banks of engine cylinders which have certain angle to each other attached to a single crankshaft. This engine design allows shorter engine block while maintaining same number of cylinders thus enables the engine to be fitted into smaller engine compartment. The angle between the two cylinder banks are between 15° to 120°, where common value is between 60° to 90°. Common number of cylinders for V-engines used in automobiles is V6 and V8 engines.

In-line engine consist of engine cylinders that is positioned in a straight line. In-line four cylinders are most widely used in-line engine worldwide. In-line configurations are most preferred since it has less components and easy to work on. It is because in-line configurations consists less cylinder heads and camshaft compared to other configurations such as 'V', 'W' or boxer.

Opposed cylinder engine consist of two banks of cylinders opposite to each other at 180° and attached to a single crankshaft. Opposed cylinder engine commonly founded in small aircraft and automobile with even number of cylinders. This type of cylinder arrangement often referred as flat or boxer engine.

On the other hand, **opposed piston engine** consist of two pistons in each cylinder with the combustion chamber at the centre between the pistons. A single combustion produces two power strokes at a time, which transferred to two separate crankshafts at each end of the cylinder. This design commonly used for large displacement engine, used for power plants, submarines or ships.

Diesel engine has two types of injection method which is direct injection or indirect injection. Direct injection method is where the fuel is injected directly into the combustion chamber. Three common type of direct injection design are quiescent chamber with multi-hole nozzle, bowl-in-piston chamber with swirl and multi-hole

nozzle and lastly bowl-in-piston chamber with swirl and single-hole nozzle. The advantages of direct injection are this system requires no glow plug for cold starting especially in the morning, finer fuel droplets formed during atomization because direct injection is commonly uses high injection pressure injector and minimum heat loss during compression. Meanwhile, the disadvantage of direct injection is high pressure fuel injection system need to be used for direct injection hence complicated design of fuel injection pump is needed.
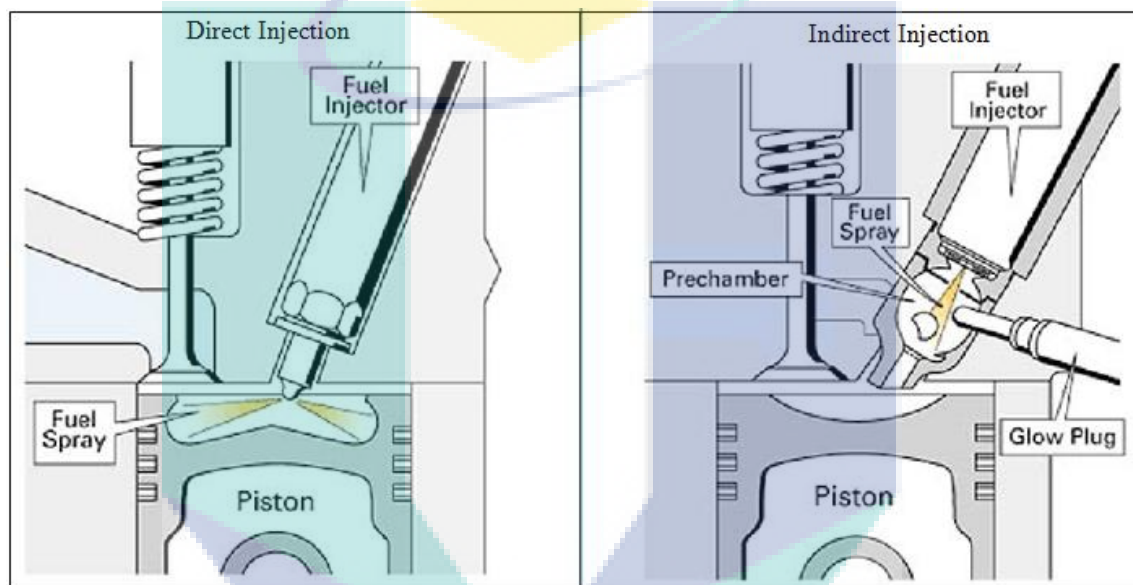
Figure 2.6: Differences between direct and indirect injection
Source: Nicolas (2013)

On the other hand, indirect injection method, also known as divided chamber or pre-chamber injection method is when the fuel is injected into the pre-chamber located at the engine head. During compression stroke, air is forced into this pre-chamber. Fuel is injected in the pre-chamber and combustion starts here before it spreads into main combustion chamber. The advantages of indirect injection are injection pressure needed for this design is low and the direction of the fuel spray is not critically affect the engine performance. Meanwhile, the disadvantages of indirect injection are the engine is difficult to start in the morning since this configuration need glow plugs. Indirect injection also has high specific fuel consumption because there is a pressure loss due to

the air movement through the duct and heat loss due to large heat transfer area. Figure 2.6 illustrate the difference between direct injection and indirect injection.

2.1.4   Diesel Engine Applications

Diesel engine is widely used in many modern applications. It is either land vehicles, power plants or vessels, diesel engine are preferred choice for power source because of its high thermal efficiency, robustness, high power output, low maintenance and fuel cost and simple arrangement designs (McAllister et al., 2011).

For land vehicles, diesel engines often used in passenger cars, trucks, buses and others. This vehicle types commonly equipped with four stroke diesel engine from small to medium size with high speed applications. While in locomotives, modern design for power generation in locomotives consists of hybrid diesel-electric system. This is differs from traditional locomotive which depends completely from diesel engine itself to generate power. Hybrid diesel-electric system use diesel engine to generate power from an electric generator. This system operates based on electric traction motors with no mechanical connection between diesel engine and the traction.

For vessels, most of the diesel engines used are two strokes, medium to large, slow speed engine. Diesel engines used in vessels are commonly large engine, which operates between 60 to 200 rpm for engine speed and can produce until 114,000 hp power output. Type of fuel used for these applications is low-grade heavy fuel. Furthermore, diesel engines also being used as power source for submarines. Nowadays, diesel engine in submarines usually paired together with electric rotor where diesel engine turns the electric generator to produce power.

2.2 TDF as Alternative Fuel for Diesel Engine

2.2.1 Production of TDF

TDF is a fuel that is produced from scrap tires. The fuel is yielded through pyrolysis process where the shredded scraps tires undergo thermal decomposition into low molecular weight products under an inert atmosphere (Amari et al., 1999). Generally, there are three types of TDF used today which are TDF with steel, TDF without steel and crumb rubber (Tillman and Harding, 2004). From the pyrolysis process for processing TDF, other products gained form the process are steel and carbon black. The Figure 2.7 below shows the pyrolysis process of TDF.
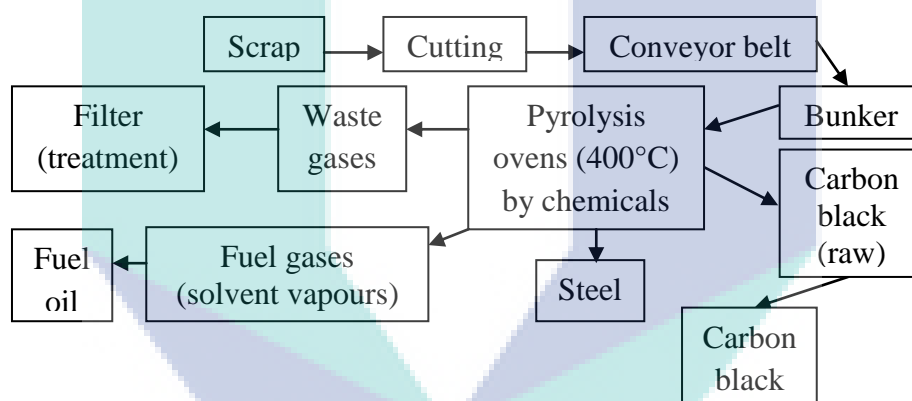
Figure 2.7: Pyrolysis process flow diagram

Source: Chong (2006)

Pyrolysis of TDF has various process conditions which have been studied by several researches. The process conditions that have been studied are heating temperature, type of catalyst and heating rate. The effects of heating temperatures and catalyst to the product obtained from tire pyrolysis have been studied by Abdul Raouf et al. (2010). From the research, it was claimed that higher temperature caused the formation of paraffin from the process. It was also claimed that aluminium oxide, Al_3O_2 (AO) is the most effective catalyst for the yield of paraffin from the reaction.

Aydin and İlkiliç (2012) concluded in their research that the optimum temperature that yielded highest liquid product was approximately 500°C. It is also found that addition of calcium oxide (CaO) and calcium hydroxide (CaOH$_2$) as catalyst in the process will lower the sulphur concentration in the liquid yield. At the end of the research, it was also concluded that the majority of the important fuel properties of fuel that were derived from the tire and its blends with diesel fuel were similar to petroleum diesel fuel.

Banar et al. (2012) studied the influence of heating temperature and heating rate to the amount of pyrolytic liquid yield. In the study, it is stated that higher pyrolytic oil is yielded when the heating temperature is between 350 °C to 400 °C and decrease when the heating temperature is between 400 °C to 600 °C. It is concluded that maximum yield of pyrolytic liquid occur at 400°C heating temperature and 5 °C/min or 35 °C/min of heating rate.

2.2.2 TDF as Alternative Fuel

TDF has potential to be used in diesel engine as an alternative fuel as stated by Murugan et al (2008d). This is due to the similar fuel properties of TDF with diesel fuel (Murugan et al., 2008b). Furthermore, Abdul- Raouf et al. (2010) stated that TDF has similar calorific value as coal.

Experiment has been conducted to determine the suitability of TDF for alternative fuel in diesel engine. Bhatt and Patel (2012) compared the chemical properties of TDF to Euro IV diesel fuel to investigate the potential of TDF to be used as an alternative fuel. At the end of their study, they concluded that TDF have comparable value of carbon content, calorific value, nitrogen, sediment, hydrogen and water content compared to Euro IV diesel. However, the disadvantages of TDF are the properties such as sulphur content, viscosity and aromatic contents are higher compared to diesel sample.

Results from engine testing show that diesel engine can operate until 90% TDF-diesel blends as observed by Doğan et al. (2012). In their studies, six different fuel

blend samples of refined TDF with neat diesel at a specific blending ratio were tested in diesel engine. Doğan reported that, the TDF content in diesel fuel did not give significant impact to engine output such as power, torque, brake thermal efficiency and brake specific fuel consumption compared to diesel. In addition, the emission of carbon monoxide, unburned hydrocarbon and smoke opacity decreased while nitrogen oxides emission increased with the increasing amount of TDF blend ratio.

Similar study was conducted by İlkılıç and Aydin (2011). Eight different samples are tested which includes different TDF blending ratio and pure 100% TDF. The findings from the study are diesel engine efficiently can operate with TDF blend ratio up to 35% without engine modifications. However, blending ratio that more than 50% results the engine to produce higher emission such as high carbon monoxide (CO), hydrocarbon (HC) and sulphur dioxide (SO_2)

Murugan S et al. (2008d) also ran an experiment to investigate the performance and emission of diesel engine operating with TDF. Three different samples of TDF where it is blended with diesel fuel at 10%, 30% and 50% blend ratio were tested in the experiment. At the end of experiment, Murugan reported that an increasing percentage of TDF in diesel fuel will contribute to higher thermal efficiency compared to diesel fuel at the same engine operating conditions. However, increasing of TDF content in diesel fuel would also cause NO_x emission to increase. Murugan also suggested that reducing the aromatic content and viscosity of TDF will improve the fuel characteristic and its possibility to be used as an alternative fuel in diesel engine.

2.2.3   Improvements of TDF for Diesel Engine Usage

There were several improvements made in order to possibly improve the TDF properties so it can give better output compared to diesel fuel. Among the improvement made is desulfurization of TDF to lower its sulphur content as reported by Aydın and İlkılıç (2012). At the end of the study, it is reported that the percentage of sulphur in TDF is reduced when TDF undergo desulphurization process. The other TDF properties values such as flash point, kinematic viscosity, heating value and distillation curves were very similar to diesel fuel.

Further research on improvement of TDF is by mixing the chemicals in TDF to improve the combustion quality. The mixing method vary according to experimental method as done by Hariharan et al. (2013) where diethyl ether (DEE) was admitted along with intake air at variable flow rates. Results show that the engine performs better when DEE is admitted into the intake manifold at rate of 170 g/h together with TDF. NO_x emission decreased when DEE is used together with TDF. However, the emission of hydrocarbon (HC), carbon monoxide (CO) and smoke was higher for DEE-TDF emission compared to diesel fuel.

Younus et al. (2013) also studied the effect of adding an additive in TDF by mixing it together with TDF instead of admitting it in the intake manifold. Ethanol and ethyl hexyl nitrate (EHN) are used as additive in TDF blend. Three different additive blend ratios were tested to study the performance and emission parameters. The output from this study shows an increment of the brake thermal efficiency (BTE) for all blend ratios compared to diesel fuel. Moreover, the brake specific fuel consumption, carbon monoxide (CO), carbon dioxide (CO_2) and hydrocarbon emission (HC) is decreased. Finally, it is concluded that the blend of TDF 20%, ethanol 10%, EHN 1% and diesel 69% is the most ideal blend ratio among the other sample according to the performance output.

Murugan S. et al. (2008a) studied the effect of TDF distillation to engine performance. In the study, the performance of two different TDF blend ratio in diesel fuel (30% TDF and 70% diesel) were compared where one sample use distilled TDF (DTDF) while the other is pure 100% TDF. The results from this experiments shows that usage of DTDF produce lower NO_x emission compared to TDF and diesel fuel. Moreover, hydrocarbon also reduced when DTDF is used compared to TDF and diesel fuel. However, smoke emission increased when DTDF is used compared to TDF and diesel fuel.

In addition, Sharma and Murugan (2013) reported that TDF has a low cetane number. Low cetane number TDF combustion lengthens the ignition delay thus resulting on poor engine performance and high emission. In order to improve the properties, TDF was blended with jathropa methyl ester (JME) which has higher cetane

number compared to diesel fuel. In their findings, JME-TDF blend at 20% ratio give an optimum performance compared to other blend. Additionally, the ignition delay and brake thermal efficiency for JME-TDF20 is almost equal to diesel fuel. The carbon monoxide, hydrocarbon and smoke emission when JME-TDF20 used is lower compared to diesel fuel. However, exhaust gas temperature and NO_x emission is higher for JME-TDF20 compared to diesel fuel.

2.3   PDF as Alternative Fuel for Diesel Engine

2.3.1   Production of PDF
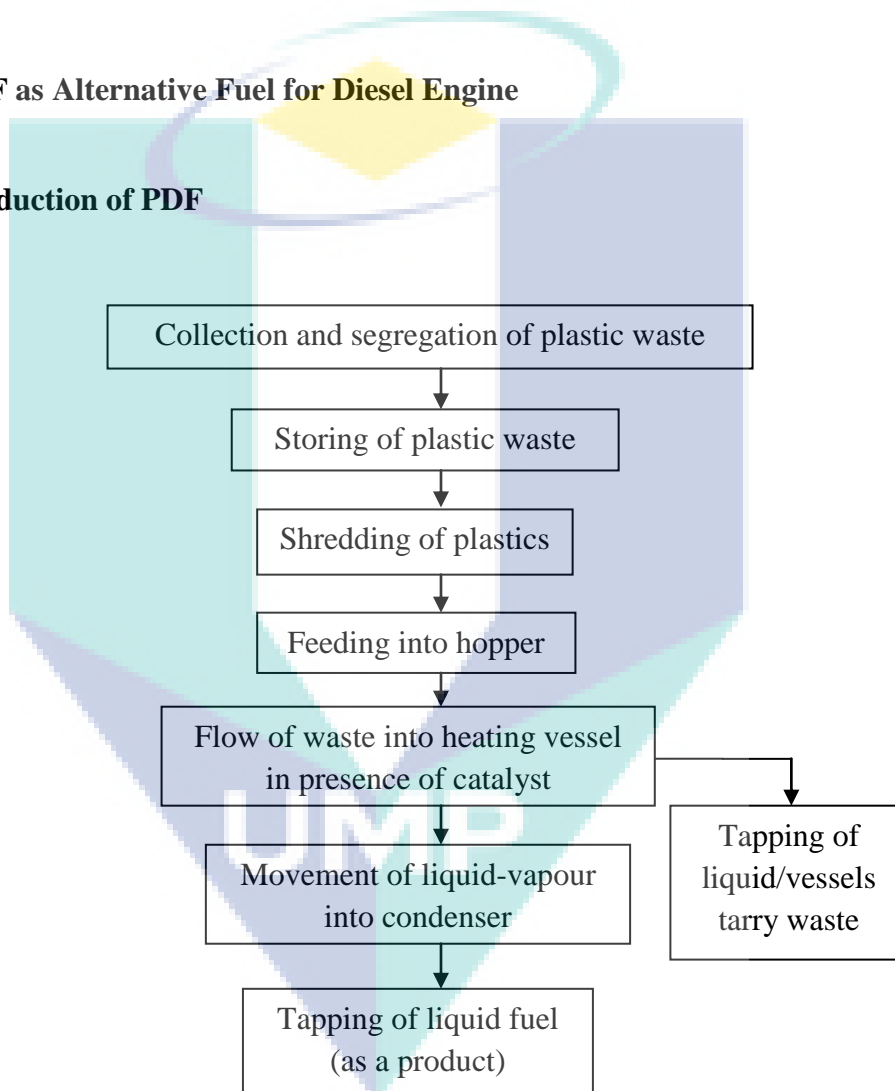
Figure 2.8: Conversion process of waste plastics to liquid fuel

Source: Harshal and Shailendra (2013)

Figure 2.8 shows the flow chart of pyrolysis process to produce PDF. PDF is obtained from thermal degradation process where the waste plastics are heated to the rated temperature with an absence of oxygen. Similar to TDF, the process of obtaining

PDF from waste plastics is known as pyrolysis process. Plastic waste is heated in a cylindrical reactor at temperature of 300 °C to 350 °C and may reach 700-900°C depends on the situation. (Harshal and Shailendra, 2013). According to Panda et al. (2010), pyrolysis process can be performed with or without catalyst where catalyst influences the rate of liquid yield in the pyrolysis process.

2.3.2 PDF as Alternative Fuel

PDF is claimed to have good potential to be used as an alternative fuel for diesel fuel thus can be considered for future transport purpose. Furthermore, engine diesel can run with 100% unblended PDF. Diesel engine fuelled with PDF produce higher thermal efficiency compared to diesel fuel (Harshal and Shailendra, 2013).

There are several studies done to investigate the suitability of PDF to be used in diesel engine. Mani et al. (2009) studied the performance of diesel engine operating with PDF. At the end of the experiment, it is concluded that diesel engine running with PDF shows stable performance with brake thermal efficiency similar to diesel. Furthermore, exhaust smoke is reduced by 40% to 50% at all loads when waste plastic fuel is used. However, the disadvantages of using PDF are the emissions such as the unburned hydrocarbon and CO shows an increment compared to diesel fuel.

Mani and Nagarajan (2009) also studied the effect of injection timing on diesel engine performance operating with waste plastic fuel. Injection timings at four different crank angles were tested which at 23°, 20°, 17° and 14° before TDC. The results shows that retarded injection timing at 14° before TDC resulted in decreased of carbon monoxide, unburned hydrocarbon and oxides of nitrogen compared to standard injection timing of 23° before TDC. Furthermore, break thermal efficiency, carbon dioxide and smoke shows an increment under all test conditions.

Effect of cooled exhaust gas recirculation (EGR) on performance of diesel engine operating with PDF also investigated by Mani et al. (2010). It is observed that NO_x emissions are reduced when cooled EGR is used against the engine. The optimum

level of EGR is at 20% based on significant reduction of HC, CO, NO_x, minimum smoke level and comparable brake thermal efficiency compare to diesel usage.

A review on the suitability of PDF to be used as an alternative fuel for diesel engine has been made by Patel and Desai (2013). In the review, it is concluded that PDF is good alternative fuel for diesel engine. Furthermore, diesel engine can run with 100% of PDF. It is also stated that higher thermal efficiency is obtained up to 75% of the rated power when PDF is used. In addition, diesel engine produce higher brake thermal efficiency when PDF is used together with retarded injection.

2.4   Fuel Properties

2.4.1   Cetane Number

Cetane number (CN) is an empirical parameter associated with the ignition delay time of diesel fuels, which is determined by means of standard tests based on the ASTM D613 standard (Cataluna and Silva, 2012). It indicates the diesel ignition delay which is the time after the fuel is injected into the combustion chamber until the first identified pressure increase during the combustion of the fuel.

The fuel with higher cetane number will have shorter ignition delay compared to fuel that have lower cetane number (Bhatt and Patel, 2012). It is also stated that TDF has lower cetane number value from regular cetane number requirement which is 42. One of the solutions to overcome the problem is by bi- fuelling or blending it with diesel fuel.

Another way to overcome the lower cetane number of TDF is through dual fuel mode as studied by Hariharan et al. (2013). In the study, it is stated that diesel engine is not able to operate with 100% TDF that may related to the lower cetane number of TDF. To overcome the problem, diethyl ether (DEE) is inducted into the intake manifold as ignition improver. The result shows that ignition delay of TDF is decreased as DEE is used as ignition improver.

Mani et al. (2011) stated that PDF has lower cetane number compared to diesel fuel that caused longer ignition delay of PDF. To overcome the problem, PDF is blended with diesel fuel. From the experiment, the ignition delay of PDF-diesel blend is increased when the PDF ratio is increased. This indicates that the cetane number of the PDF-diesel fuel is decreased as the PDF ratio increase.

2.4.2 Fuel Density

Density is defined as mass of the liquid divided by its volume at 15 °C or 20 °C, written in units of mass and volume, together with the standard reference temperature (Murphy et al., 2012). The fuel density affects the engine performance directly by influencing the fuel injection system (S.A.Shahir et al., 2014)

Aydın and İlkılıç (2012) stated that the TDF has the highest density compared to diesel fuel. Even though the TDF has undergone desulphurization process, its density still higher compared to diesel fuel. Through fuel blending between TDF and diesel fuel, the density of TDF is decreased as stated by Sebola et al. (2013). However, the changes of blend ratio between TDF and diesel fuel does not give significant trend to the blended fuel density.

Hossain and Davies (2013) also reviewed that the density of TDF is higher compared to diesel fuel. The density value gives indication to the specific energy content and ignition quality. Higher density also causes higher NO_x emission when the TDF is used as fuel.

Several researches claims that PDF has lower density compared to diesel fuel (Mani and Nagarajan, 2009), (Pratoomyod and Laohalidanond, 2013), (Harshal and Shailendra, 2013). Lower density of fuel may affect the mass of fuel injected into the combustion chamber where lower density cause less mass of fuel that injected into the combustion chamber. This condition will cause less power and engine torque.

2.4.3   Viscosity

Viscosity of a fluid describes the fluid's internal resistance to flow or also can be assumed as measure of fluid friction (Hossain and Davies, 2013). Fuel with high viscosity has several effect to engine operations such as poor fuel atomization during spray process and increases the carbon depositions on fuel filter (S.A.Shahir et al., 2014). Higher viscosity causes less penetration of fuel spray throughout the combustion chamber hence cause poor combustion quality (Adam et al., 2011).

TDF has higher kinematic viscosity than specified limit for EURO V diesel engine (Bhatt and Patel, 2012). High viscosity cause larger fuel droplets during injection phase. Larger fuel droplets cause less surface area, hence cause poor mixing between fuel and air. This condition cause poor engine performance and high emission of TDF.

High viscosity of TDF can also cause problems to the engine in long run (Murugan et al., 2008a). The problems include the formation of carbon deposits and also sticking of oil ring. High viscosity of TDF is caused by large molecular mass and chemical structure. However, according to Murugan et al. (2008c), highly viscous fuel can be used in diesel engine by performing either engine modification or fuel modification.

Mani et al. (2011) stated that the properties of PDF is closer to diesel fuel except for viscosity. It is stated that PDF has high viscosity thus cause high smoke level and low thermal efficiency when used in diesel engine. Furthermore, the viscosity of PDF is reduced when blended with heavy oil thus results in better engine performance (Kumar et al., 2013).

2.4.4   Calorific Value

The calorific value of a fuel measures the energy released as heat when a compound undergoes complete combustions with oxygen under standard conditions (Flagan and Seinfeld, 2012). This value is measured in units of energy per unit of the

substance, usually mass where commonly expressed in unit MJ/kg. The calorific value commonly measured using bomb calorimeter where the amount of heat released during the combustion of a specified amount of the tested fuel inside the oxygen bomb is measured. Fuels with different calorific values will produce different power output (S.A.Shahir et al., 2014).

Bhatt and Patel (2012) stated that TDF has high and comparable calorific value compared to diesel fuel hence make it possible to be used as fuel. However, Banar et al. (2012) stated that TDF has lower calorific value compared to diesel fuel. Further investigation is conducted to determine the relation of calorific value to the engine output. İlkılıç and Aydın (2011) investigated the effect of TDF usage in diesel engine. 100% unblended TDF is tested in diesel engine and the power and torque output is compared to diesel fuel. From the results obtained, it can be concluded that TDF produce lower power and torque compared to diesel fuel as the calorific value for TDF is lower compared to diesel fuel.

PDF also has lower calorific value compared to diesel fuel as stated by Harshal and Shailendra (2013). To improve the properties of PDF, it is blended with diesel fuel. Blending the PDF with diesel fuel results in higher calorific value of PDF-diesel fuel blends compared to unblended PDF as stated by Kumar et al. (2013). However, calorific value is decrease as the ratio of PDF in diesel fuel is decrease. The decreasing trends of calorific value as the PDF ratio in diesel fuel increase cause the power and torque output also decrease as stated by Pratoomyod and Laohalidanond (2013).

2.4.5   Sulphur Content

Sulphur content naturally occurs in fuels and the straight run of diesel fuel cause significantly higher sulphur content than gasoline (Pundir, 2010). The sulphur content affects the emission produced by diesel engine where sulphur contribute to the formation of particulate matter (PM) (Tan et al., 2009). Saiyasitpanich et al. (2005) concluded that the increase of sulphur content will cause the formation of particulate matter increase significantly.

Bhatt and Patel (2012), Islam et al. (2008) and Frigo et al. (2014) stated that the sulphur content in TDF is higher compared to diesel fuel. High sulphur content precludes TDF to be used as fuel in road vehicles. High amount of sulphur content can be reduced through desulphurization of TDF. Additive addition such as calcium hydroxide during production process of TDF also can reduce the sulphur content (Williams, 2013).

According to Mani and Nagarajan (2009) and Patel and Desai (2013), PDF has lower sulphur content compared to diesel fuel and TDF. This indicates that PDF will produce lower amount of particulate matter when combusted compared to diesel fuel and TDF. Lower amount of sulphur content also cause significant reduce on sulphur dioxide (SO_2) emission (Naima and Liazid, 2013).

2.4.6   Flash Point

Flash point measures the lowest temperature where combustible mixture can be ignited in air by a flame or above its surface (Janès and Chaineaux, 2013). These parameters are related to the precaution steps to be taken during storage, handling, transportation and use of diesel in safe way. Fuel with flash point of 90°C or higher is considered as non-hazardous (Hossain and Davies, 2013).

Aydın and İlkılıç (2012) and Bhatt and Patel (2012) stated that TDF has slightly lower flash point compared to diesel fuel. It is also stated that lower flash point for TDF gives it advantageous situation in terms of burning the fuels. However, Banar et al. (2012) claimed that the flash point of TDF is higher compared to diesel fuel hence it can be stored safely at room temperature.

PDF has lower flash point compared to diesel fuel as stated by Harshal and Shailendra (2013) and Mani and Nagarajan (2009). Kumar et al. (2013) blended the PDF with diesel fuel at several blend ratio. It is observed that the flash point of the blended PDF-diesel fuel is decreasing as the PDF blend ratio is increased.

2.5   Engine Performance Analysis

In this section, measured and calculation data analysis for engine testing are discussed. Engine testing analysis includes engine power, torque, combustion pressure, ignition delay, exhaust gas temperature and exhaust gas emissions. All the measured parameters are described into several subsections.

According to Heywood (1988), engine performance is more accurately defined as the maximum power or torque occurs at every speed within useful engine operating range. Engine performance indicates the output from an engine after the input (fuel and air) is combusted in the combustion chamber. The performance parameters that commonly measured are power, torque, combustion pressure, combustion temperature, fuel consumption and exhaust emission.

Engine performances are determined by engine testing where the engine is coupled to a dynamometer to measure its performance. The dynamometer functions by exerting load to the engine at certain level and speed. There are two common dynamometer testing which is engine dynamometer and chassis dynamometer. Engine dynamometer measures engine power and torque directly from the engine crankshaft. This method is only applicable to stationary engine or engine that taken out from the vehicle. The chassis dynamometer measures the power and torque that is transferred to its drive roller from vehicle wheel.

2.5.1   Engine Torque and Power

Engine torque is commonly measured by dynamometer. The engine is placed on a test bed and the flywheel is coupled to the dynamometer rotor. The dynamometer will exert load to the engine. Engine torque is a measure of an engine ability to do work and commonly written as 'T'. Engine torque that measured according to the torque transmitted to the dynamometer is known as brake torque.

Engine power is a known as rate of work done by the engine. The equation that describes the engine power is shown in Equation 2.24 and Equation 2.25. Since brake

torque is used in the equation, the power value obtained from the equation is known as brake power.

$$\text{Brake Power, } P_b \text{ (kW)} = \text{Brake Torque, } T_b \text{ (Nm)} \times \text{Engine Speed, } N \text{ (rpm)} \quad (2.24)$$

$$\text{Brake power, } P_b = 2\pi NT \quad (2.25)$$

For indicated power (P_i) and indicated torque (T_i), it is measured through pressure data for the gas in the cylinder. Pressure data is obtained through pressure sensor that mounted directly into the cylinder to measure combustion pressure. When this indicated torque and indicated power can be determined, one more parameter which is friction loss or friction power can be calculated through equation as shown in Equation 2.26.

$$\text{Indicated power, } P_i = \text{Brake power, } P_b + \text{Friction power, } P_f \quad (2.26)$$

Most of the TDF undergoes testing are blended with diesel fuel. Since researches that conducted by Doğan et al. (2012) and Hariharan et al. (2013) claimed that diesel engine would malfunction when 100% unblended TDF is used, blending the TDF with diesel fuel enables TDF to be used in diesel engine.

Doğan et al. (2012) tested five samples of blended TDF-diesel fuel with up to 70% TDF blend ratio with diesel fuel as reference fuel. It is concluded that the blend ratio does not have significant effect to the engine torque and power until 70% blend ratio. Moreover, it is stated that the factors that affect the engine torque and power is the fuel density, viscosity and calorific value.

Frigo et al. (2014) also investigated the performance of blended TDF-diesel fuel. There are six different TDF-diesel fuel blend ratios with highest blend ratio is 45% TDF. The result shows that the blend ratio also does not give significant impact to the engine power and torque until 20% blend ratio. As the blend ratio exceeds 20%, the engine power and torque starts to decrease. It is also stated that the factors affecting to

engine output is the reduction of cetane number for every blend ratio as the TDF ratio is increase.

Experiment that was conducted by İlkılıç and Aydın (2011) showed significant power and torque change as the TDF blend ratio is increased. When the TDF blend ratio is increase, the power and torque output will decrease. Moreover, all the blended TDF-diesel fuel blends will produce lower power and torque output compared to diesel fuel. The factors that affecting the power and torque for the experiment is the variations of calorific value for each test fuels.

PDF also undergo blending process with diesel fuel to be used in diesel engine. However, Harshal and Shailendra (2013) and Mani and Nagarajan (2009) concluded that 100% unblended PDF can be used in diesel engine. Pratoomyod and Laohalidanond (2013) studied the power and torque output of blended PDF. Four different blend ratios are tested with 75% PDF blend are the highest blend ratio. It is concluded that engine power and torque are decrease when the PDF blend ratio is increased.

2.5.2 Ignition Delay

Ignition delay can be described as a time region between the start of injection to the point where the pressure time-time curves separates from the motoring curve which is also known as compression pressure curve (Ganesan, 2012). Moreover, Pundir B.P (2010) also explains the ignition delay as the time between the start of injection and the start of combustion where the start of combustion is identified by a sudden increase in the slope of P-θ curve. The factor affecting the ignition delays of the fuel is the cetane number. As the cetane number increases, the ignition delay is shorter (Bhatt and Patel, 2012).

The mixing process between TDF and diesel fuel affects the ignition delay of every blend. According to Doğan et al. (2012), as the blend ratio of TDF in diesel fuel increases, the ignition delay is prolonged. It is also reported that longer ignition delay will provide more time for air to mix with the injected fuel in the combustion chamber hence produce higher brake thermal efficiency (BTE).

Prolonged ignition delay also causes more fuel existed in the combustion chamber during delay period, hence causes a rapid heat release when the combustion started (Frigo et al., 2014). This condition will cause knocking to occurs during engine operation. It is also claimed that the engine knocking is clearly perceptible during engine operation due to long ignition delay period. Therefore, İlkılıç and Aydın (2011) stated that the diesel engine knocking phenomenon can be eliminated by reducing the ignition delay.

Hariharan et al. (2013) proposed that one of the alternatives that are available to increase the cetane number of TDF and its blends is by blending it with fuels that has high cetane number. In the experiment, TDF-diesel fuel blend is combusted with diethyl ether that has cetane number greater than 125. Diethyl ether is admitted into the combustion chamber by an injection process into the intake manifold. It is concluded that usage if diethyl ether as ignition improver could shorten the ignition delay.

Kumar et al. (2013) reviewed that PDF that is blended with diesel fuel also has longer ignition delay compared to diesel fuel. The maximum blend ratio that gives acceptable knocking level is 40%. Higher blend ratio will cause severe knocking effect thus affect the engine performance. Mani et al. (2011) also stated that PDF-diesel fuel blend has longer ignition delay compared to diesel fuel. The factors that affect the longer ignition delay of PDF are poor spray characteristics of PDF and also lower cetane number.

2.5.3   Peak Pressure

EL-Kasaby and A.Nemit-allah (2013), Enweremadu and Rutto (2010) and Rodríguez et al. (2011) stated that the combustion peak pressure are strongly related to the ignition delay. As the ignition delay prolonged, the peak pressure that is produced during combustion is higher due to higher amount of fuel presence in the combustion chamber during ignition delay period.

Lower peak pressure due to shorter ignition delay has advantages to diesel engine operation as stated by Hariharan et al. (2013). Lower peak pressure resulted in

low noise level and also contributes to the smooth engine operation. The NO_x emission level also decreases as the peak pressure decreases, since lower peak pressure causes lower combustion temperature.

Hossain and Davies (2013) reviewed that the usage of crude, unblended TDF in diesel will produce higher level of peak pressure compared to diesel fuel. Moreover, Murugan et al. (2008a) stated that TDF that is blended with diesel diesel fuel also produces high peak pressure compared to diesel fuel. High peak pressure of TDF-diesel fuel blends is caused by longer ignition delay, where it is attributed to higher viscosity and lower volatility of the fuel.

PDF and its blends also has higher peak pressure compared to diesel fuel (Mani et al., 2011). Higher peak pressure of PDF also related to longer ignition delay compared to diesel fuel that additionally results in higher rate of heat release. The cetane number of PDF that is lower than diesel fuel also cause longer ignition delay thus producing higher peak pressure.

2.6   Diesel Engine Emissions

Fuel combustion in internal combustion engine emits undesirable exhaust emissions. The emission gives effect to the environment and cause problems such as acid rain, global warming, health problems and many more. The main causes that contribute to these problems are non-stoichiometric combustion, impurities in the air and fuel and also dissociation of nitrogen. The types of emission includes unburned hydrocarbon (HC), carbon monoxide (CO), nitrogen oxides (NO_x) and particulate matter (PM) (Pulkrabek, 2004).

2.6.1   Exhaust Gas Temperature

The combustion temperature indicates the amount of energy released when the combustion occur. The exhaust gas temperature measurement served as an indicator of the combustion temperature that is related to the heat release (EL-Kasaby and A.Nemit-allah, 2013). Moreover, exhaust gas temperature shows the efficiency of fuel

combustion. The increase of exhaust gas temperature reduces the conversion of heat energy contains in fuel to useable work (Enweremadu and Rutto, 2010).

İlkılıç and Aydın (2011) stated that TDF and its blends produce lower exhaust gas temperature compared to diesel fuel. When TDF blend ratio is increased, the exhaust gas temperature also decreased. The factors that affect the exhaust gas temperature include combustion temperature, incomplete combustion and retarded combustion. Furthermore, Doğan et al. (2012) stated that increasing the TDF blend ratio will increase the volatility of the fuel. Commonly, high volatility fuel will reduce the exhaust temperature due to higher vaporization cooling effect. The effect will results in lower exhaust gas temperature when the TDF blend ratio increases.

PDF and its blends produce higher exhaust gas emission compared to diesel fuel (Kumar et al., 2013) due to higher oxygen content and higher boiling point of PDF. High oxygen content and high boiling point cause higher exhaust gas temperature of PDF compared to diesel fuel.

2.6.2   Carbon Oxides (CO_x)

The fuel/air equivalence ratio affects the carbon monoxide (CO) emissions of internal combustion engine. CO formed as a result of incomplete combustion in rich air-fuel mixture due to air deficiency. Compression ignition engine always well operates on lean stoichiometric where the lean combustion will produce low level of carbon monoxide emissions (Pulkrabek, 2004).

The carbon dioxide (CO_2) is a naturally existent gas in the atmosphere and common product of diesel combustion. The proportion of carbon dioxide also depends on the engine operating conditions. CO_2 contained in the automotive exhaust gas is not classified as pollutant. However, CO_2 causes the greenhouse effect and global climate change (Pulkrabek, 2004). Since the Industrial Revolution period begins, the content of carbon dioxide in the atmosphere continuously rises, mostly because of widely used fossil fuel to generate energy (Baranescu and Challen, 1999).

The combustion of TDF and its blends produce higher level of CO compared to diesel fuel (Murugan et al., 2008d). The presence of low molecular weight compounds which affect the atomization process thus resulting in local rich mixtures which contributes to the high level of CO emission formed during combustion.

However, Doğan et al. (2012) claimed that CO emission is reduced when TDF blend ratio is increased. The factor that affects the CO emission level is the viscosity of the fuel. When the TDF blend ratio is increased, the viscosity of the fuel decreases hence improves the preparation of combustible mixture during the combustion process. This factor lowers the CO emission level when the ratio of TDF is increased.

Harshal and Shailendra (2013) concluded that PDF produce higher level of CO emission compared to diesel fuel. The reason that causes higher CO emission level is incomplete combustion of PDF due to reduced in-cylinder temperatures. Kumar et al. (2013) also stated that PDF produce higher level of CO emission that is caused by the absence of oxygenated compounds in PDF hence causes incomplete combustion.

Mani et al. (2011) also stated that PDF-diesel fuel blends will produce higher level of CO compared to diesel fuel. This is caused by the poor mixture preparation, reduced in-cylinder temperatures and local rich regions. However, Mani also stated that the CO emission reduces when the power output is higher. This is because the ignition delay reduces at higher power outputs and the fuel presents in the combustion chamber during delay is reduced hence cause less CO formation.

2.6.3   Nitrogen Oxides (NO_x)

Nitric oxide (NO) and nitrogen dioxide (NO_2) are often grouped together as oxides of nitrogen (NO_x). Nitrogen and oxygen will react to each other at high combustion temperatures. Therefore, high combustion temperature and existence of oxygen are the factors that contribute to NO_x formation. When sufficient amount of oxygen is presence, higher peak pressure will cause higher level of NO_x formed (Ganesan, 2012).

Unlike other pollutants, NO_x is a side output of the fuel combustion and not an incomplete step in it. The main source of NO formation is the oxidation of atmospheric nitrogen. Apart from that, the fuel that contains significant amount of nitrogen can be additional source of NO through oxidation of the fuel that contains nitrogen.

$$O + N_2 \rightarrow NO + N \tag{2.27}$$

$$N + O_2 \rightarrow NO + O \tag{2.28}$$

$$N + OH \rightarrow NO + H \tag{2.29}$$

For nitrogen dioxide (NO_2) gas, it is formed by rapid conversion of NO in the flame zone where the reactions are shown by following equations:

$$NO + H_2O \rightarrow NO_2 + OH \tag{2.30}$$

$$NO + O_2 \rightarrow NO_2 + O \tag{2.31}$$
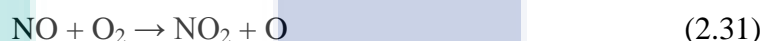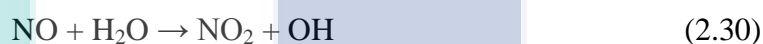
The NO formation rate is influenced by high gas temperature and high oxygen concentrations and also equivalence ratio. The maximum rate of NO formation occurs when the equivalence ratio is stoichiometric and rapidly decreases when the mixture is rich or lean.

NO_x emission is increase with the increasing of TDF blend ratio (Doğan et al., 2012). The factor that contributes to the increasing of NO_x is the higher fuel density with the increment of the TDF blend ratio. Additionally, higher aromatic content in TDF also cause higher level of NO_x emission when during TDF combustion. Murugan et al. (2008d) also stated that NO_x emission level produce by TDF-diesel fuel blends combustion is higher compared to diesel fuel. The NO_x emission level is influenced by the combustion temperature where higher combustion temperature will cause higher level of NO_x emission.

In contradiction, Frigo et al. (2014) claimed that NO_x emission is decrease as the TDF blend ratio is increase. This is related to the cetane number of TDF blend that decreases as the TDF ratio increase. As a result, the ignition delay increases and the

combustion occur in a larger volume with lower ambient pressure and ambient temperature hence cause lower NO_x emission.

As for PDF, Kumar et al. (2013) claimed that NO_x emission increase when the PDF blend ratio in diesel fuel is increase compared to diesel fuel. The increasing amount of NO_x is caused by the oxygenated hydrocarbon that contains in PDF. The oxygenated hydrocarbon promotes better combustion thus produce higher combustion temperature that contributes to higher formation of NO_x.

Mani et al. (2011) also stated that NO_x emission level increase when PDF is consumed compared to diesel fuel. The factor that causes increasing level of NO_x is higher rate of heat release during PDF combustion. PDF has high aromatic content fuel with ring structure. Fuel which has ring structure will produce high adiabatic flame temperature that results in high rate of heat release. Higher rate of heat release will cause higher NO_x emission.

2.7   Fuel Spray Characteristics

Diesel fuel is injected into the combustion chamber through fuel injector. The basic operating principle of fuel injector is the fuel is forced injected through a small nozzle with a large pressure difference across the nozzle orifice. The fuel injection pressure depends on the system that used either distributor type injection pump, in-line injection pump or common rail injection pumps (Heywood, 1988).

Upon excitation from nozzle, the fuel wills undergoes atomization process where the surface area of the fuel droplets is increase. This is to increase the rate of heat transfer from the surrounding gases to the fuel (Lefebvre, 1989). Since the nozzle size and injection pressure is constant (depending on the engine setup), the properties of the fuel used in the engine will give affect the fuel spray characteristics.

Fuel viscosity is one of the factors that affect the fuel spray characteristics. The fuel with high viscosity will produce larger fuel droplets (Lefebvre, 1989). Large fuel droplets will reduce the surface area of the fuel hence will cause less air molecules that

react with the fuel during air-fuel mixing process lead to the less efficient combustion process.

Fuel density also influences the fuel spray characteristics. The fuel density is related to the fuel spray momentum (Youn et al., 2011). High density fuels will produce high initial spray momentum hence cause deep penetration through the combustion chamber. This results in good air utilization since the air on the periphery of the chamber react with the fuel (Heywood, 1988).
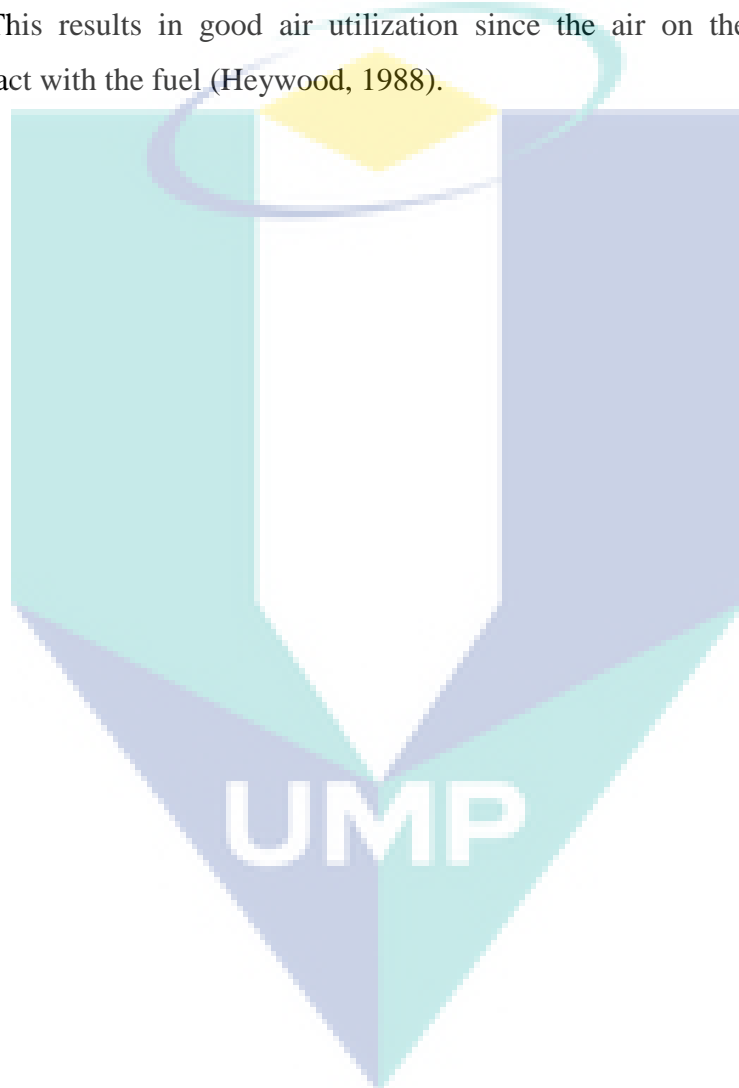
CHAPTER 3

METHODOLOGY

3.1   INTRODUCTION

Figure 3.1 shows the categories of alternative fuel that is mainly used today (Sharma and Murugan, 2013). Generally, alternative fuels are divided into two categories which are first generation biofuels and second generation biofuels. From the figure, biodiesels and alcohol which are widely used as alternative fuel in nowadays are categorized as first generation biofuels while the second generation biofuels is produced from the feedstock such as automobile tires, rubber, plastic and agro waste.
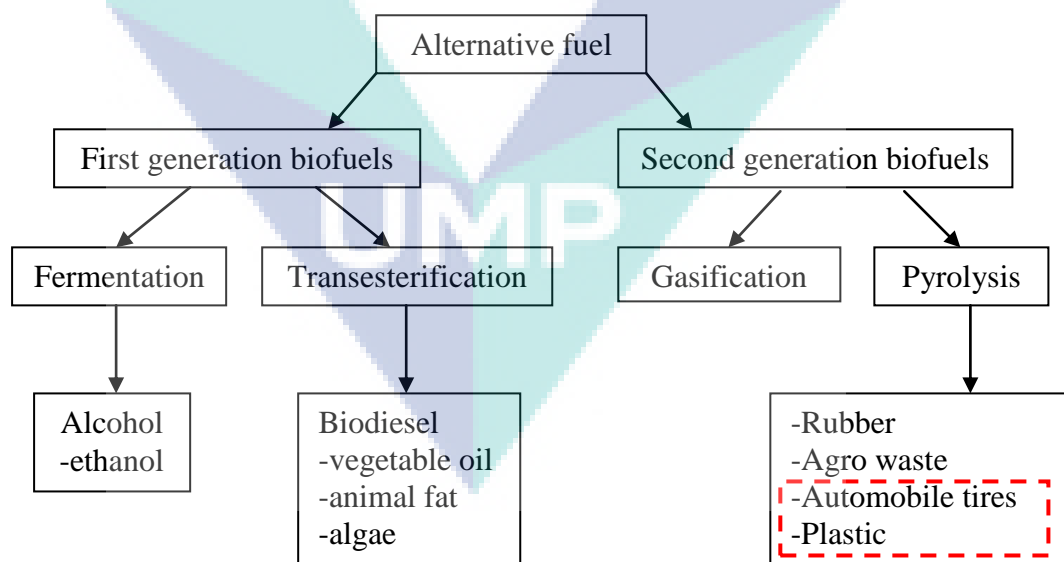
Figure 3.1: Categories of alternative fuels

Source: Sharma and Murugan (2013)

Based on the recommendations by Aydın and İlkılıç (2012), further improvement needed for TDF quality in term of fuel properties by blending TDF with diesel fuel while Mani et al. (2011) stated that further PDF testing in high speed engine is recommended. Therefore, the present work focused on the TDF and PDF as the test fuels where it is originated from the waste source which is automobile tires and plastics. The aspects that are studied include fuel properties of the TDF, PDF and its blends. The engine performance when the fuels are used in the diesel engine are will also be analyzed. For the purpose, the fuel properties will be determined through lab testing and the engine performance will be determined through engine testing.

3.2 Diesel Engine Test Rig Design

For engine testing purposes, an engine test rig is designed. Figure 3.2 shows the schematic diagram of the proposed engine test rig. It consists of a diesel engine, dynamometer system, data acquisition (DAQ) system, exhaust gas analyzer, air-volume measurement and external fuel tank.

1: Diesel Engine YANMAR TF120M
2: Engine Flywheel
3: NBK Flexible Coupling
4: Hydraulic Gear Pump (Dynamometer)
5: Pressure Gauge
6: Stop Valve
7: Cooling Radiator
8: Hydraulic Oil Tank
9: Sensor Interface
10: LCS Data Logger
11: Computer
12: Exhaust Gas Filter
13: Exhaust GAs Analyzer
14: Crank Angle Sensor
15: In-cylinder Pressure Sensor
16: Air-Volume Measurement
17: Diesel Fuel Tank
18: Alternative Fuel Tank
19: Stop Valve
20: Stop Valve
21: Exhaust Gas Manifold
22: Alternative Fuel Filter

Figure 3.2: Test rig schematic diagram

3.2.1   Diesel Engine

A diesel engine is used for testing purpose. Specific engine characteristics need to be determined beforehand. The first characteristic is the engine configuration which is a single cylinder engine. Single cylinder engine is preferred for engine testing for its simplicity and easy to operate. Furthermore, the engine performance can be analyzed more accurate since all the parameters that affect the engine output is based on the combustion that occurs in a single combustion chamber only.

The second characteristic that is taken into account is the injection system of the engine. The performance characteristics in the combustion chamber are measured using pressure sensor. Therefore, direct injection system is selected instead of indirect injection system due to the location of the pressure sensor that can be easily mounted. While for indirect injection system, the sensor needs to measure the combustion process that happens in a small pre-chamber. This will cause difficulties to mount the pressure sensor since the pre-chamber has a small volume.

The third characteristic is the engine cooling system. The engine should have water cooled system since it will be placed on a stationary stand in lab experiment. Water cooled system give more efficient cooling effect compared to air cooled system for an engine that operates in lab environment. Furthermore, the cooling system for the engine should be attached to the engine itself where this characteristic eliminates the requirement for external engine cooling system.

Based on the required characteristic, a single cylinder diesel engine YANMAR and the engine model is TF120M is chosen. This engine is a single cylinder engine with direct injection system. Furthermore, YANMAR TF120M is water cooled engine and attached cooling system according to the predetermined engine characteristics that decided. Further engine specifications are shown in Appendix 1. Figure 3.3 shows the YANMAR TF120M engine.

Figure 3.3: YANMAR TF120M diesel engine

3.2.2   Engine Stand Design

An engine stand is required to mount the engine. For the purpose, an engine stand design is proposed. The design of the engine stand is shown in Figure 3.4. The aspect that is taken into consideration during the stand design is the engine will have low centre of gravity when it is mounted to the stand. This is to prevent the moment of overall system when the engine is operating that will cause excess vibration.
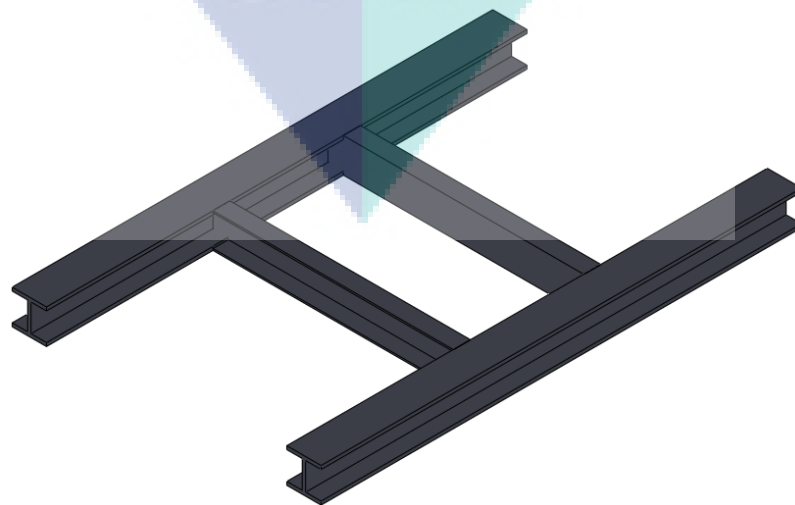
Figure 3.4: Proposed engine stand

The material that will be used to construct the engine stand is I beam (50 mm height × 50 mm wide × 3 mm thickness) and C channel (50 mm height × 25 mm wide × 3 mm thickness). The engine mounting size on the engine stand is according to the engine technical drawing that shown in Appendix 2.

3.2.3   Dynamometer

Dynamometer is another part for this test rig setup. Dynamometer function is to give load to the engine, forcing the engine to do work to overcome the load that is exerted on it. By measuring the amount of work done by the engine to overcome the load exerted to it, the brake work and brake power of the engine can be measured. The dynamometer is coupled to the engine crankshaft using flexible couplings or shafts.

The type of dynamometer that proposed in this test rig is hydraulic dynamometer. A hydraulic gear pump is used as dynamometer due to the small size, simple and easy to assembly. For this purpose, a positive displacement gear pump is used as dynamometer as shown in Figure 3.5.
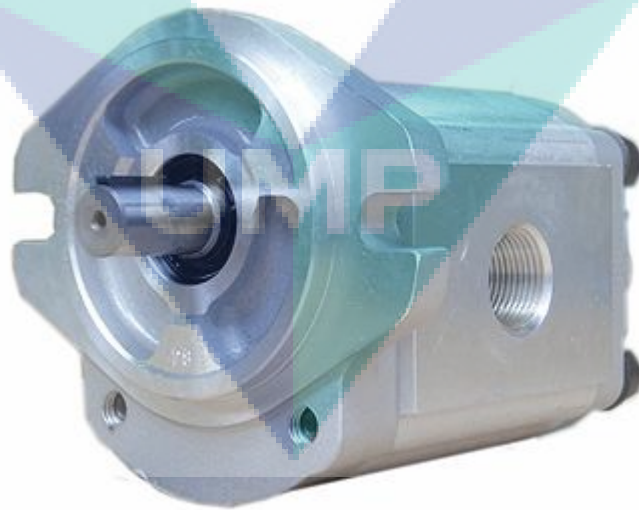
Figure 3.5: Hydraulic gear pump

The gear pump that chosen is from brand Hydrome model HGP-3A-F23. The gear pump specifications are shown in Appendix 3. The gear pump sizing is calculated to fulfil the requirement for the full-load engine operation at whole range of engine

speed. The equations that were involved in pump sizing determination are stated by McNamee et al (2010):

$$T_{pump}(\text{Nm}) = \frac{(p.d_{pump})}{2\pi} \qquad (3.1)$$

From Equation 3.1, the minimum pump size for dynamometer purpose is determined. The torque that obtained from equation 3.1 is hydraulic torque. For determining the hydraulic power, Equation 3.2 is used.

$$P_{hydraulic}(\text{kW}) = p\,(\text{Pa}) \times Q\,(\text{m}^3/\text{min}) \qquad (3.2)$$

$$Q = \frac{d_{pump}.\omega}{2.\pi} \qquad (3.3)$$

3.2.4 External Fuel Tank
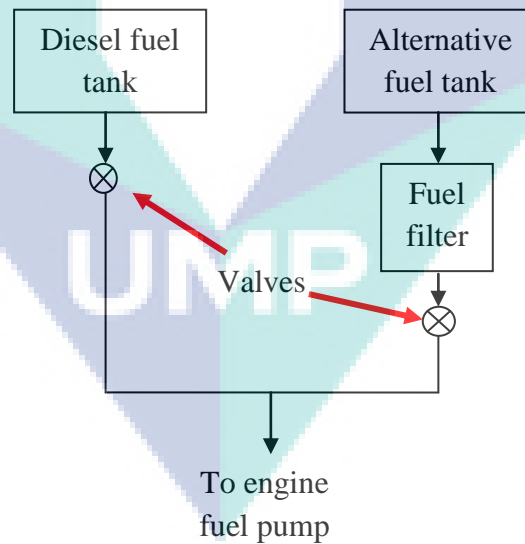
Figure 3.6: External fuel tank diagram

For alternative fuel testing, external fuel tank is preferred since the flow of tested fuels needs to be switched as the engine is operating. For the purpose, an external fuel tank is proposed as shown in Figure 3.6. It consists of two tanks, each for diesel fuel and alternative fuel. A fuel filter is placed after the alternative fuel. The fuel flow will be controlled using valves.

3.2.5   Dynamometer Bracket

A custom bracket is needed to hold the gear pump when the gear pump is connected to the engine flywheel. For this purpose, a custom bracket is designed using SolidWorks software and fabricated to mount the gear pump. The raw material used for this bracket is hardened mild steel which the thickness is 20 mm. The design of the bracket is shown in Figure 3.7. Detail drawings of the bracket are shown in Appendix 4.
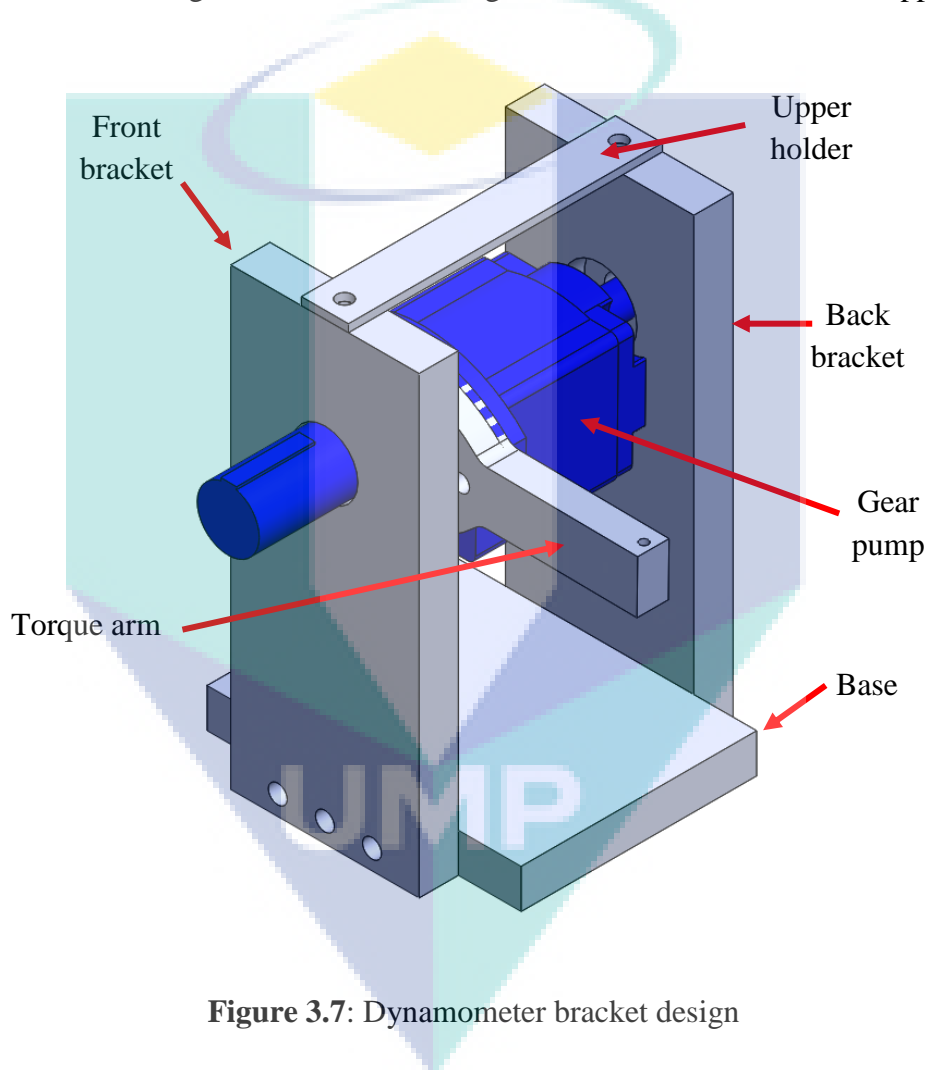
Figure 3.7: Dynamometer bracket design

3.2.6   Air Volume Measurement

The amount of air consumed by the engine can be determined using several apparatus such as air flow meter or manometer. The amount of air consumed is determined through the pressure drop of air through the orifice. Determination of this parameter enables the air-fuel ratio to be calculated as the fuel consumption also considered. The main part for this system is an orifice and a manometer. Figure 3.8 shows the proposed intake air volume measurement schematic diagram.
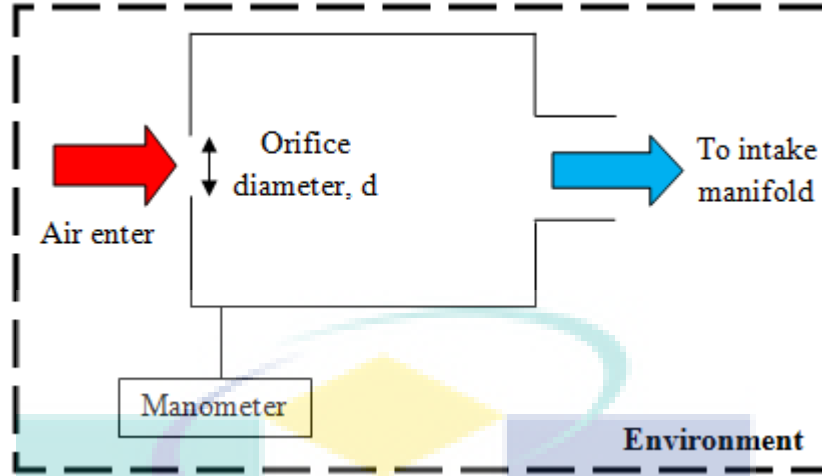
Figure 3.8: Air volume measurement diagram

An orifice is fitted to the airbox to create laminar airflow between surroundings and inner airbox. The size of the orifice is calculated based on engine specifications. The equation that is involved in determining the orifice size is shown by equation 3.4 (Martyr and Plint, 2007);

$$V = 0.1864 \, C_d \, d^2 \sqrt[2]{\frac{T_a}{P_a}} \, h \, (\text{m}^3/\text{s}) \tag{3.4}$$

The maximum air consumption of the engine can be calculated from equation 3.5 where the engine speed is taken at the maximum power occurs.

$$V = \eta_v \frac{V_s}{k} \frac{n}{60} \, (\text{m}^3/\text{s}) \tag{3.5}$$

The minimum size for the airbox is determined from equation 3.6;

$$V_b = \frac{[417 \times 10^6 \times k^2 d^4]}{N_c V_s n_{min}^2} \, (\text{m}^3) \tag{3.6}$$

The volume of air that consumed by the engine at several engine speed is determined through Equation 3.7, Equation 3.8 and Equation 3.9.

$$\text{Air velocity} = 1096.2 \sqrt{\frac{P_v}{D}} \tag{3.7}$$

$$\text{Air density}, D = 1.325 \times \frac{P_B}{T_a} \tag{3.8}$$

$$\text{Flow in cu. ft./min} = \text{duct area in sq. ft} \times \text{air velocity in ft./min} \tag{3.9}$$

3.3   Test Rig Fabrication

3.3.1   Engine Stand Fabrication

An engine stand is fabricated to mount the engine as shown in Figure 3.9. The stand is fabricated using I beam and C channel as proposed. The beams and the channels are welded together using metal inert gas (MIG) welding. The welding process is conducted properly to ensure the engine stand is able to withstand the diesel engine high vibration during operation.
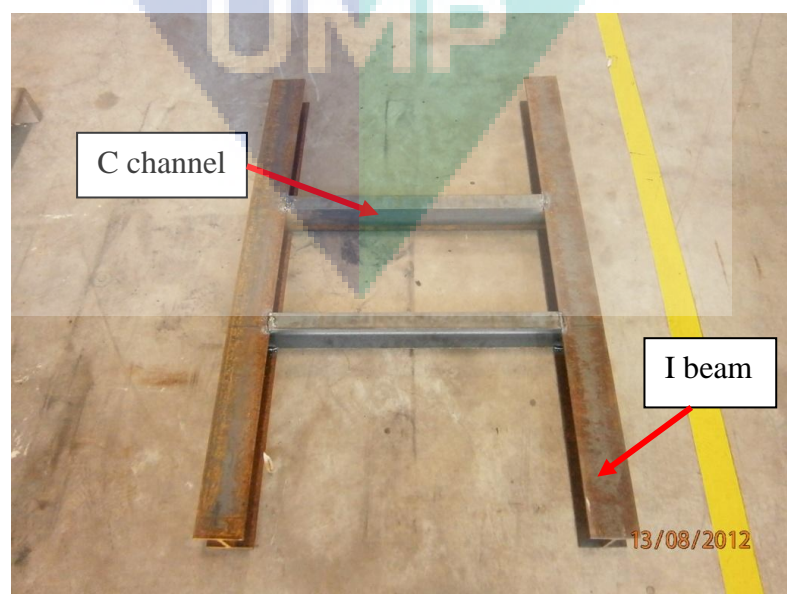
Figure 3.9: Engine stand

Four pieces of cylinder shaped rubber mounting as shown in Figure 3.10 are used to mount the engine. The mountings are made from solid rubber with M10 × 1.25 studs. These mountings are used to absorb the vibration that occurs when diesel engine is operating and also to mount the engine properly on the stand. The dimension for mounting placement at the engine stand is according to the dimension of the hole at the engine base which is 370 mm length × 170 mm wide.
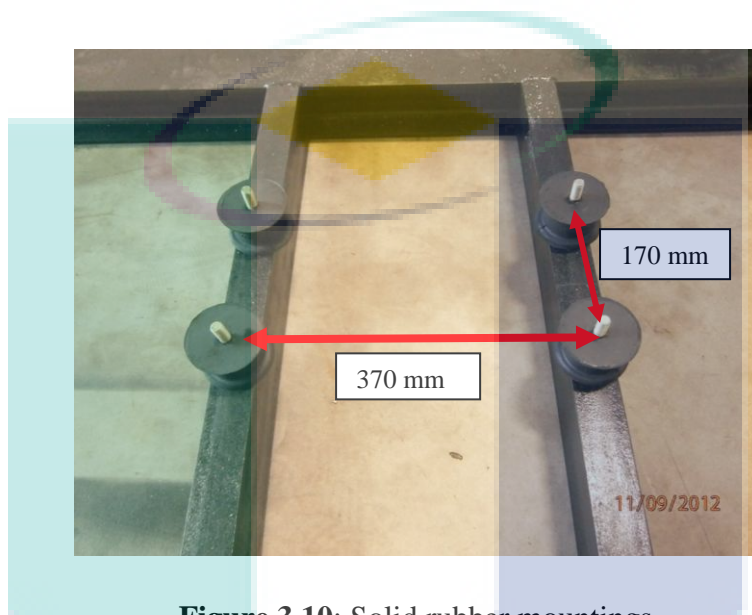
Figure 3.10: Solid rubber mountings

3.3.2 Dynamometer System
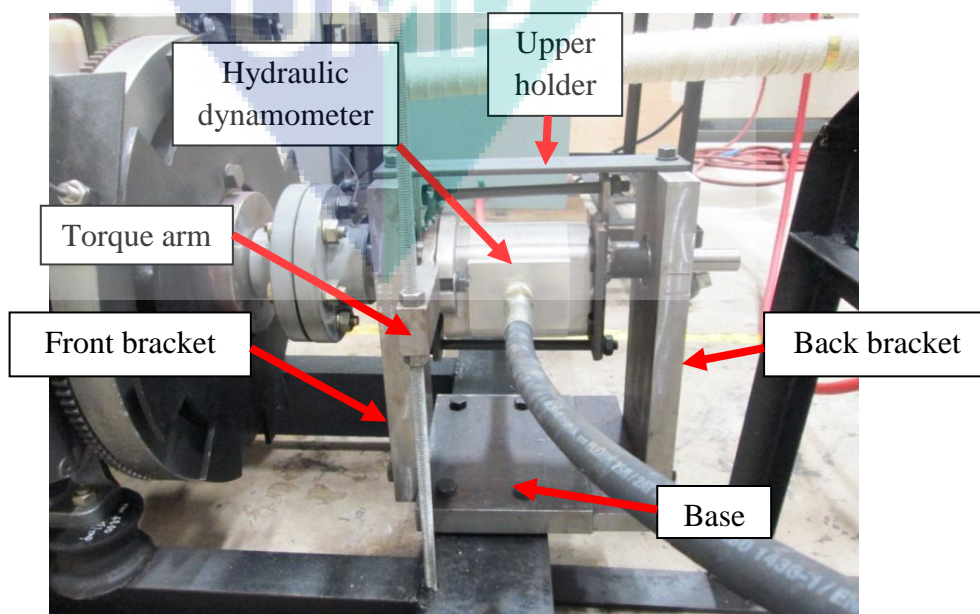
Figure 3.11: Hydraulic dynamometer bracket

Figure 3.11 shows the dynamometer bracket that has been fabricated with the hydraulic dynamometer mounted to it. It consists of front bracket, back bracket, base, upper holder and torque arm. The bracket is mounted to the engine stand using four pieces of M12 x 1.25 bolts.

A screw type valve as shown in Figure 3.12 is used to control the load exerted by the dynamometer to the engine. This type of valve is chosen for its durability to withstand high temperature and pressure without leakage around valve. Furthermore, screw type valve enables controllable load exerted to the engine compared to other type of valve.
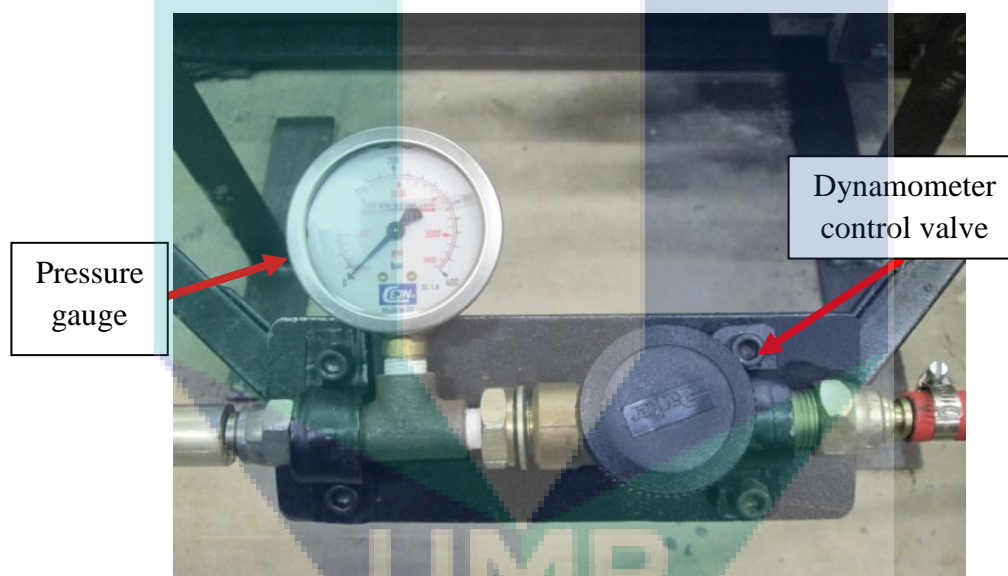
Figure 3.12: Dynamometer control unit

The load exerted to the engine is shown by a pressure gauge placed between the valve and gear pump. From the pressure reading, the amount of torque and power exerted by the dynamometer can be determined using Equation 3.1 and Equation 3.2.

The AWS 60 grade hydraulic oil is used as working fluid for this dynamometer system. The hydraulic oil is stored in a 90 litre storage capacities reservoir tank as shown in Figure 3.13. Large amount of hydraulic oil is used for this dynamometer system to prevent the hydraulic fluid become too hot in a short time during operations. High hydraulic oil temperature will damage the gear pump during operation. Equation 3.10 is used to measure the minimum size of the storage tank (McNamee et al., 2010).

$$\text{Tank capacity} = \text{pump capacity (L/min)} \times 2 \text{ or } 3 \qquad (3.10)$$

Figure 3.13: Hydraulic oil reservoir tank

In addition, a radiator with cooling fan is used to maintain the safe operating temperature of hydraulic oil when load is exerted to the engine. The hydraulic oil temperature will rise during engine operation due to the friction in the gear pump and friction inside the control valve. The radiator used is shown in Figure 3.14.
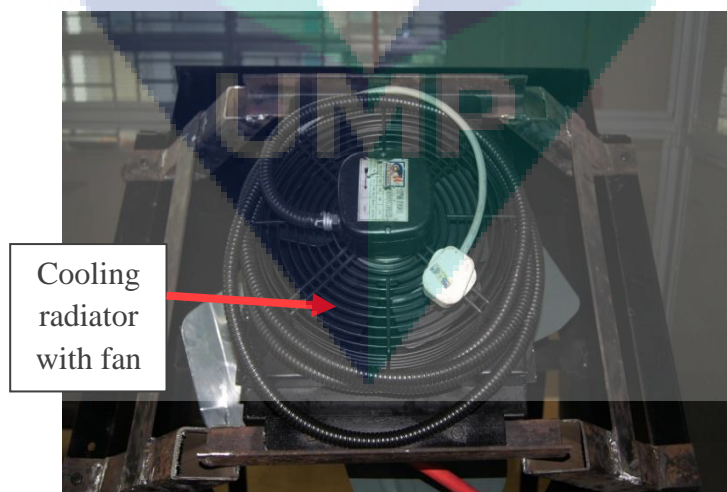
Figure 3.14: Hydraulic oil cooling radiator

A high pressure hose as shown in Figure 3.15 is connected between the control valve and gear pump. The hose is among the critical parts in the dynamometer system because during operation, this high pressure hose will withstand the pressure and high

temperature that occur when the load exerted by the dynamometer to the engine. The chosen hose is able to withstand until 33 MPa pressure.
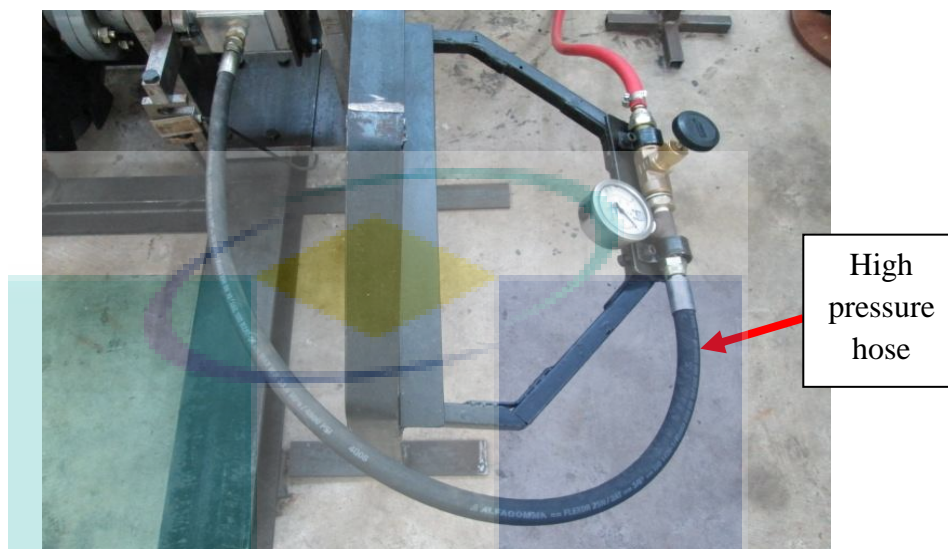
Figure 3.15: High pressure hose

A flexible flanged shaft coupling is used to connect the hydraulic dynamometer to the engine flywheel as shown in Figure 3.16. The coupling is chosen because it is able to absorb the vibrations that occur between the engine and the dynamometer. The vibration source can be the vibration from the engine or miss alignment between the engine flywheel and the dynamometer shaft.

The coupling is chosen based on engine maximum torque that is transmitted to the dynamometer. The coupling model is NBK type shaft coupling with six bolts. The coupling is made of cast iron according to Japanese Industrial Standard (JIS) 5501. The standard specifications for the coupling are shown in Appendix 5.

A custom pulley is designed and fabricated to connect between the engine flywheel and the flexible flanged shaft. The material used for custom pulley is hardened mild steed. The custom pulley is shown in Figure 3.17. The technical drawing of the pulley is shown in Appendix 6.
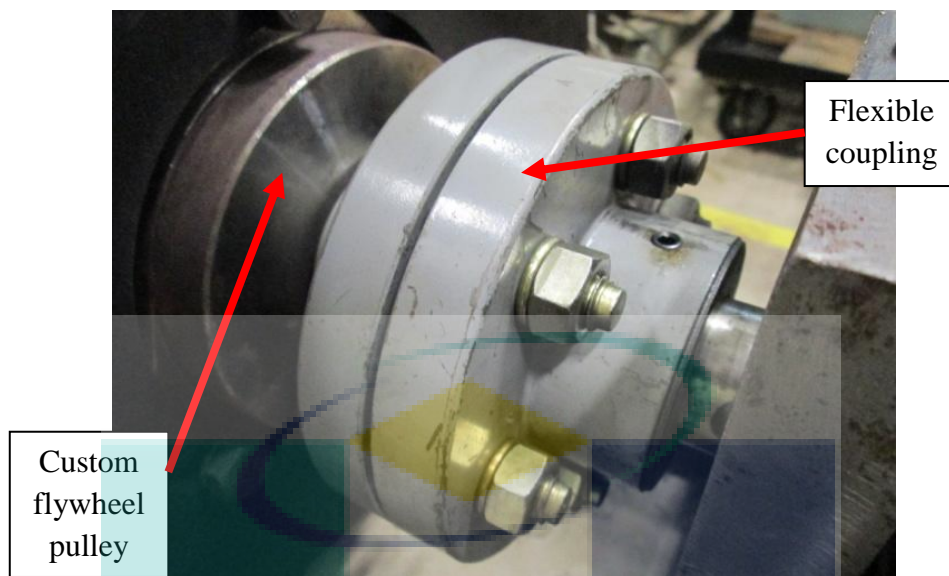
Figure 3.16: Flexible flanged shaft coupling

Figure 3.17: Custom flywheel pulley

A 'S' type load cell is mounted to lever arm that bolted to the dynamometer as shown in Figure 3.18. This load cell measures the brake torque that exerted by the engine to the dynamometer. From the measurement, the brake power also can be determined through calculations. The specifications of the load cell are shown in Appendix 7. The load cell is connected to the National Instruments (NI) data logger and then connected to the computer.
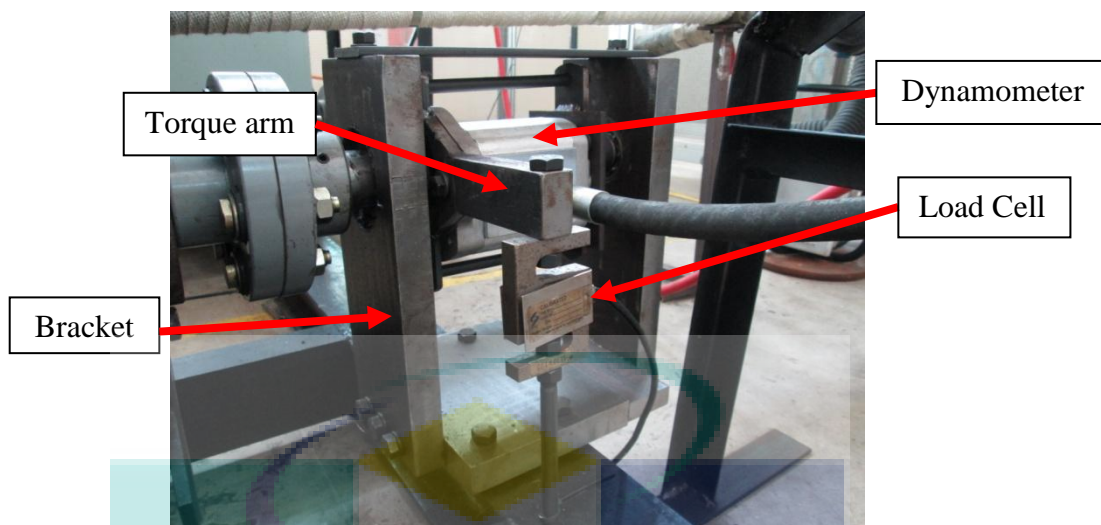
Figure 3.18: S type load cell

The load cell is calibrated using certain weight and graph of current versus weight is plotted. From the chart, the equation of the straight line is calculated and any amount of force that exerted to the load cell can be measured through the current yielded by the load cell. The calibration chart of the load cell is shown in Appendix 8.

3.3.3   External Fuel Tank

Figure 3.19 shows the external fuel tank to supply the tested fuel to the engine fuel pump. The tank is made from two beakers with 1 litre capacity each. The fuel is supplied into the fuel pump using transparent 3/4" hose from the beaker. The purpose of using the transparent fuel line is to ensure that the fuel flow can be easily observed during experiment.

The fuel tanks are placed one metre from the ground to enables the fuel flows into the fuel pump by gravitational force. The amount fuel flow can be controlled by a ball valve. For alternative fuel, a filter is placed to the fuel line to avoid particles in TDF from entering the fuel pump thus could damage the fuel pump.

Alternative fuel tank

Fuel filter

Valve

Diesel fuel tank
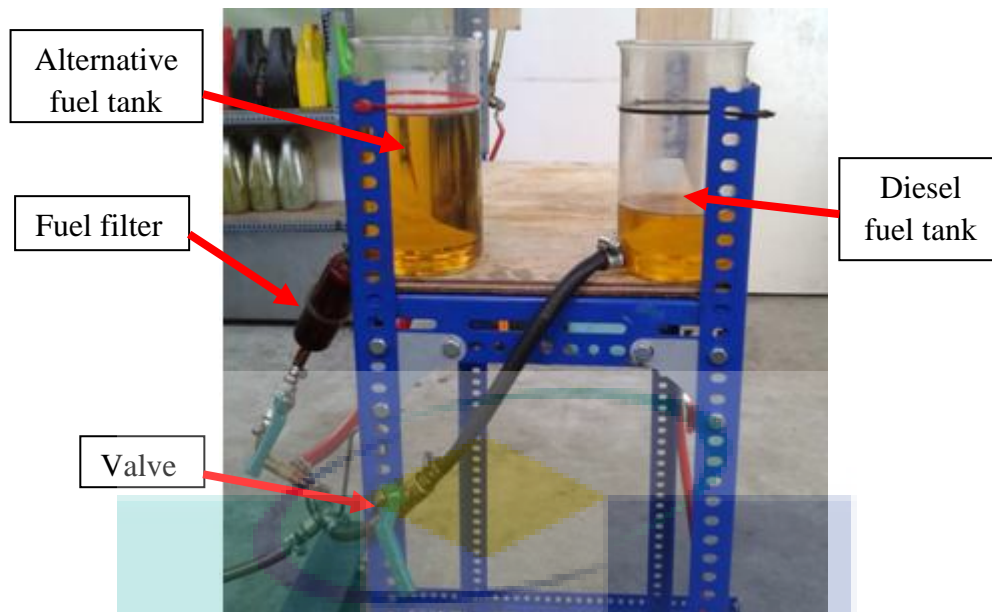
Figure 3.19: External fuel tank

3.3.4   Air Volume Measurement System

Figure 3.20 shows the fabricated air volume measurement system for the engine. It consists of cylinder container, an orifice, manometer, and 2.5 inch diameter hose that is connected the container to the intake manifold. Figure 3.21 shows the 23.1 mm diameter orifice that fabricated using wire cut CNC machine.

Container

Manometer

Figure 3.20: Air volume measurement system
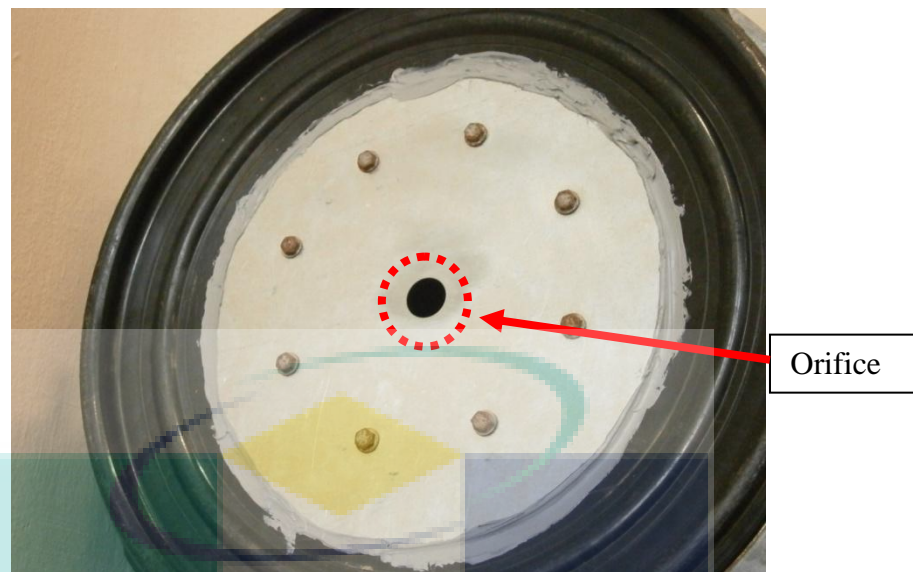
Figure 3.21: The 23.1 mm diameter orifice

Pressure drop across the orifice is measured using manometer from Dwyer Mark II model as shown in Figure 3.22. The specifications for the manometer are shown in Appendix 9.
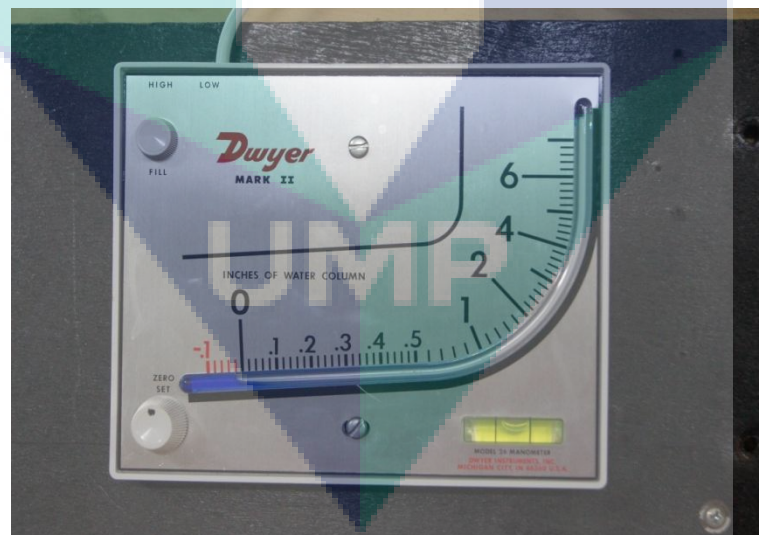
Figure 3.22: Manometer

3.3.5   Diesel Engine Modifications

Some modifications are done to the diesel engine for alternative fuel testing. Firstly, the original engine fuel tank that attached to the engine is removed. Since this engine will run with alternative fuel, the fuel will be channelled into the engine fuel

pump from external fuel tank. The picture of the engine with the fuel tank after removal is shown in Figure 3.23. Referring to Figure 3.24, the fuel from external fuel tank will enter the fuel pump through the upper pipe labelled as 'A'. Next, the fuel will be pumped out through the pipe labelled as 'B' to the fuel injector.

Figure 3.23: Diesel engine without original fuel tank
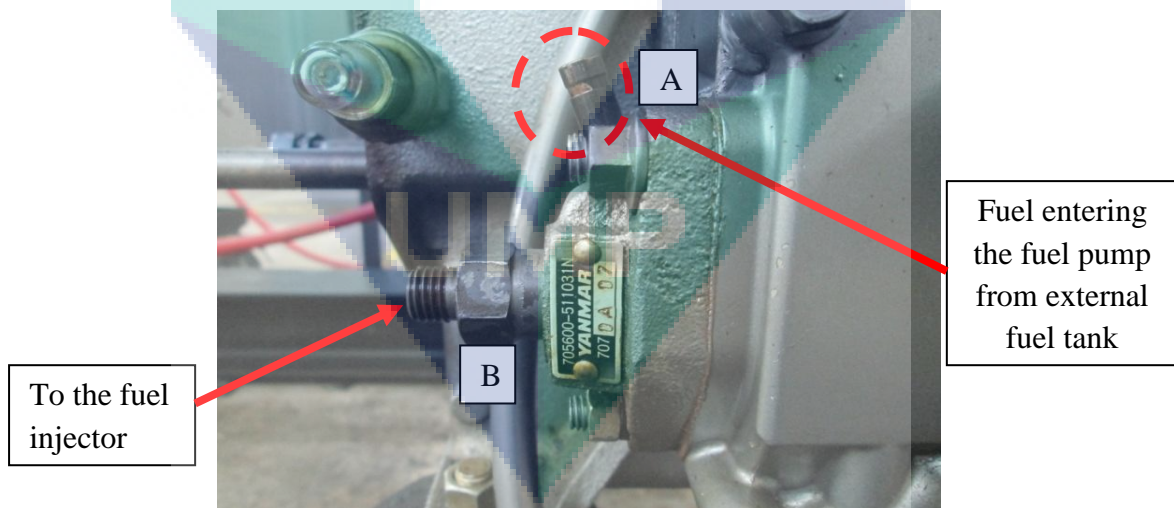
Figure 3.24: Engine fuel pump

The exhaust manifold is also modified for the experiment. The muffler is detached from the exhaust manifold. Then a pipe with 2" diameter is welded to the end of the detached manifold. Figure 3.25 shows the exhaust manifold that has been modified.
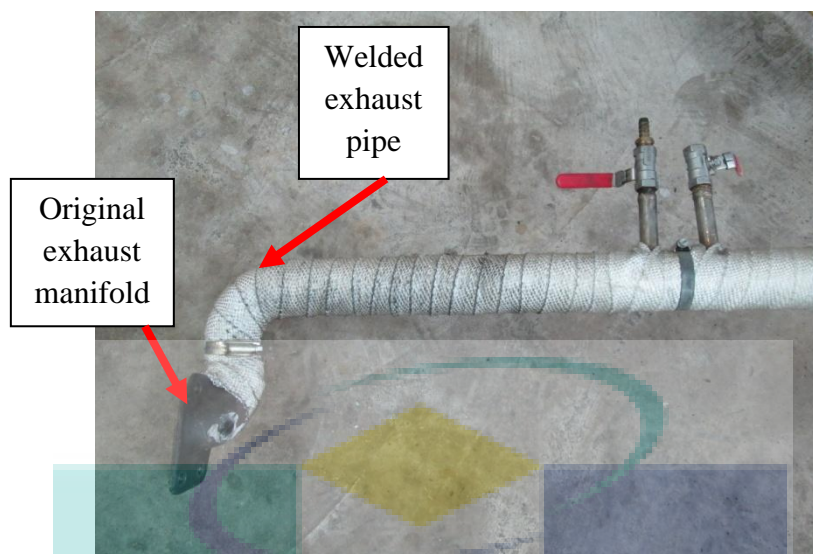
Figure 3.25: Modified exhaust manifold

3.3.6   Data Acquisition (DAQ) System Setup

Engine combustion characteristics are measured using data acquisition (DAQ) system supplied by TFX Engineering, USA. It consists of cylinder pressure sensor, magnetic type crank angle sensor, sensor interface, transfer cable and LCS data logger. All the hardware is shown in Figure 3.26.

Engine combustion characteristics are determined using cylinder pressure sensor as shown in Figure 3.28. To mount the cylinder pressure sensor, the engine head is modified by drilling a hole from the top of the engine head to the combustion chamber. A M8 x 1.25 size thread is made through the hole. The sensor is mounted using a custom adapter to the engine head. Figure 3.27 shows the modification diagram that has been done to the engine head. Figure 3.29 shows the position of the sensor on the top of the engine head while Figure 3.31 shows the hole that links between the combustion chamber and the pressure sensor in the combustion chamber.

The custom adapter is made from stud bolt with M8 x 1.25 size. A hole with 2 mm diameter is drilled through the stud bolt using SuperDrill CNC machine. Then a thread with size M5 x 0.5 is made at the top of the bolt. Figure 3.30 shows the cross sectional diagram of the custom adapter to mount the cylinder pressure sensor to the engine head.

Figure 3.26: DAQ system
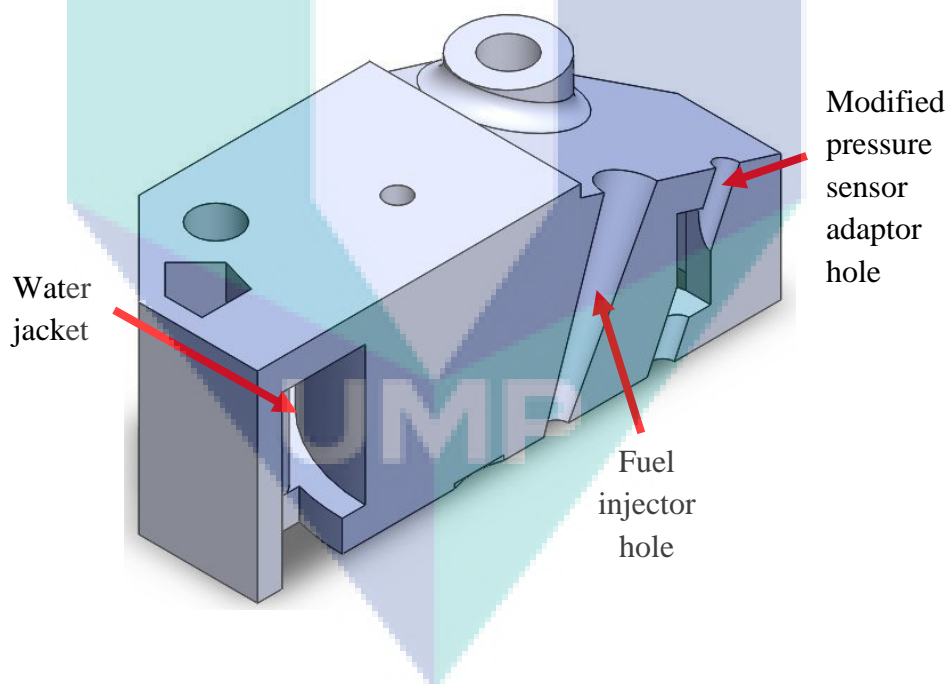
Figure 3.27: Modification diagram of engine head (cross sectional diagram)
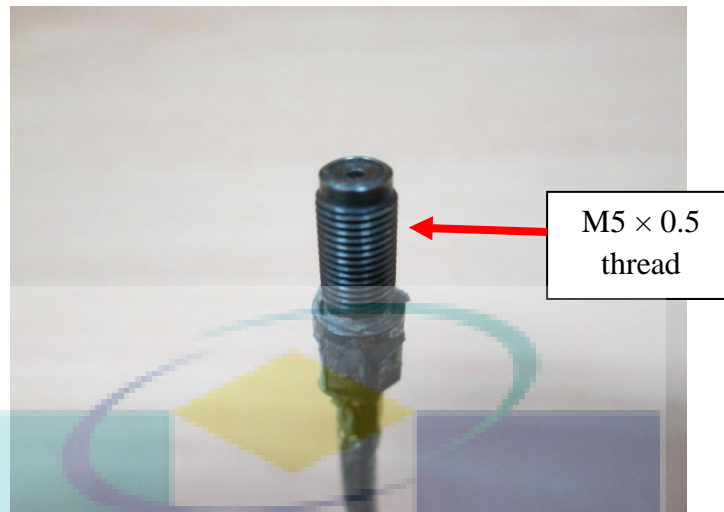
Figure 3.28: Cylinder pressure sensor

Figure 3.29: Cylinder pressure sensor at the top of engine head
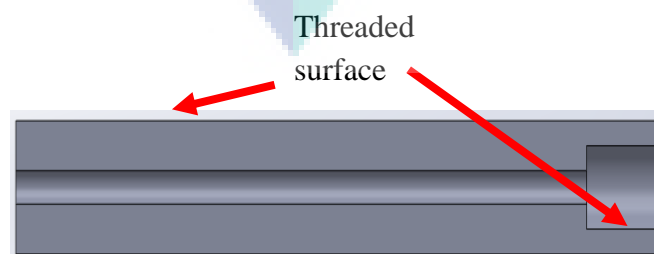
Figure 3.30: Custom cylinder pressure sensor adaptor (cross sectional diagram)
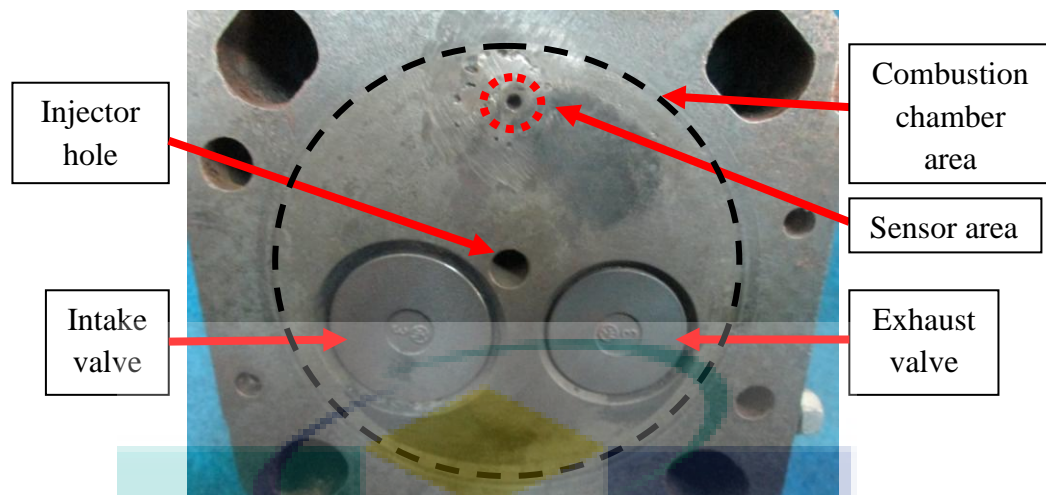
Figure 3.31: Sensor area in the combustion chamber

A magnetic type crank angle sensor as shown in Figure 3.32 is mounted to the engine to measure the crank angle for every crank rotation. A custom bracket is fabricated using angle iron which has 2 mm thickness to hold the sensor parallel to the trigger wheel as shown in Figure 3.33. The clearance between the crank sensor tip and trigger wheel is calibrated to be not more than 3 mm. If the distance is more than 3 mm, the crank angle cannot be measured accurately by the sensor. On the other hand, if the distance is too narrow, the trigger wheel will have possibility to hit the crank sensor due to vibration during operation and damage the crank sensor.

Figure 3.32: Magnetic type crank angle sensor
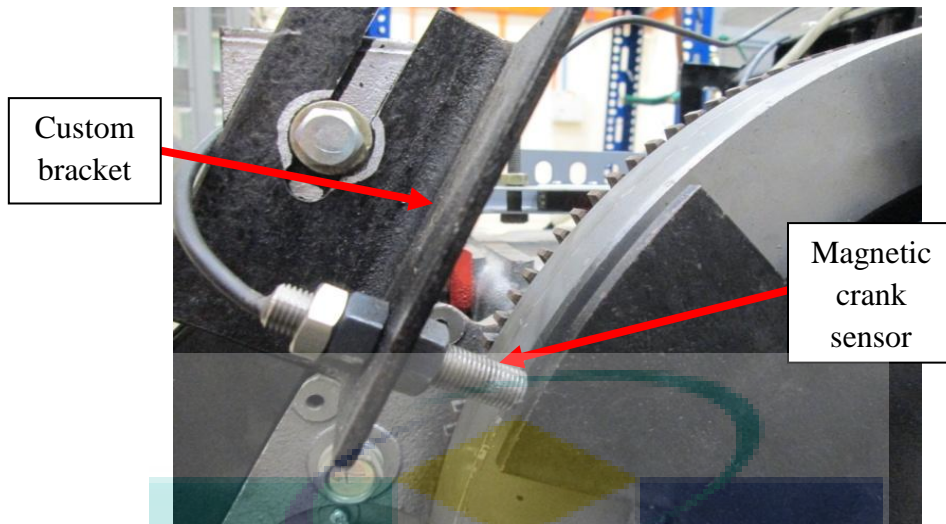
Figure 3.33: Crank angle sensor position

A trigger wheel is required to enable the magnetic crank sensor measure the angle of every crankshaft rotation. For the purpose, an eight teeth trigger wheel as shown in Figure 3.34 is designed and fabricated using 5 mm steel plate. The trigger wheel is bolted to the engine flywheel as shown in Figure 3.35 using M12 × 1.25 bolts. The technical drawing of the trigger wheel is shown in Appendix 10.

Figure 3.34: Trigger wheel
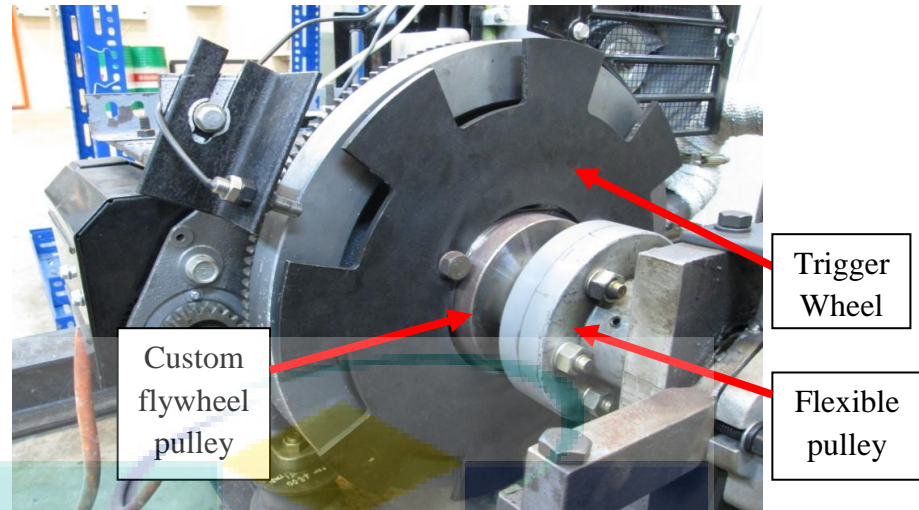
Figure 3.35: Trigger wheel at the engine flywheel.

The in-cylinder sensor and crank angle sensor is connected to the sensor interface and LCS data logger. The obtained data are then shown at the computer that connected with the LCS data logger. The assembled DAQ system is shown in Figure 3.36.

Figure 3.36: DAQ system assembly

For engine speed sensor, a photoelectric sensor is used. A bracket is fabricated using angle iron to mount the speed sensor as shown in Figure 3.37. The sensor measures the engine speed through the flywheel rotation. The speed sensor reading is

displayed through digital tachometer that directly connected to the sensor as shown in Figure 3.38.
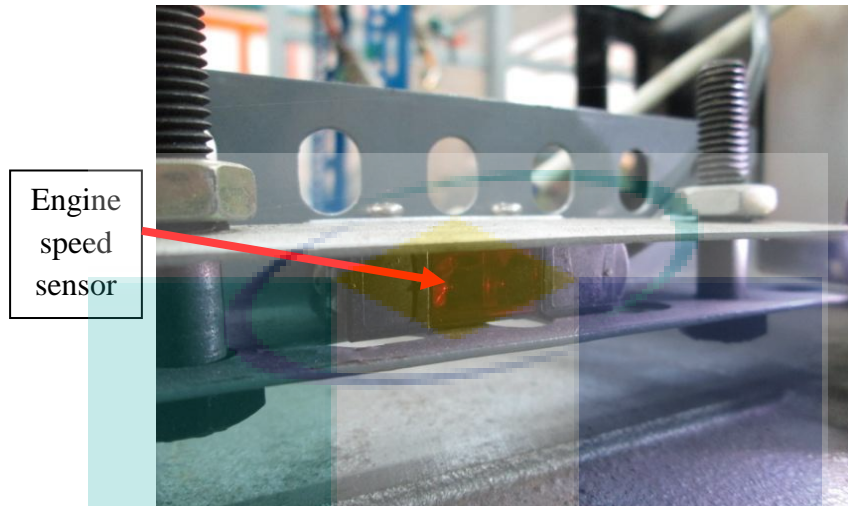
Figure 3.37: Engine speed sensor
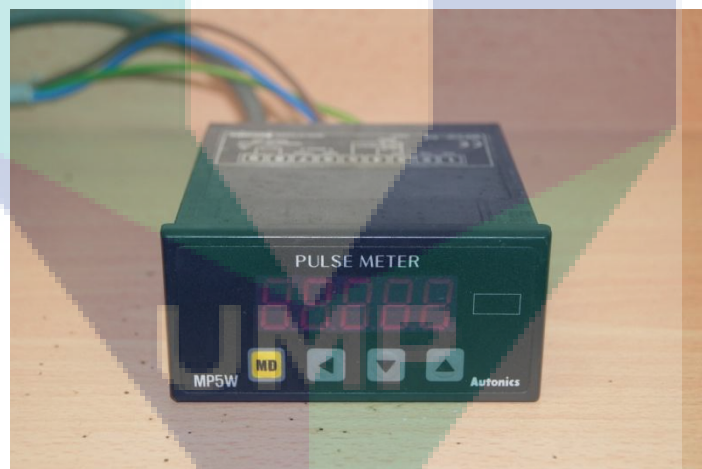
Figure 3.38: Digital tachometer

3.3.7 Thermocouples

For temperature measurement, the engine is fitted with three units of K-type thermocouples to measure intake temperature, exhaust temperature and ambient temperature. The locations of these thermocouples are strategically placed to ensure the accuracy of the measurements. Figure 3.39 shows the modification that made to the intake manifold. A hole is drilled to the intake manifold to fit the thermocouple. The thermocouple that is fitted to the intake manifold is labelled as T_1

Figure 3.39: Modified intake manifold

A hole is also drilled to the exhaust manifold to measure the exhaust gas temperature. Figure 3.40 shows the hole that was drilled into the exhaust manifold to mount the thermocouple. The thermocouple that is used to measure the exhaust gas manifold is labelled as T_2.

Figure 3.40: Drilled exhaust manifold

The thermocouple that is used to measure the ambient temperature is placed near the air volume measurement system as shown in Figure 3.41. The thermocouple is labelled as T_3. All thermocouple is connected to the multipoint temperature indicator as shown in Figure 3.42. This multipoint temperature indicator can display until six different temperatures.

Figure 3.41: Thermocouple placement for ambient temperature measuring
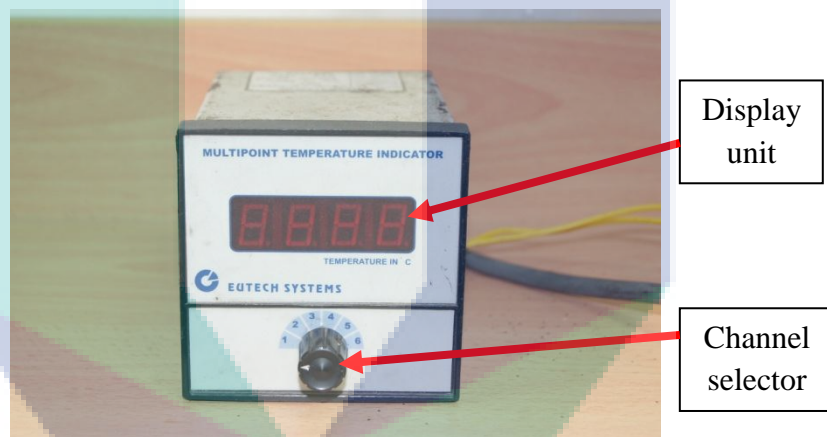
Figure 3.42: Multipoint temperature indicator

3.4   Exhaust Gas Measurement

After the combustion occurs in the combustion chamber, the fuel-air mixture is converted to the exhaust gas as a product after combustion. The content of exhaust gas emissions from the combustion will be measured and analyzed as a part of engine performance parameters. In this experiment, the parameters that have been analyzed are exhaust gas content and exhaust gas temperature.

For exhaust gas content measurements, KANE portable gas analyzer from model AUTO5-3 is used for the purpose. The exhaust gas is collected through the connecting pipeline that is connected to the valve at the exhaust manifold and

channelled to the exhaust gas analyzer. The KANE exhaust gas analyzer is shown in Figure 3.43. The specifications of the gas analyzer are shown in Appendix 11.

Figure 3.43: KANE exhaust gas analyzer

Engine performance testing is conducted at engine performance laboratory located at Universiti Malaysia Pahang. Figure 3.44 and Figure 3.45 shows the testing facilities that have been assembled. It consist of modified YANMAR TF120M single cylinder diesel engine, a hydraulic dynamometer system, external fuel tank, a calibrated airbox with Dwyer Mark II manometer for air intake measurement, TFX Engineering data acquisition (DAQ) system and KANE emission measurement system.
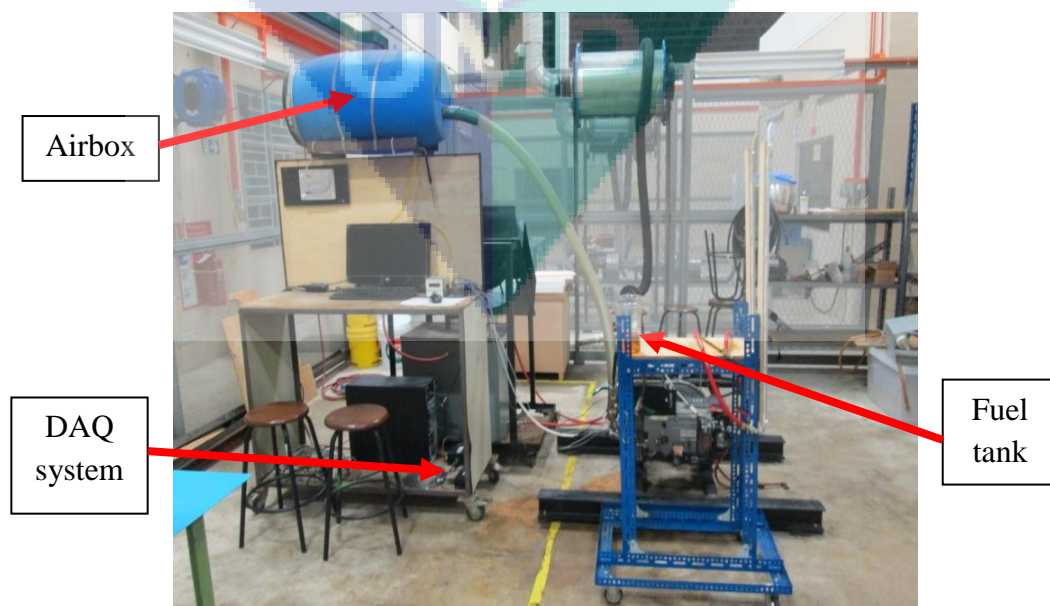
Figure 3.44: Completed engine test rig (front view)
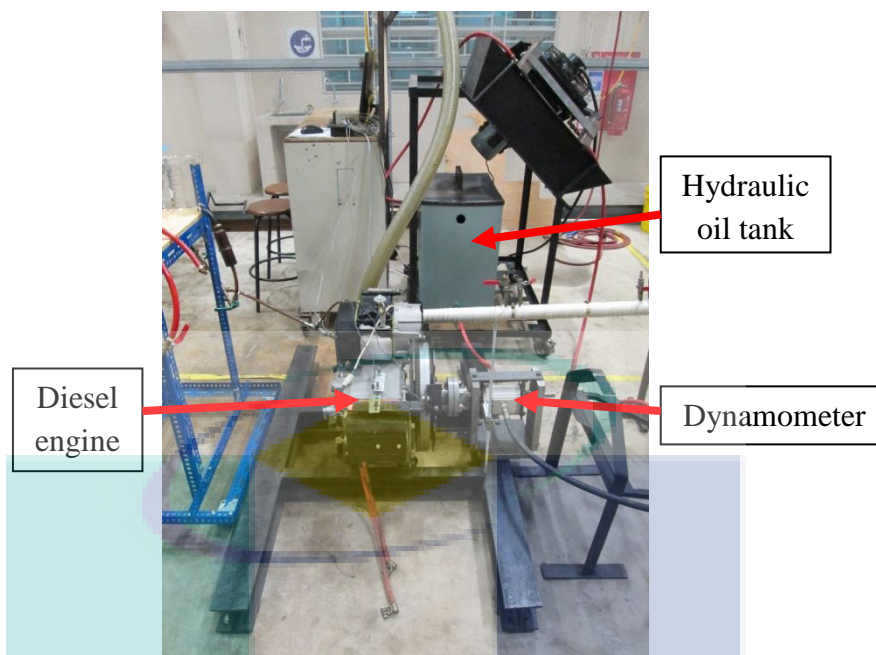
Figure 3.45: Completed test rig (side view)

3.5   Test Fuels and Sample Preparation

In this project, there are three base fuels which have been used during the engine testing. The first fuel is commercial diesel which has been used widely in Malaysia. The diesel used for this project is Dynamic Diesel supplied by Petroliam Nasional Berhad (PETRONAS) which the properties of the fuel were shown in Appendix 12.

The second and third test fuel is TDF and PDF. The TDF is supplied by Kajang Tire Recycle Oil Sdn Bhd and PDF is supplied by Syngas Sdn. Bhd. This fuel is produced from scrap tires and waste plastics through pyrolysis process as reviewed in Chapter 2.

Fuel samples are prepared through mechanical mixing process. A mechanical mixer as shown in Figure 3.46 is used to stir the blended fuel. The diesel fuel is blended with TDF at several blend ratios. The fuel blend is stirred for minimum 15 minutes. Three fuel blends are prepared which are 10% TDF blend ratio, 30% TDF blend ratio and 50% TDF blend ratio. There are total of six tested fuels in this experiment which is diesel fuel, pure TDF, 10% TDF blend, 30% TDF blend, 50% TDF blend and pure PDF.

Figure 3.46: Mechanical mixer

Based on the conclusion by Doğan et al. (2012), it is stated that diesel engine is unable to run with unblended TDF. Therefore, TDF is blended with diesel fuel to improve the properties of TDF thus make TDF can be used in diesel engine (Aydın and İlkılıç, 2012). Thus, the TDF in this testing are blended with diesel fuel at several blend ratios.

Blend ratio of 10%, 30% and 50% between TDF and diesel fuel are chosen. This is to observe the trends of performance output when the TDF ratio in diesel fuel is increased. All the comparisons of TDF, TDF10%, TDF30% and TDF50% are made based on performance of diesel fuel as base data. This is because for an alternative fuel, it should be able to give same or better performance output when used in the engine. If the alternative fuel gives lower performance output compared to diesel fuel, initiative can be taken to increase the performance output either by modifying the engine system, refining the fuel properties or adding a combustion catalyst. For PDF, comparisons are made between pure PDF, pure TDF and diesel fuel because both PDF and TDF are originated from waste. This is to compare the potential between the two types of waste source fuels to be used as alternative fuel.

During the experimental study, TDF-diesel fuel blends are labelled as TDFXX%, where XX signifies the volumetric blending percentage of TDF in the diesel fuel. As for example, TDF10% represents the volumetric blend of 10% TDF with 90%

diesel. All the blended fuels are stored in lab environment, under room temperature and pressure.

3.6   Fuel Properties Testing

All prepared sample is undergone properties testing. The properties that are determined include fuel, density, kinematic viscosity, flash point and gross calorific value. The fuel properties are determined since it affects the engine performance as the fuel is tested in diesel engine. Fuel properties testing enable more understanding about the relations between the fuel properties and performance output.

3.6.1   Fuel Density

The density of the fuel is determined through the density meter as shown in Figure 3.47. The sample is prepared and inserted into the sampling tube. Next, the prepared sample is inserted in the density meter and the density meter measurement is started. The density value is being displayed on the density meter display unit.

Figure 3.47: Density meter

3.6.2 Kinematic Viscosity
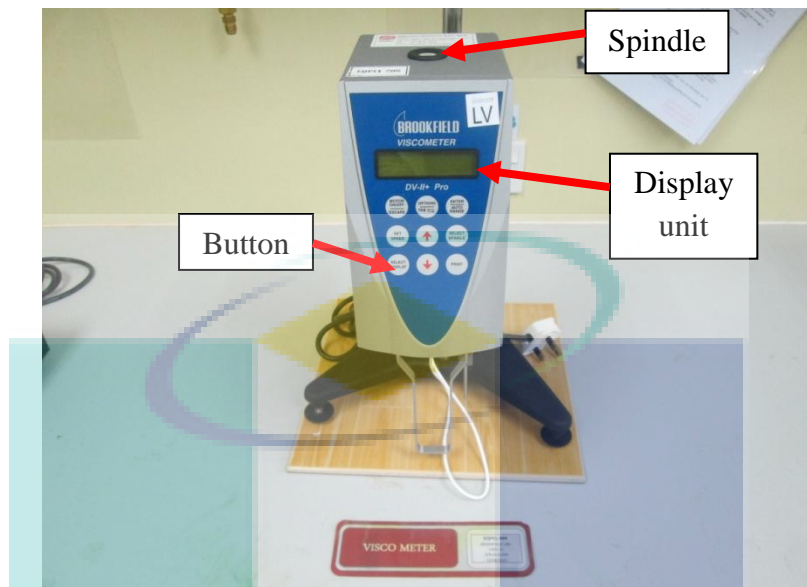
Figure 3.48: Viscometer

Kinematic viscosity of all tested fuels is determined using viscometer. Figure 3.48 shows the viscometer that is used for measuring the fuel kinematic viscosity. The step taken to operate this apparatus is as follows: first, the viscometer is set to Autozero mode. To set the viscometer to Autozero mode, the spindle is moved and any key is pressed to begin its Autozero.

Second, a spindle is choosen and screwed into the long shaft and then enter button is pressed. The speed of the spindle was set at 20 rpm. The kinematic viscosity value is being displayed at the display unit.

3.6.3 Flash Point

Figure 3.49: Flash point tester

Figure 3.49 shows the flash point tester that was used to determine the flash point of the fuels. To operate the tester, small amount of fuel ranged from 2 mL to 4 mL is injected into the sample cup. Then the measuring process is started. The flash point value is being shown at the tester display unit.

3.6.4 Gross Calorific Value

The gross calorific value of all samples is determined using bomb calorimeter. Bomb calorimeter consists of bomb, sample pan, fuse wire and jacket. Figure 3.51 shows the overall bomb calorimeter that was used.

For the gross calorific value testing, approximately 1 gram of test fuel is placed in the sample pan. The sample pan is placed on the coil. Next, 10 cm of nickel fuse is attached to the coil as shown in Figure 3.50. This nickel fuse is electrically heated to act as a source of ignition to the fuel. Then, the coil is placed inside the bomb. The bomb is filled with oxygen at 30 atm pressure.

The bomb is immersed in steel water bucket that was filled with distilled water at the standard temperature. Two litre of distilled water is poured into the steel bucket. Then, the measuring process is started. The result is printed when the process is finished.
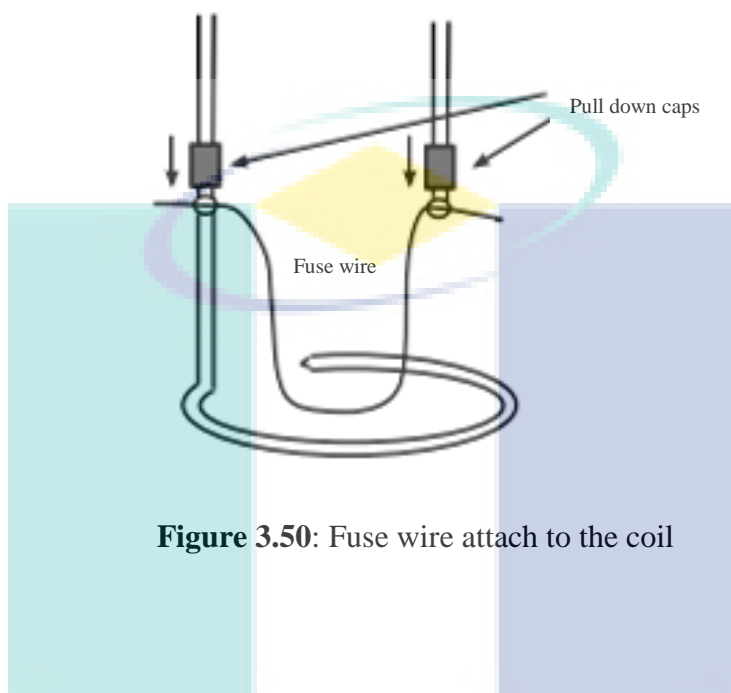
Figure 3.50: Fuse wire attach to the coil
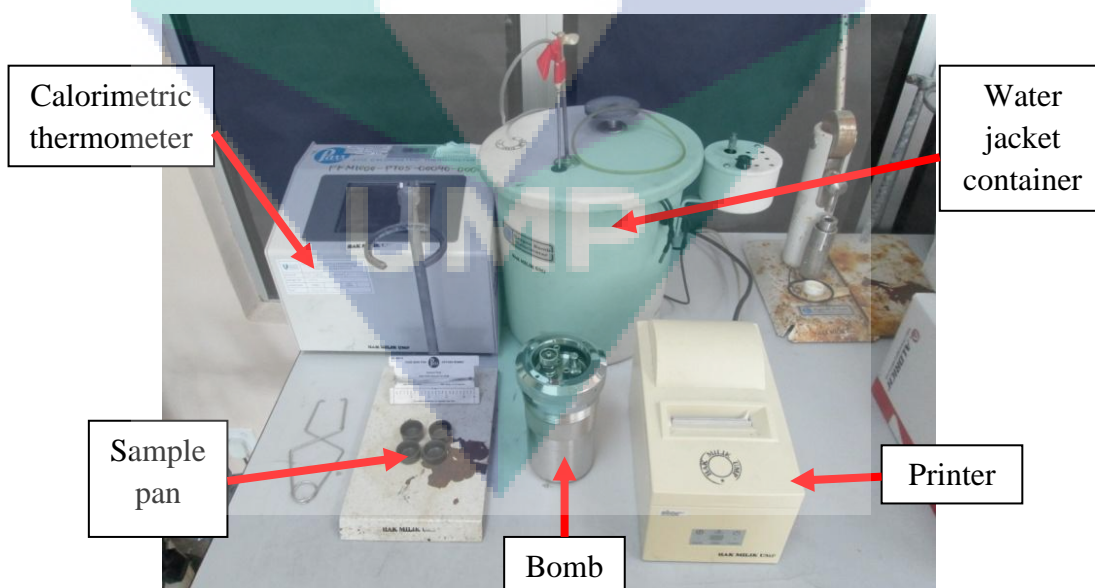
Figure 3.51: Bomb calorimeter

3.7   Engine Test Operating Conditions and Procedure

This experiment is conducted according to SAE J1349- Standard Engine Power Test Code as a reference. The operating environment is in the lab environment. Before the experiment is conducted, the engine is let idle for at least 15 minutes. This is to ensure that the engine had reached the optimum operating temperature before the experiment begins.

The test engine speeds are ranged from 1200 rpm until 2400 rpm. This range is chosen based on the standard performance curve of the engine as shown in Appendix 14. Five engine speeds are chosen which started from 1200 rpm, followed by 1500 rpm, 1800 rpm, 2100 rpm and 2400 rpm. For combustion characteristics analysis, the analysis will focused on three conditions which is low, moderate and high speed region. Low engine speed region indicates the engine performance output at minimum engine speed while high engine speed region indicates the engine performance at maximum engine power. Moderate engine speed region indicates the performance between low and high engine speed, where it can be assumed as medium operating condition of the engine. Therefore, 1200 rpm is chosen for the analysis at low engine speed region while 1800 rpm is chosen for medium speed region as the maximum torque occurs during this engine speed. High engine speed region of 2400 rpm is chosen for high engine speed region because the maximum power occurs at this engine speed.

The test cycles are manually controlled using engine speed as variable parameters. The test operating conditions that were manipulated during operations are variable engine speed with constant 20Nm load exerted to the engine. For the beginning, the engine is operated with test fuel at 1200 rpm engine speed without any load exerted to the engine. After the engine speed is stabilized, the load is exerted to the engine by closing the control valve slowly. Performance data is taken after the speed remained stable for at least one minute ((SAE), 2011). The procedure is repeated for another engine speed which is 1500 rpm, 1800 rpm, 2100 rpm and 2400 rpm.

In this experiment, diesel fuel is first used for performance data measurement. The obtained data will be the base data for comparison. This is followed by TDF10%, TDF30%, TDF50%, pure TDF and pure PDF.

3.8   Pre-testing

Pre-testing is conducted to ensure the completed test rig setup is functioned well. For pre-testing, diesel fuel is used as test fuel. From the pre-testing, the interface as shown in Figure 3.52 is obtained. The figure shows the combustion pressure, compression pressure and also combustion temperature. The list at the right side of the interface shows the parameters such as the engine speed, indicated power, torque, IMEP, maximum combustion pressure and others.
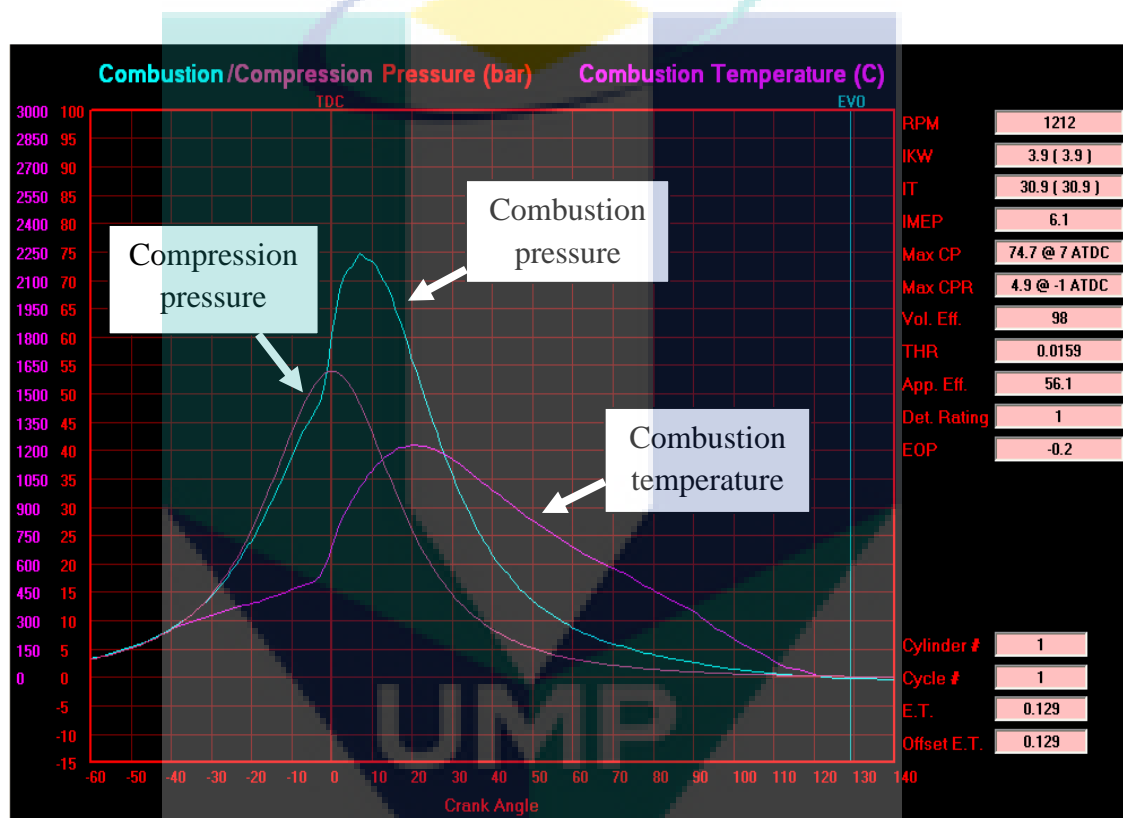
Figure 3.52: Software interface sample

3.9   Summary

In this chapter, all the information regarding the methodology involved for this experiment is discussed. The methodology that discussed in this chapter is based on the scopes that need to be covered in this thesis. The methodology covered includes the test rig design and fabrication, design of experiment, sample preparation, properties testing and also pre-testing.

CHAPTER 4

RESULTS AND DISCUSSIONS

4.1   Introduction

This chapter presents the data on chemical properties of TDF and its blends. The properties include fuel density, kinematic viscosity, gross calorific value and flash point. The properties difference between diesel fuel and TDF is discussed. The trend when the TDF blend ratio is increased is also discussed. The properties of the fuels are related to the performance output as the fuels undergo engine testing. Next, the performance data such as power, torque, ignition delay and peak pressure of TDF and its blends when used in diesel engine is presented and discussed. The performance difference between each fuel is analyzed. Then, the exhaust gas emissions of TDF and its blends when used in diesel engine also discussed.

The next part of this chapter will be discussed on the chemical properties and the performance of PDF when used as fuel. Hereby, the PDF data will be discussed and compared between diesel fuel and TDF. The fuel properties that are presented in this chapter are fuel density, kinematic viscosity, flash point, and sulphur content. After that, the performance of PDF used in diesel engine is presented and discussed. The parameters determined are engine torque, power, ignition delay and combustion pressure. Finally, the exhaust gas emissions of PDF is also presented and compared with diesel fuel and PDF.

4.2   TDF Fuel Blends Properties

Table 4.1 shows the properties of the test fuels. There are four properties were determined which are density, kinematic viscosity, flash point and gross calorific value. All the properties are discussed in the next subsection.

Table 4.1: Properties of test fuels

		Diesel	TDF 10%	TDF 30%	TDF 50%	TDF
Density	kg/m^3	841.6	865.2	877	881	923
Kinematic Viscosity @ 40°C	mm^2/s	4	4.1	3.8	3.81	5.1
Flash Point	°C	84	140	113	99	44
Gross Calorific Value	MJ/kg	42.5	45.2	43.4	42.9	38

4.2.1   Fuel Density

Figure 4.1 shows the density of TDF and its blends. From the figure, it can be observed that the density of TDF is higher compared to diesel fuel by 9.8%. The density of TDF10% is higher compared to diesel fuel by 2.8% while TDF30% is higher by 4.2%. In addition the density of TDF50% is higher compared to diesel fuel by 4.6%. Referring to the graph, it can be seen that the density of TDF-diesel fuel blends increases as the TDF ratio in diesel fuel increase.

Higher fuel density enables a higher mass of fuel to be injected into the combustion chamber at a same injection volume, injection pressure and injection timing. Thus, high fuel density may result to higher engine performance output. However, higher fuel density may require some modifications to the fuel pump for some cases to enables the fuel to be used in the diesel engine. This is because more work may require by the fuel pump since higher fuel density cause greater fuel resistance through the fuel line and fuel injectors. For this experiment, the engine runs well without any modifications to the engine fuel pump system.
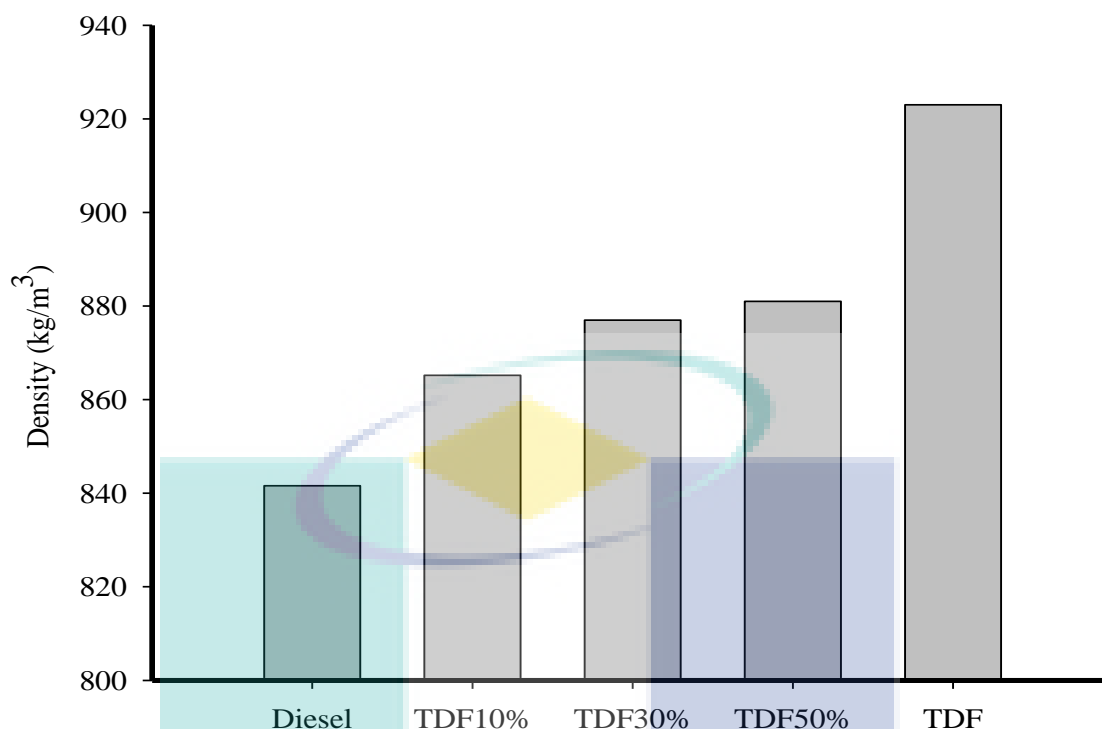
Figure 4.1: Density of test fuels

4.2.2 Kinematic Viscosity

Figure 4.2 shows the variations of kinematic viscosity for test fuel. Referring to the graph, the viscosity of TDF is higher compared to diesel fuel by 27.5%. After TDF is blended with the diesel fuel, the kinematic viscosity of TDF-diesel fuel blends at 30% and 50% are slightly lower compared to diesel fuel by 4.75% difference for both fuel. The kinematic viscosity for TDF10% is slightly higher compared to diesel fuel by 2.5%. From the figure, it can be concluded that blending the TDF with the diesel fuel could lower the kinematic viscosity of TDF. The kinematic viscosity of TDF-diesel fuel blends shows comparable value compared to diesel fuel.

High kinematic viscosity of TDF can cause poor fuel atomization, incomplete combustion and formation of the engine deposits. Thus, blending the TDF with diesel fuel improves kinematic viscosity of TDF thus improves the performance when it is used as fuel. The trend is shown in the Figure 4.2 where the kinematic viscosity of TDF10%, TDF30% and TDF50% is lower compared to TDF.
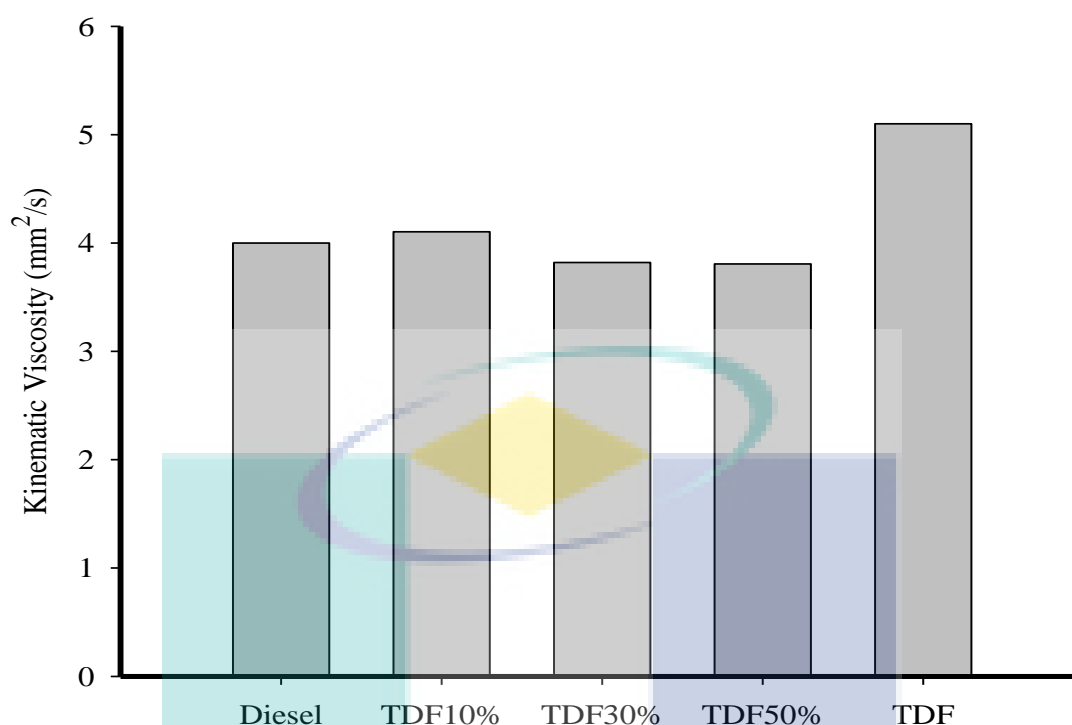
Figure 4.2: Kinematic viscosity of test fuels

4.2.3 Flash Point

Figure 4.3 shows the variations of flash point for all the fuels. From the figure, it is observed that the flash point of TDF is lower compared to diesel by 47.6%. Meanwhile, for TDF-diesel fuel blends, all blended fuels have higher flash point compared to TDF and diesel fuel. TDF10% has higher flash point compared to diesel fuel by 66.6% while TDF30% has higher flash point by 34.5%. TDF50% has higher flash point by 17.9%. From the figure, it can be seen that blending the TDF and diesel fuel will produce TDF-diesel blends that have higher flash point compared to TDF and diesel fuel. Furthermore, it also can be seen from the figure that the flash point decreases when the ratio of TDF in the diesel fuel is increased.

Higher flash point does not give any effect to the combustion directly. It involved in handling, transportation and storage where higher flash point make the handling process much safer. Thus, from the figure, the TDF-diesel fuel blends is safer to handled since it has higher flash point compared to TDF and diesel fuel.
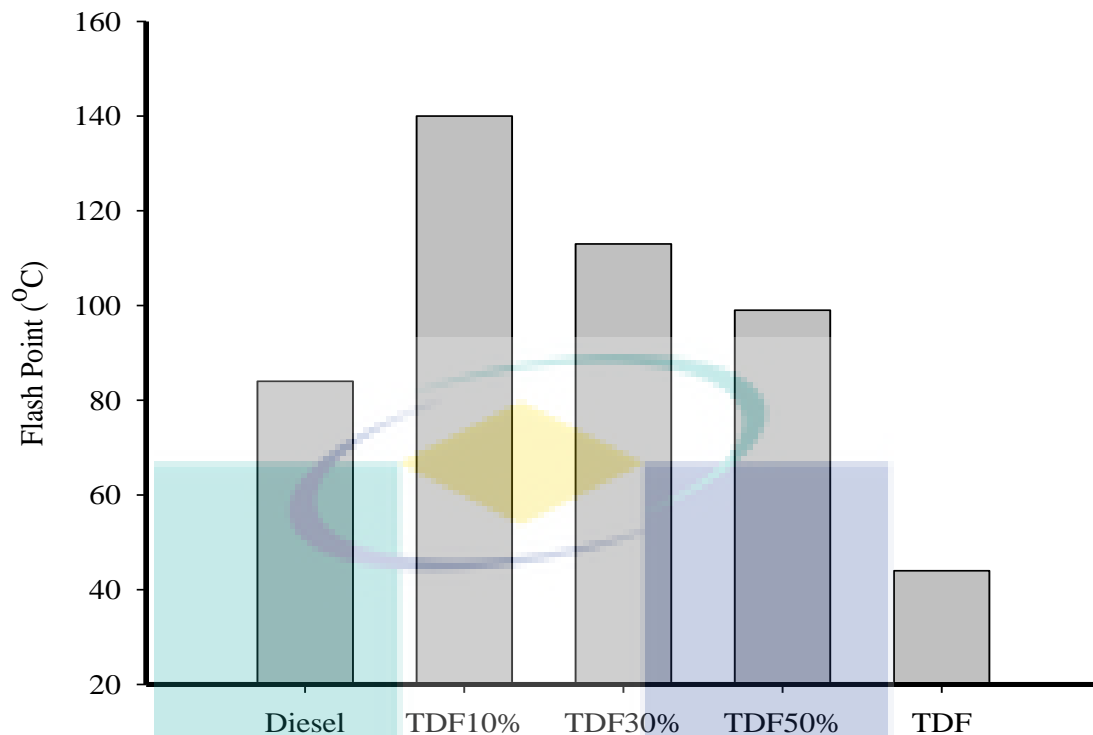
Figure 4.3: Flash point of test fuels

4.2.4   Gross Calorific Value

Figure 4.4 shows the gross calorific value of all test fuels. From the figure, it can be observed that the gross calorific value of TDF is lower compared to diesel fuel by 12%. When the TDF and diesel are blended, the gross calorific values of all TDF-diesel fuel blends are higher compared to TDF and diesel fuel. TDF10% has the highest gross calorific value by 6.4% compared to diesel fuel followed by TDF30% at 2.1% and TDF50% at 0.9% higher compared to diesel fuel. From the figure, it can be observed that when the TDF is blended with the diesel fuel, the gross calorific value is higher compared to diesel fuel and TDF. In addition, similar trend with the flash point, when the ratio of TDF that blended with diesel fuel is increased, the gross calorific value is decreased.

Lower gross calorific value cause more amount of fuel needed to produce same amount of energy. This will cause higher specific fuel consumption of the fuel. For the fixed amount of fuel that injected into the combustion chamber, the fuel that has lower gross calorific value will produce lower performance output.
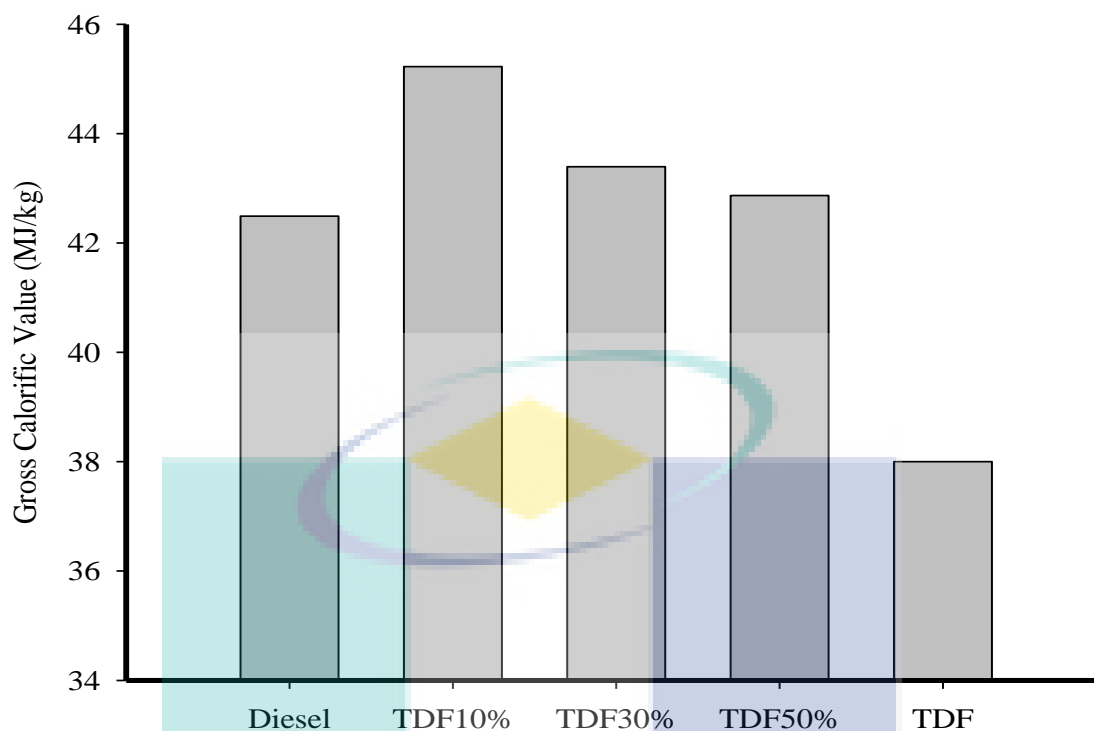
Figure 4.4: Gross calorific value of test fuels

4.3   PDF Fuel Properties

Table 4.2 shows the comparison of fuel properties between diesel fuel, TDF and PDF. The properties that are listed are fuel density, kinematic viscosity, flash point, gross calorific value and sulphur content. TDF fuel properties also included to be compared with PDF since both fuel are sourced from waste. Furthermore, both fuels are obtained from pyrolysis process.

All the properties are discussed in the next subchapter. The properties of the PDF are discussed and compared to diesel fuel and TDF to determine the potential of PDF as alternative fuel.

Table 4.2: Fuel properties of diesel, TDF and PDF

		Diesel	TDF	PDF
Fuel density	kg/m^3	841.6	923	771
Kinematic viscosity	mm^2/s	4	5.1	2.1
Flash point	°C	84	44	72
Gross calorific value	MJ/kg	42.5	38	34.7
Sulphur content	%	0.042	0.811	0.019

4.3.1 Fuel Density
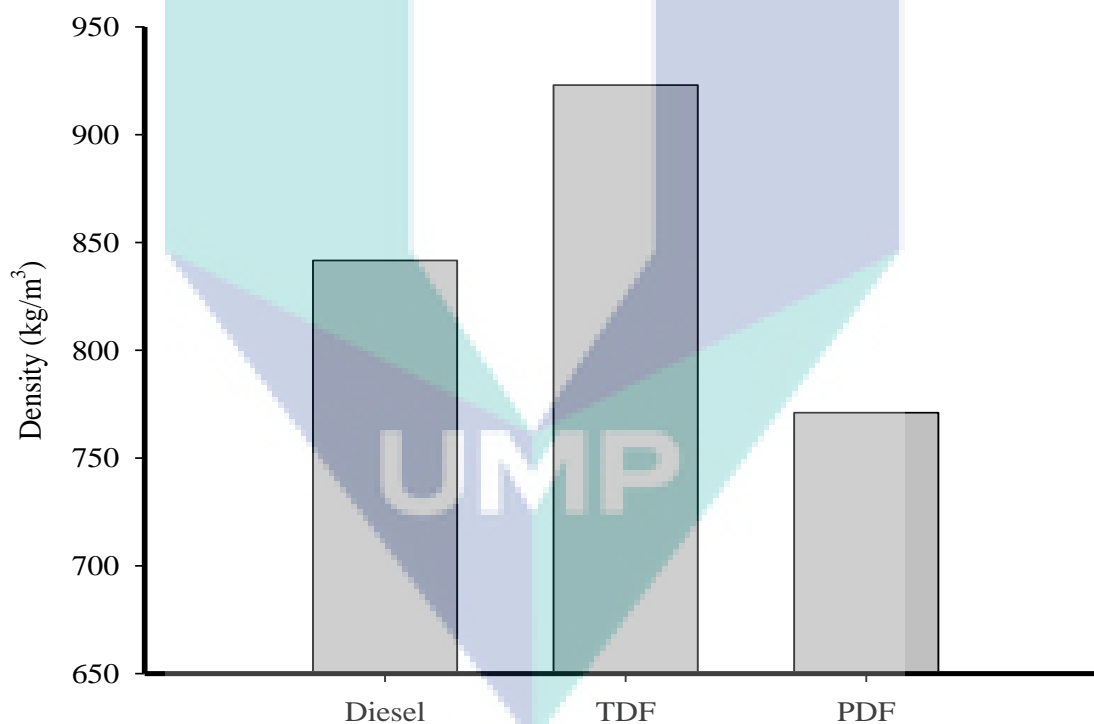
Figure 4.5: Fuel density

Figure 4.5 shows the fuel density of the fuels. From the figure, it can be observed that PDF has lowest density at 771 kg/m^3 compared to other fuel. It has lower density compared to diesel fuel by 8.4% and 16.5% lower compared to TDF. Low fuel density will cause low amount of mass injected into the combustion chamber for the same volume. This will produce low energy when the combustion of the fuel occurs.

From the figure, it is expected that the PDF will produce low engine output compared to the other fuel. However, combustion performance will also depend on the other properties such as gross calorific value and the quality of the fuel sprays.

4.3.2   Kinematic Viscosity
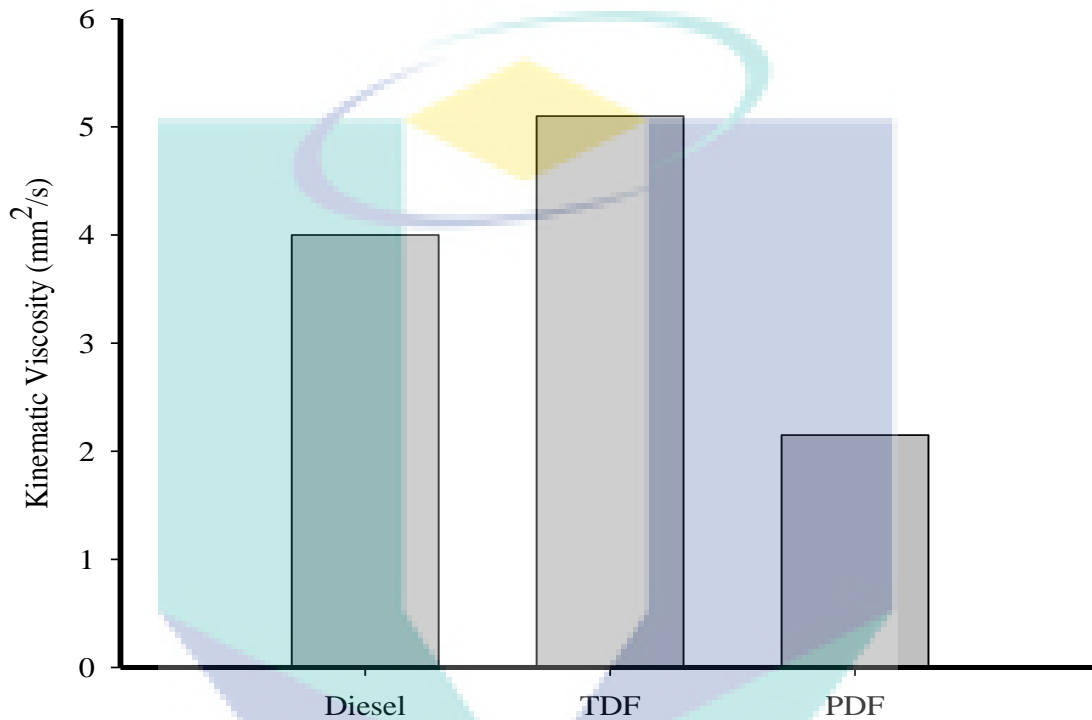
Figure 4.6: Kinematic viscosity

Figure 4.6 shows the kinematic viscosity of the fuels. From the graph, it can be observed that kinematic viscosity of PDF is lower at 2.1 mm^2/s compared to diesel fuel and TDF. Kinematic viscosity of PDF is lower compared to diesel fuel by 46.3% and lower compared to TDF by 57.9%. Low kinematic viscosity will contributes to finer fuel droplets of the PDF compared to other fuel hence producing better combustion quality. Lower kinematic viscosity of PDF also enables the fuel spray to penetrate deeper into the combustion chamber hence producing better combustion quality.

However, low kinematic viscosity may not able to provide the lubrication effect to the fuel pump and injector plunger, thus, cause leakage and faster wear on the engine

parts. On the other hand, high kinematic viscosity will cause larger fuel droplets formed thus cause poor combustion performance quality and increase emission level.

4.3.3   Flash Point
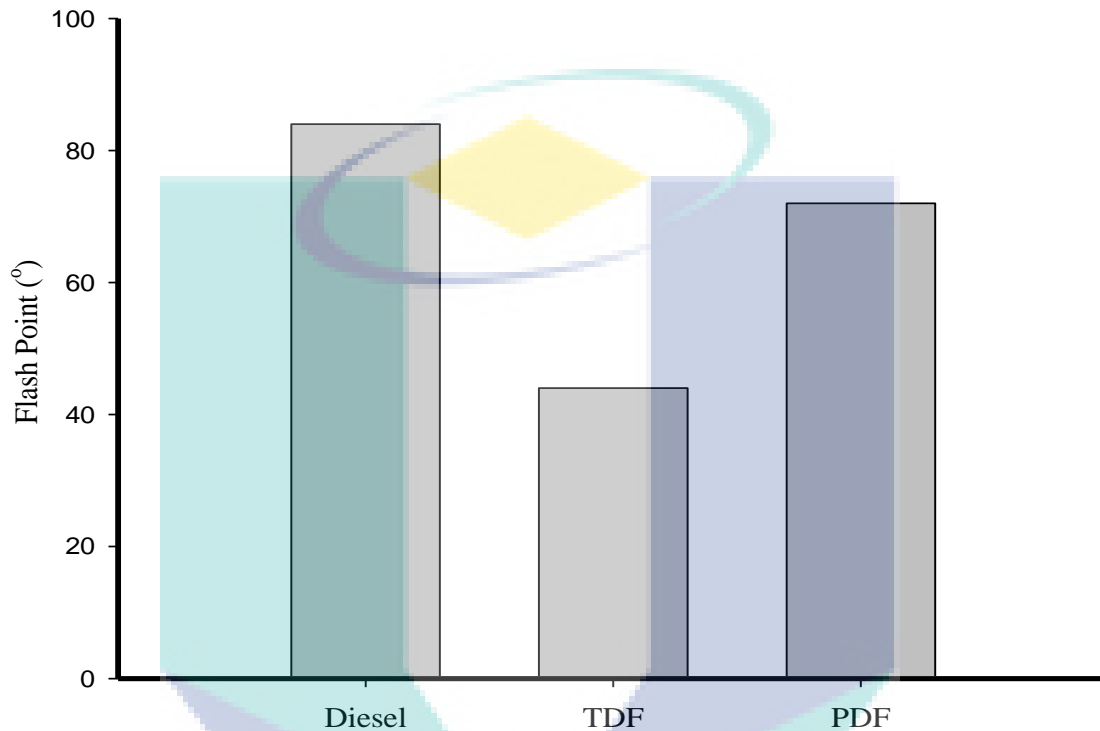
Figure 4.7: Flash point

Figure 4.7 shows the flash point of diesel fuel, TDF and PDF. From the graph, it can be observed that PDF has lower flash point compared to diesel fuel by 14.3%. However, PDF has higher flash point compared to TDF by 63.6%. Higher flash point does not affect the combustion of the fuel. It is related to the fuel handling and storage. The fuel has flash point lower than 37.8°C is considered flammable and need an extra caution when handling the fuel during experiment. According to the Figure 4.7, TDF has the lowest flash point which is 44°C. All test fuel used in this experiment (diesel fuel, TDF and PDF) has flash point larger than 37.8°C thus, the fuels is not categorized as flammable.

4.3.4 Gross Calorific Value
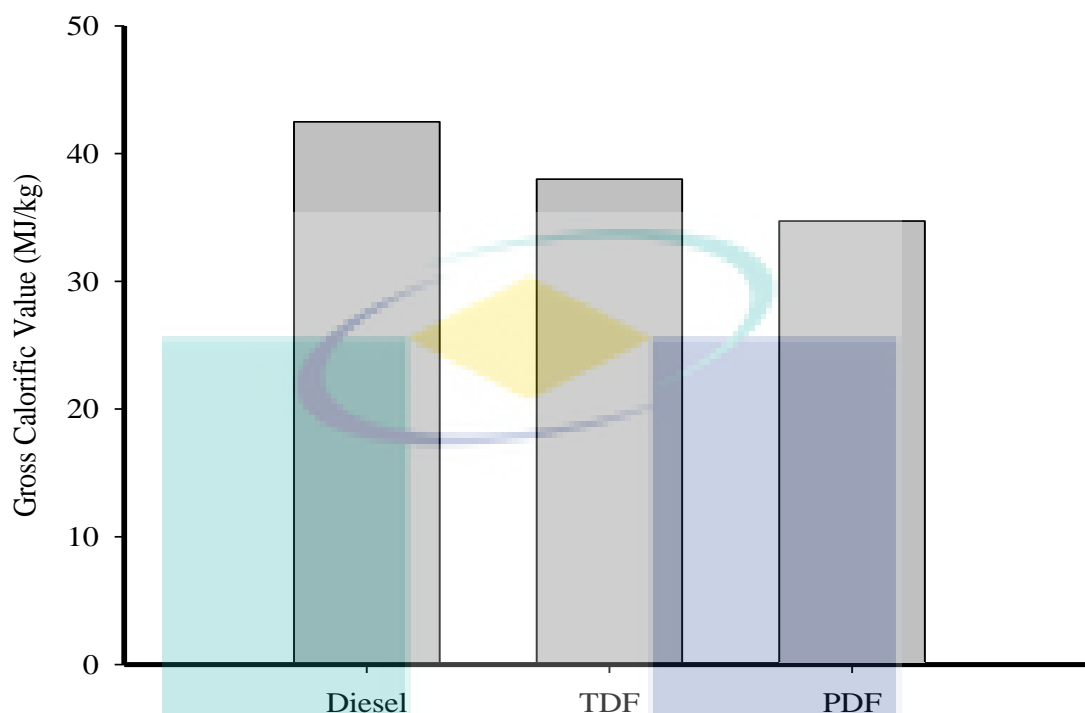
Figure 4.8: Gross calorific value

Figure 4.8 shows the gross calorific value of the fuels. From the figure, it can be observed that PDF has lowest amount of gross calorific value compared to TDF and diesel fuel. PDF has lower gross calorific value compared to diesel fuel by 18.3% and lower compared to TDF by 8.6%. Lower gross calorific value of PDF indicated that PDF will produce lower energy when combusted compared to other fuels.

4.3.5 Sulphur Content

Figure 4.9 shows the sulphur content of the fuels. From the figure, it can be observed that the sulphur content of PDF is lower compared to diesel fuel and TDF. PDF has lower sulphur content compared to diesel fuel by 54.8% and 97.6% lower compared to TDF. Lower sulphur content of PDF indicates that this fuel will produce lower emission level compared to diesel and TDF. High amount of sulphur leads to high emission of sulphur oxides (SOx). The particulate matter (PM) emission is also increases.
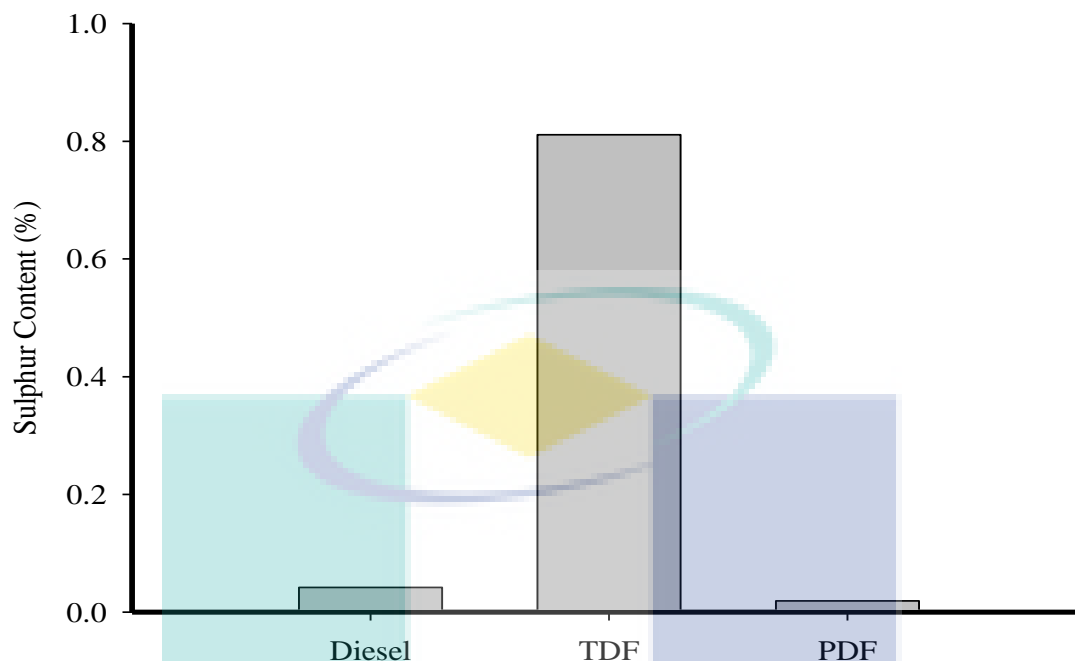
Figure 4.9: Sulphur content

4.4 Engine Performance when TDF is used as Fuel

4.4.1 Engine Torque

Figure 4.10 shows the variation of engine torque versus engine speed for test fuels. The torque output value varies from 32.3 Nm to 43.7 Nm for engine speed ranged between 1200 rpm to 2400 rpm. The results show that the torque for every fuel usage is increase as the engine speed increase. From the figure, it can be seen that TDF10% marked highest torque output which is averagely 4.6% higher compared to diesel fuel followed by TDF30% which is averagely 2.3% higher than diesel fuel. TDF50% produce 2.2% higher torque output in average compared to diesel fuel and TDF produce 3.69% lower torque output in average compared to diesel fuel. The figure shows that the TDF-diesel fuel blends marked higher torque output compared to diesel fuel and TDF. The phenomenon is due to the level of gross calorific value measured in TDF-diesel fuel blends which are much higher compared to diesel fuel and TDF as shown and described in Figure 4.4. Higher gross calorific value of a fuel will produce higher amount of energy when during combustion process.
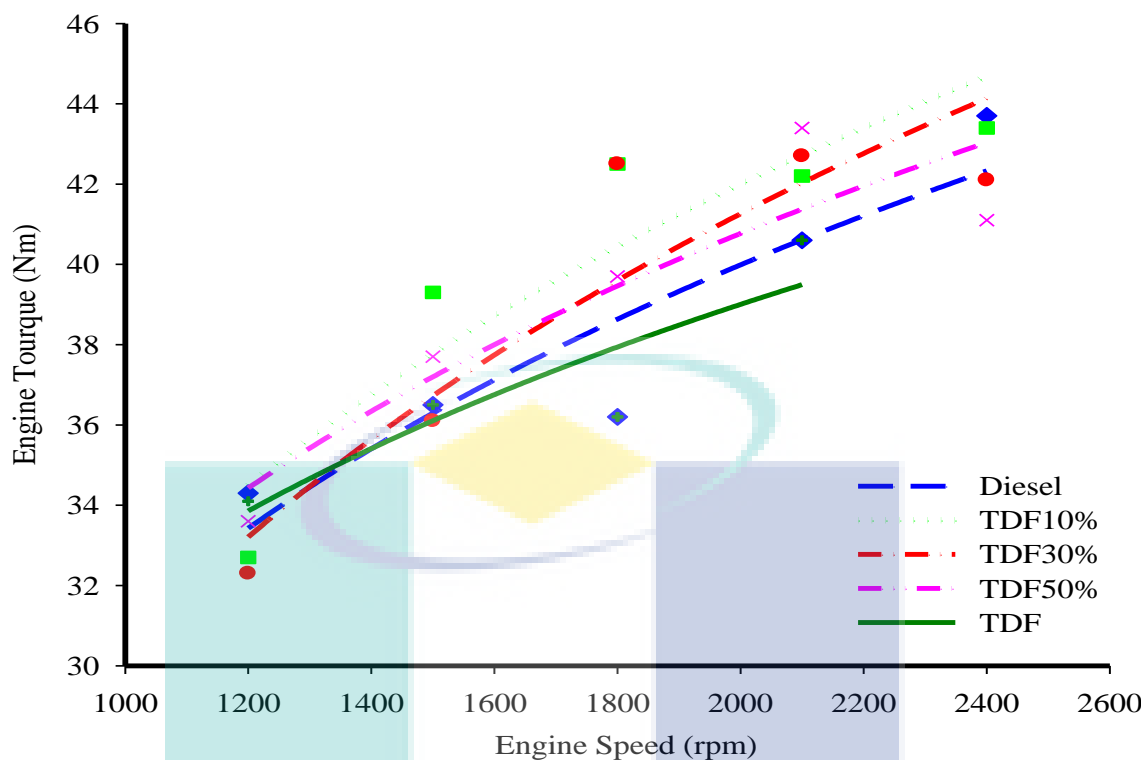
Figure 4.10: Engine torque for all test fuel

From Figure 4.10, it can be observed that the TDF-diesel fuel blends will produce higher torque output when the fuel is used in diesel engine compared to diesel fuel and TDF. This is because the gross calorific value increases when TDF is blended with diesel fuel. However, as the TDF blend ratio in diesel fuel increases, the gross calorific value decreases. This condition causes the torque output also decrease when higher TDF blend ratio is used.

4.4.2   Engine Power

Figure 4.11 shows the engine power output for every fuel type with increasing engine speeds. The power obtained from this testing is ranging from 4.1 hp to 11 kW with the corresponding engine speed from 1200 rpm to 2400 rpm. The figure shows that the power output for every fuel is increasing as the engine speeds is increasing. From the figure, it can be seen that TDF10% marked highest power output which is averagely 4.9% higher compared to diesel fuel followed by TDF30% which is averagely 3% higher than diesel fuel. TDF50% produce 2.18% higher power output in average

compared to diesel fuel and TDF produce 8.38% lower torque output in average compared to diesel fuel
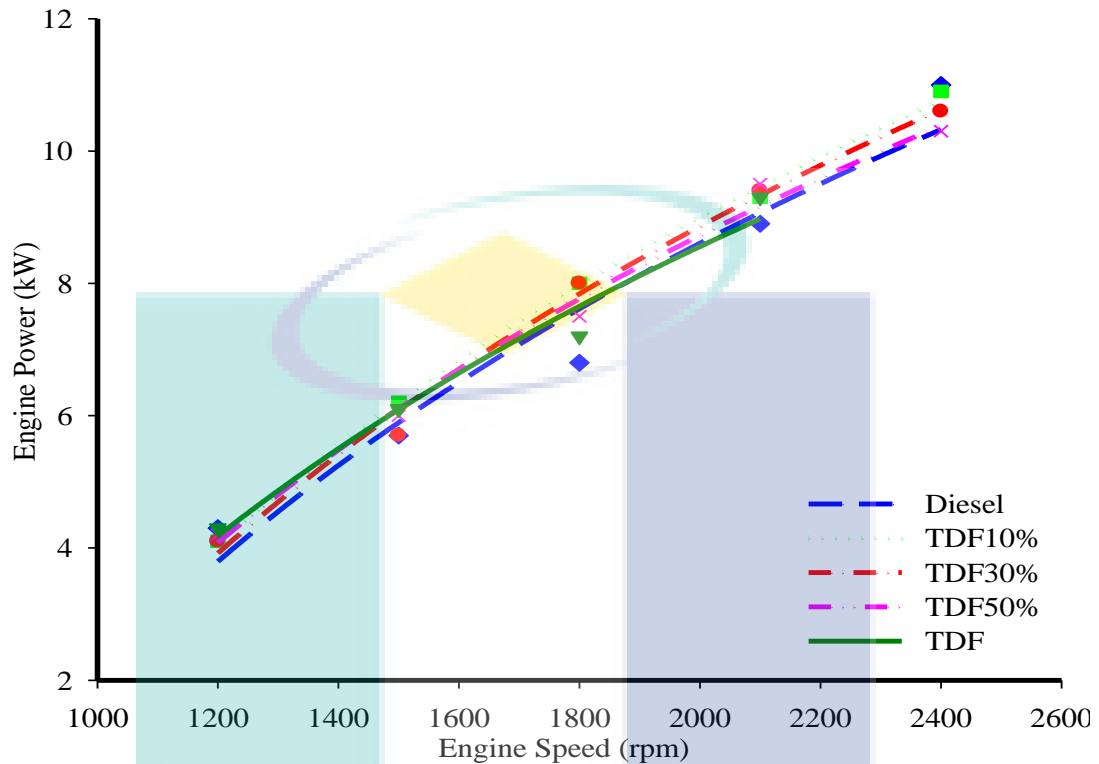
Figure 4.11: Engine power for all test fuel

From the figure, it can be observed that TDF10% records the highest power output, followed by TDF30%, TDF50%, diesel fuel and TDF. The condition is relates to the gross calorific value of the test fuels as shown in Figure 4.4. The trend that shown in Figure 4.11 shows similarity with the trend in Figure 4.10 where TDF10% produce highest torque output and TDF produce lowest torque output where the trend can be related to the gross calorific value of the fuels.

4.5 Combustion Characteristics of TDF

4.5.1 Cylinder Pressure at 1200 rpm
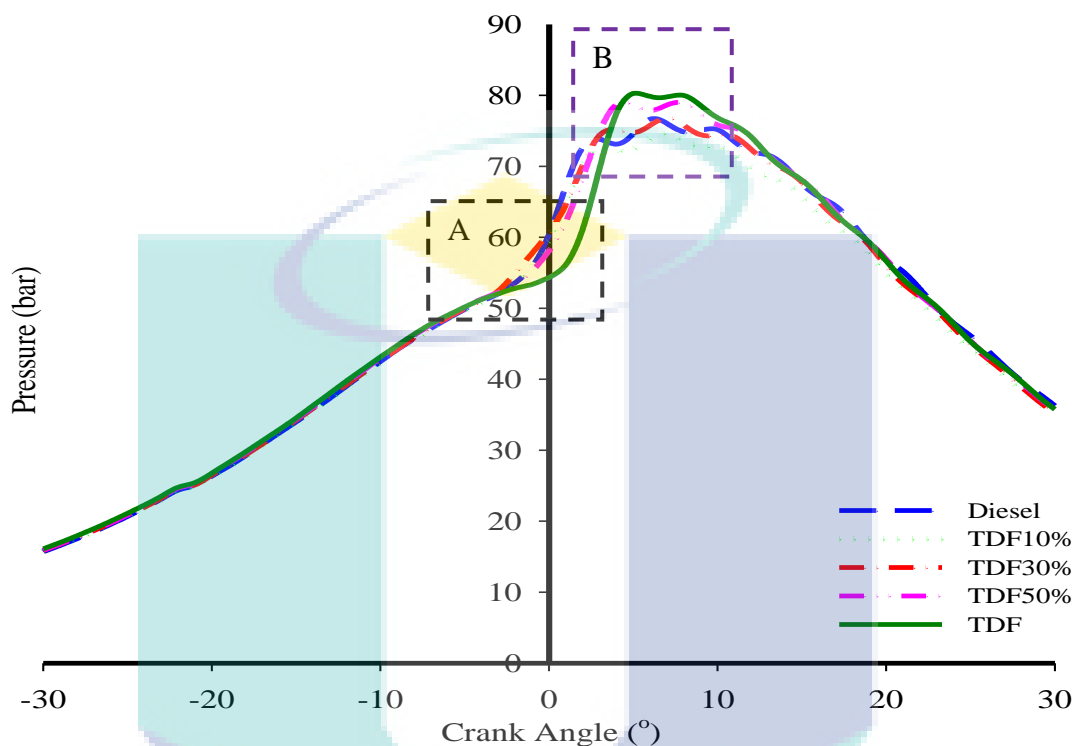
Figure 4.12: Cylinder pressure at 1200 rpm

Figure 4.12 shows the cylinder pressure curves versus crank angle at low engine speed of 1200 rpm for all test fuel. Five different fuel sample tested are diesel, TDF10%, TDF30%, TDF50% and TDF. Referring to Figure 4.12, two regions are focused in the Figure 4.12 which is the region A for fuel ignition delay and the region B for the combustion peak pressure.

Figure 4.13 describes the region A for the ignition delay of all test fuels at 1200 rpm. From the figure, it can be observed that the ignition delay for diesel, TDF10%, TDF30% and TDF50% is almost the same where the ignition starts at approximately 1° bTDC. However, TDF shows significant difference compared to other fuel where the combustion starts at about 1° aTDC compared to the other fuels which starts to combust at about 1° bTDC.
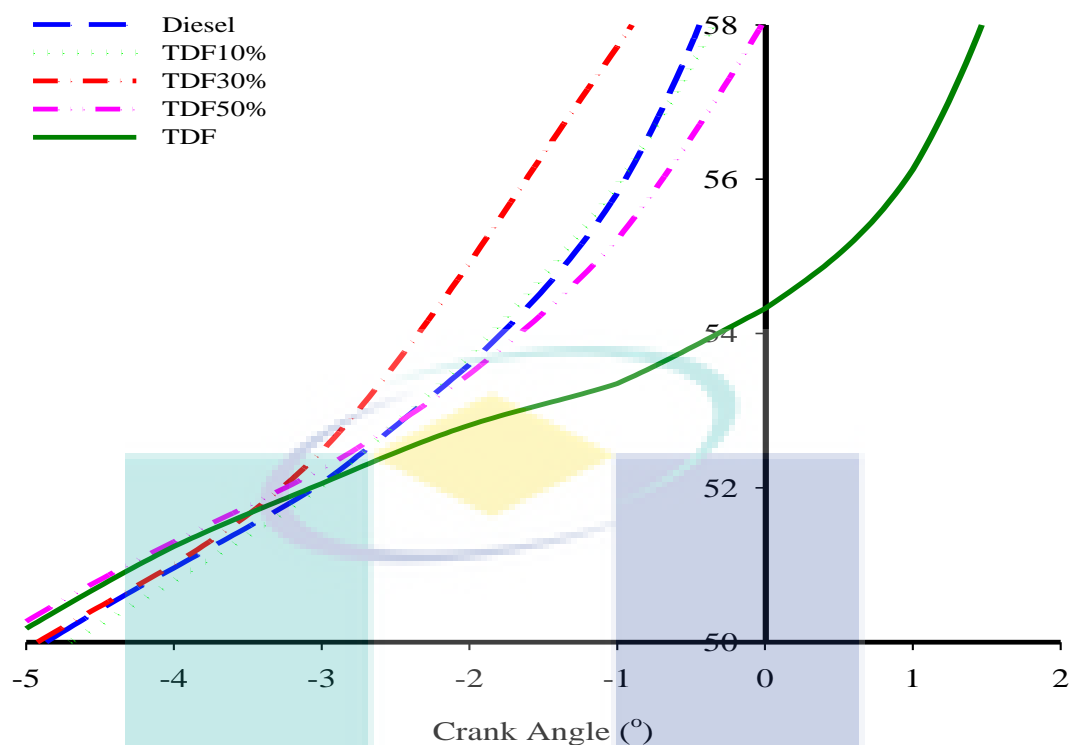
Figure 4.13: Ignition delay at 1200 rpm

Ignition delay of TDF10%, TDF30% and TDF50% occurs at almost the same crank angle compared to diesel fuel. The reason of this trend is the engine speed which is in low speed region enables the combustible air-fuel mixture to form sufficiently between the moments when the fuel is injected into the combustion chamber until the start of combustion. This condition will cause the combustion of TDF fuel blends occurs at almost the same crank angle.

It also can be seen from Figure 4.13 that the ignition delay of TDF is the longest compared to other test fuel. This can be related to the low cetane number of the TDF. The cetane number of TDF is below the acceptable range for diesel engine usage (Bhatt and Patel, 2012). Thus, low cetane number of TDF results longest ignition delay among the test fuels.

Furthermore, longer ignition delay for TDF will contribute to the rough and un-smooth diesel engine operations. Longer ignition delay will cause more fuel presence in the combustion chamber during the time after the fuel is injected until the combustion

start. Therefore, when the combustion starts, the rapid, uncontrolled combustion phase will take place at the beginning, where rapid and higher pressure rise will occur as a result of large amount of fuel inside the combustion chamber. This condition will cause audibly knocking sound, sometimes referred as "diesel knocks" thus resulting rougher diesel engine operations. The diesel knocks can be heard clearly during experiment especially at the low engine speed region during TDF combustion.
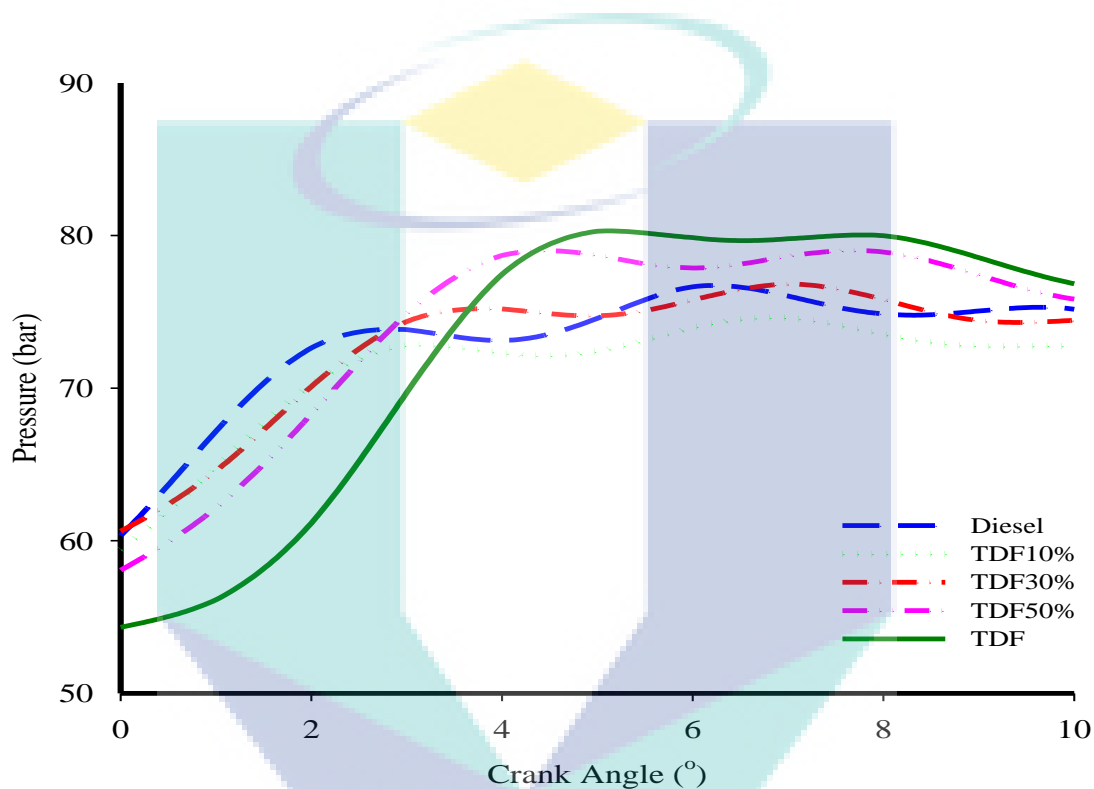
Figure 4.14: Peak pressure at 1200 rpm

Figure 4.14 shows the peak pressure for all fuels at 1200 rpm. Referring to Figure 4.12, peak pressure refers to the region 'B'. Referring to the figure, the peak pressure for diesel fuel is 76.6 bar at 6° aTDC crank angle while TDF10% produce 74.6 bar at 7° aTDC. TDF30% produce 76.8 bar at 7° aTDC, TDF50% produce 78.7 bar at 5° aTDC and lastly TDF produce 80.2 bar at 5° aTDC. From the figure, it can be observed that the peak pressure of TDF is the highest among of all fuel. This can be related to the longest ignition delay of the TDF. As mentioned earlier, longer ignition delay causing more fuel accumulated in the combustion chamber during the ignition

delay period. This condition causes more rapid and higher pressure rise when the combustion occur hence producing highest peak pressure compared to other test fuels.

For TDF-diesel fuel blends, the peak pressure shows increasing trends with the increasing of TDF ratio in the diesel fuel. According to Figure 4.14, TDF50% is the highest among TDF-diesel fuel blends, followed by TDF30% and TDF10%. The variations of peak pressure can be related to the fuel density. Since the fuel density increases as the TDF blend ratio increases, more fuel is combusted for the same volume injected into the combustion chamber hence producing higher peak pressure.

4.5.2   Cylinder Pressure at 1800 rpm

Figure 4.15 shows the cylinder pressure curves versus crank angle at moderate engine speed of 1800 rpm. From the figure, it can be observed that the combustion characteristics for each fuel shows significant difference in term of the ignition delay and the combustion peak pressure.
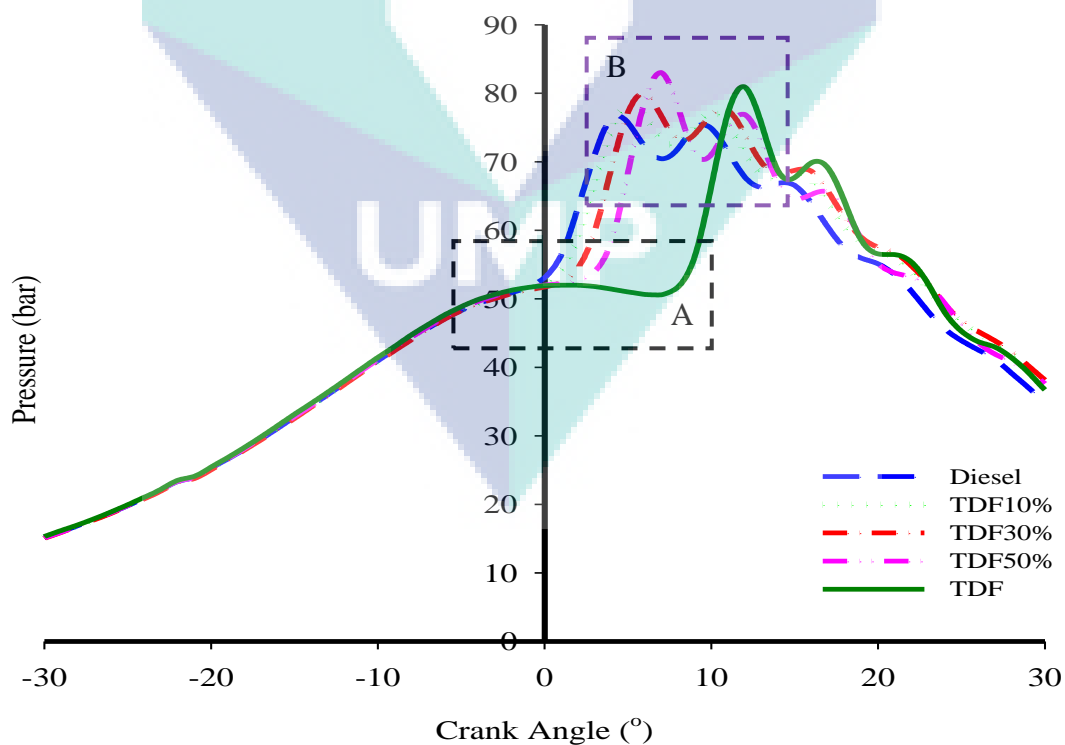
Figure 4.15: Cylinder pressure at 1800 rpm

Figure 4.16 shows the ignition delay for every fuel in separated axis. Referring to Figure 4.15, ignition delay refers to the region 'A'. From the Figure 4.16, it can be observed that the ignition delay of diesel fuel is the shortest, followed with TDF10%, TDF30%, TDF50% and TDF. It can be seen from the figure, increasing percentage of TDF blends will results longer ignition delay.
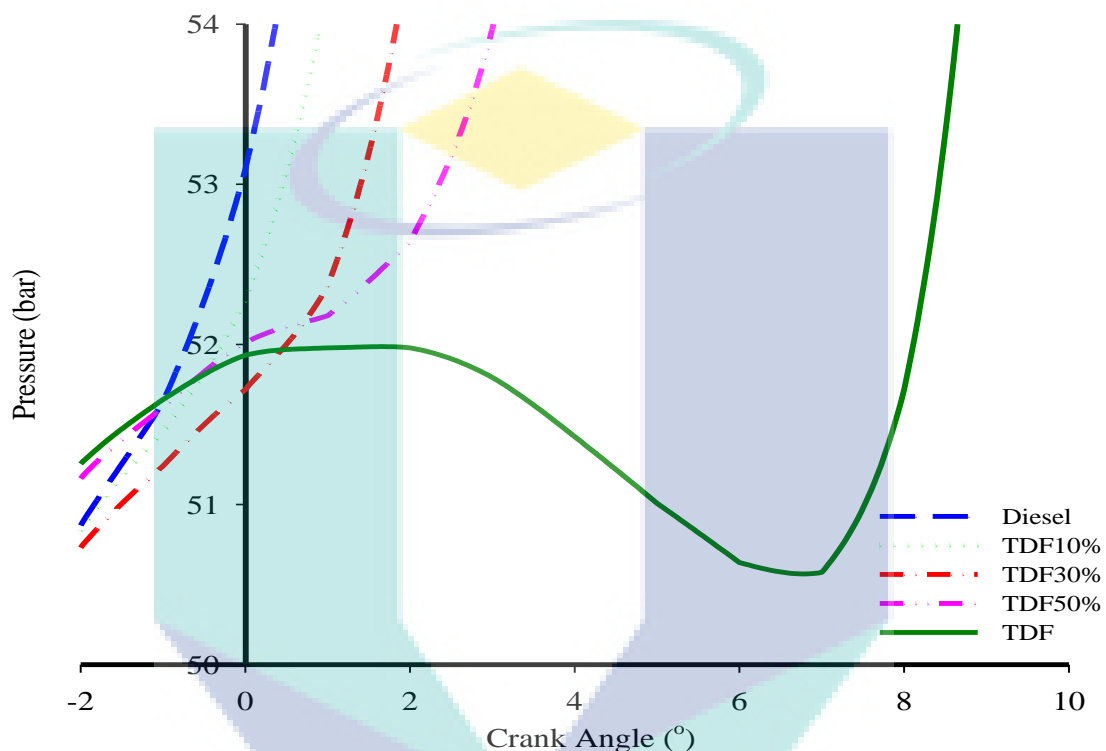
Figure 4.16: Ignition delay at 1800 rpm

The phenomenon can be related to the density of every test fuel where the ignition delay becomes longer as the density of the test fuels increase. Variations in fuel density determine the spray quality hence affect the air-fuel mixing. Higher fuel density cause greater fuel resistance to the flow. The condition cause poor atomization of the fuel. Poor atomization will cause poor mixing between the fuel and air thus results ignitable air-fuel mixture formed in a long time period, thus, affects the ignition delay for each fuel. Furthermore, the ignition delay of the TDF is the longest compared to the other fuel. As for comparison, the crank angle difference between TDF and TDF50% is about 4° crank angle difference. As engine speed increases while the other engine parameter such as injection pressure, injection timing and compression ratio are

constantly maintained, the combustion for TDF occurs late at 7° aTDC. This phenomenon can be related due to the low cetane number of TDF.

Figure 4.17 shows the peak pressure at 1800 rpm. Referring to Figure 4.15, peak pressure refers to area 'B'. It can be observed from the graph that the peak pressure of every fuel increases with the increase in TDF ratio in diesel fuel. Diesel fuel produces 76.3 bar peak pressure at crank angle of 4° aTDC while TDF10% produces 77.2 bar at 10° aTDC. Meanwhile, TDF30% produce 77.5 bar of peak pressure at 11° aTDC and TDF50% produce 83 bar of peak pressure at 7° aTDC. Lastly, TDF produces 80.9 bar of peak pressure at 12° aTDC.
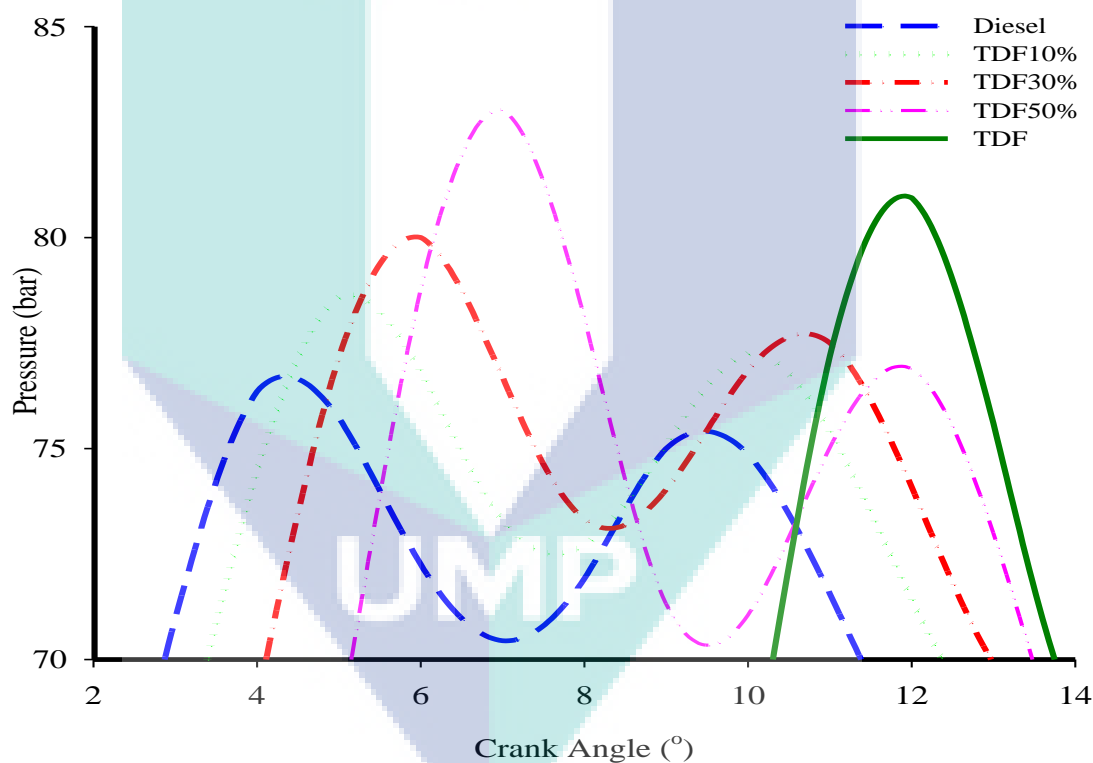
Figure 4.17: Peak pressure at 1800 rpm

This trend is due to longer ignition delay of TDF-diesel fuel blends compared to diesel fuel. Diesel fuel marked lowest cylinder pressure, followed by TDF10%, TDF30%, TDF and TDF50%. The trend of peak pressure of each fuel can be seen where the peak pressure increases with the increasing of ignition delay. Peak pressure is much affected by the level of the fuel density. Higher fuel density will cause more fuel

to exist in the combustion chamber thus enables higher mass of fuel to be combusted. This condition also cause higher peak pressure. Referring to Figure 4.1, the density of each fuel increases as the ratio of TDF increases. With the combination of the above mentioned factor (ignition delay and fuel density), more fuel is combusted when the ignition starts thus resulting on higher peak pressure.

Meanwhile, observation on cylinder pressure for TDF at 1800 rpm shows slightly decrease compare to peak pressure of TDF50%. Even though the ignition delay of TDF is the longest and fuel density is the highest, the peak pressure for TDF decrease as the engine speed increases. Compared to the peak pressure for TDF at 1200 rpm, it yields the highest peak pressure as the ignition delay for TDF is the longest. The decrease in peak pressure at 1800 rpm is because of the ignition of TDF occurs too late where the compression pressure in the cylinder starts to decrease as the piston starts to move downward. This is because of the low cetane number of TDF compared to other fuels. This is proved by TDF curve in Figure 4.16. From the curve, it can be seen that the pressure is drop starts from $2°$ to $7°$ crank angle before it starts to increase rapidly as the combustion occur. For the other fuel, the combustion occurs most when the compression pressure is almost at the highest.

4.5.3   Cylinder Pressure at 2100 rpm

Figure 4.18 shows the cylinder pressure for each fuel at high speed which is 2100 rpm. From the figure, it can be observed that the combustion characteristics (ignition delay and peak pressure) for each fuel shows clear difference compared to each other. Similar trend also can be seen at moderate speed pressure curve which was shown in Figure 4.15.

Figure 4.19 shows the ignition delay at high engine speed (2100 rpm). Referring to Figure 4.18, the ignition delay refers to the area 'A'. From the figure, it can be seen that the ignition delay increase as the TDF ratio in the diesel fuel increase. Diesel fuel shows shortest ignition delay, followed by TDF10%, TDF30%, TDF50% and TDF. It also can be observed from the graph that when the engine speed is increased, the ignition delay of all test fuels is longer in term of crank angle. This trend can be related

to the change of fuel density for the test fuels. As the ratio of TDF blend increase, the fuel density also increases. Higher density cause higher fuel flow resistance in the injection system, thus cause poor fuel atomization. Poor fuel atomization cause longer ignition delay of the fuel.
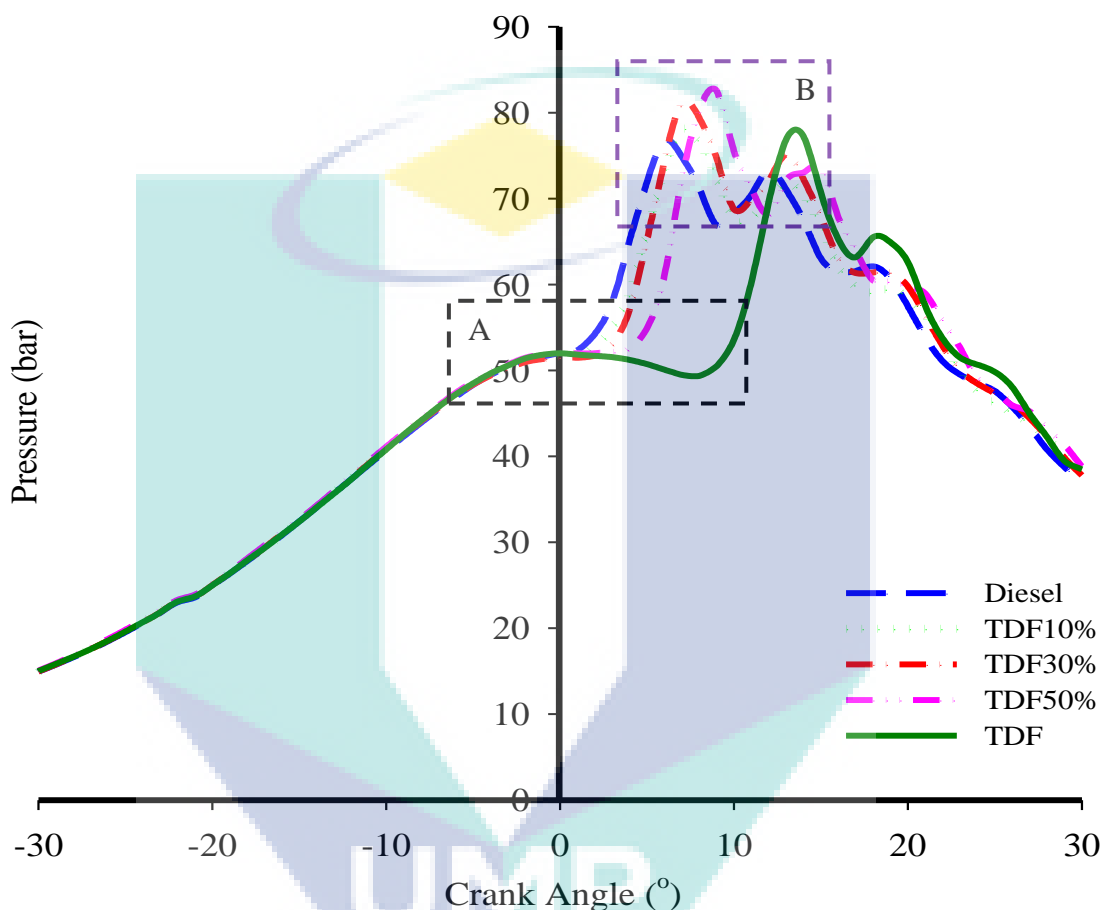
Figure 4.18: Cylinder pressure at 2100 rpm

Figure 4.20 shows the peak pressure at high engine speed (2100 rpm). Referring to the Figure 4.18, the peak pressure refers to the area 'B'. Diesel fuel produce peak pressure of 76.8 bar at 6° aTDC while TDF10% produce 78 bar of peak pressure at 7° aTDC. Moreover, TDF30% produce 81 bar of peak pressure at 7° aTDC and TDF50% produce 82.5 bar of peak pressure at 9° aTDC. Lastly, TDF produce 76.9 bar of peak pressure at 13° aTDC. From the figure, it can be observed that the peak pressure of every test fuel is increase as the TDF ratio in the diesel fuel is increase. Diesel fuel yields the lowest peak pressure, followed by TDF, TDF10%, TDF30% and TDF50%.

Ignoring peak pressure of TDF aside, the trend of every blended fuel is the same as the moderate speed figure curve. Thus, increasing the blend ratio of TDF in diesel fuel will prolong the ignition delay. This will result in higher peak pressure as a result of rapid pressure rise as more fuel enters the combustion chamber before the ignition starts.
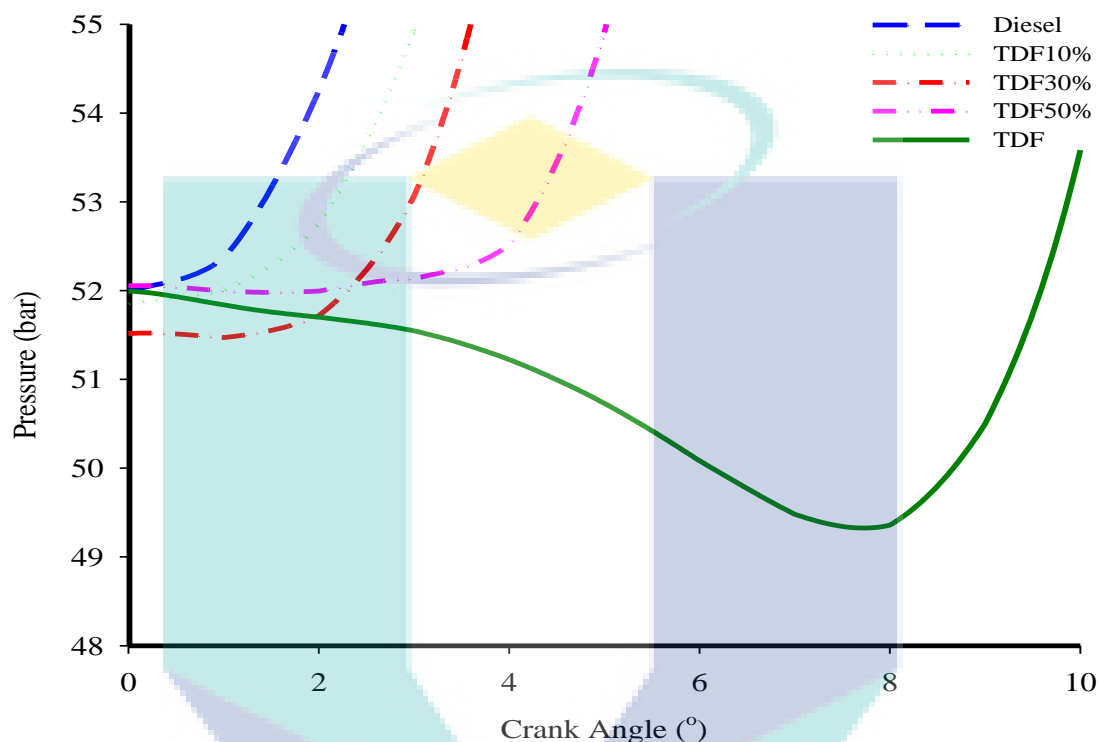
Figure 4.19: Ignition delay at 2100 rpm

The peak pressure for TDF become lower compared to the peak pressure at 1800 rpm because of the combustion of TDF occurs when the compression pressure in the combustion chamber starts to decrease as the piston moving downward. This is caused by the very long ignition delay of TDF. Referring to the TDF pressure curve in Figure 4.18, the pressure curve decreases from 1° crank angle until 8° crank angle before the pressure curve rapidly increase as the fuel is combusted. Combustion that occurs at this crank angle will cause poor engine performance.
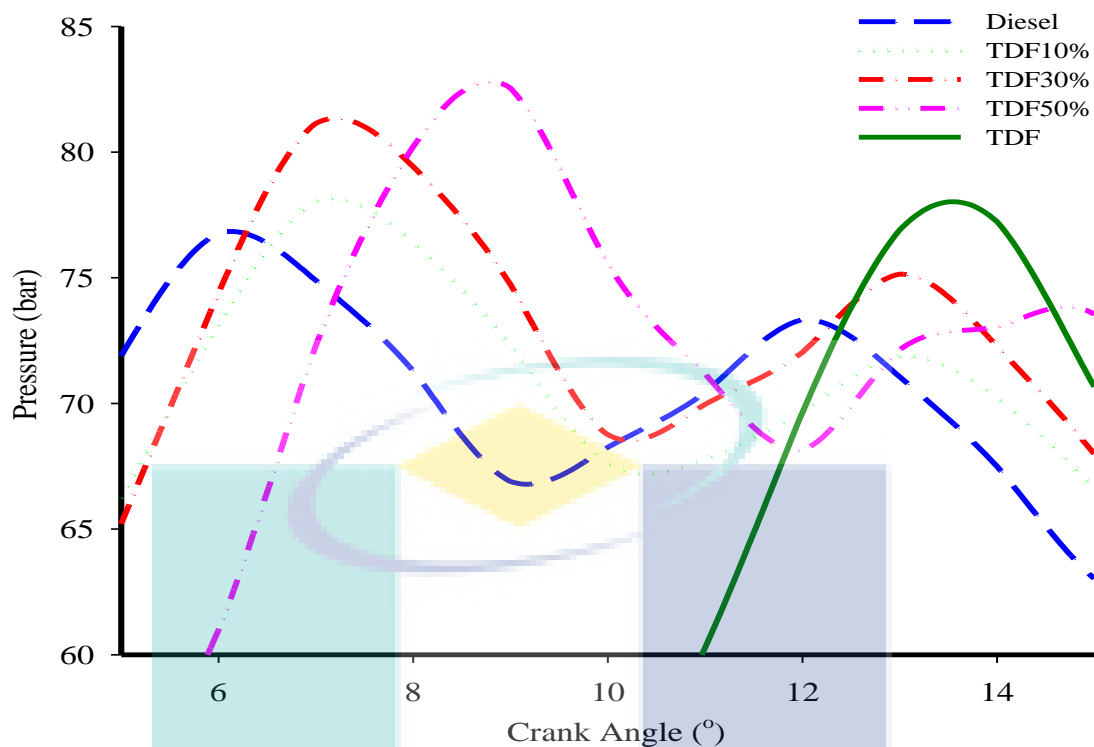
Figure 4.20: Peak pressure at 2100 rpm

4.6   Backfire Phenomenon

As mentioned in previous section 4.5.1, low cetane number will cause longer ignition delay especially for TDF. This means the time region starting from the fuel injected into the combustion chamber until the ignition of the fuel occur, becomes longer in term of crank angle. As the engine speed increase through the low speed region, medium speed region and entering high speed region, the ignition delay obviously becomes longer. At the high speed region, when the exhaust valve starts to open, some of the unburned fuel enters the exhaust manifold. The high temperature of exhaust manifold will cause the fuel that entering the exhaust manifold combust. This condition will cause a backfire observed at exhaust manifold together with explosion sound when the TDF is used. The backfire phenomenon will occur as the engine speed exceeds 2200 rpm.

Figure 4.21 shows the backfire that occurs at the exhaust manifold as the engine speed is increased more than 2200 rpm. This proves that TDF has very long ignition

delay compared to other fuel. The non-combustible TDF will enter the exhaust manifold when the exhaust valve starts to open when the expansion stroke ends. The heat from the exhaust manifold will cause the TDF to combust. The effect of this phenomenon includes worse emission level and also bad engine performance. This phenomenon indicates that the TDF is not suitable for high speed application since it will cause bad performance and worse emission level.
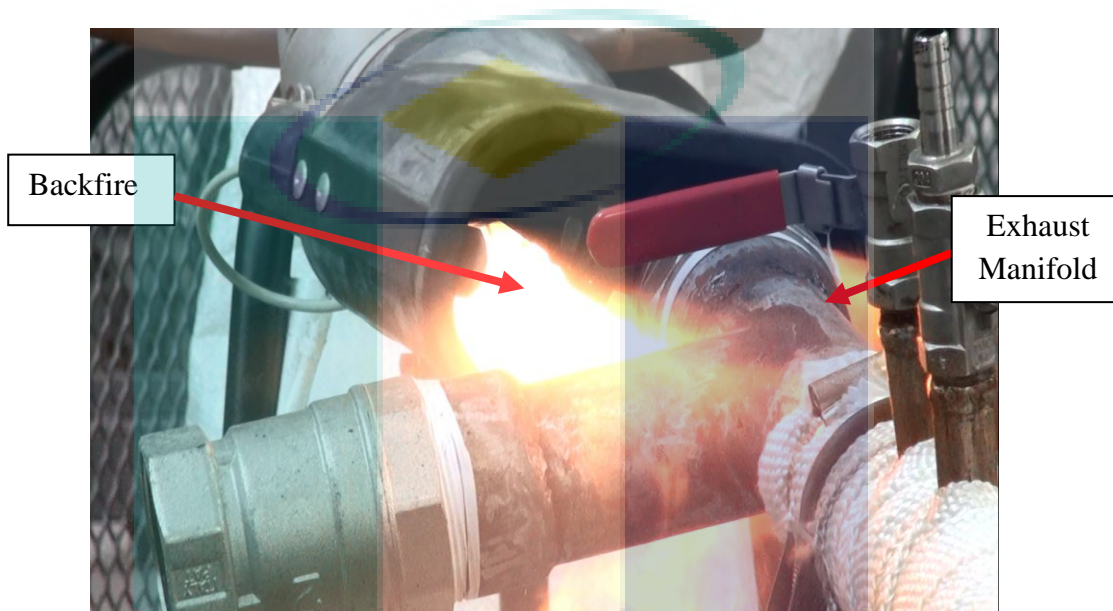
Figure 4.21: Backfire phenomenon

4.7 Exhaust Gas Emissions of TDF

4.7.1 Exhaust Gas Temperature

Figure 4.22 shows the variation of exhaust gas temperature versus engine speed for all test fuel. From the figure, it can be observed that diesel fuel produce the lowest exhaust gas temperature. This is followed by TDF10% which average at 2.1% higher compared to diesel fuel. TDF30% is 3.4% higher compared to diesel fuel in average and TDF50% is 7.9% higher in average compared to diesel fuel. Referring to the figure, TDF produce the highest exhaust gas temperature compared to all fuels.

The trend occurs due to the higher heat release rate of TDF-diesel fuel blends that was developed during the premixed combustion phase. As observed in Figure 4.13,

Figure 4.16 and Figure 4.19, the ignition delay period is increase as the ratio of TDF blends is increase. Longer ignition delay causes more fuel to exist in the combustion chamber during ignition delay period, causing a rapid, higher rate of heat release when the combustion occur. The combustion condition will cause the exhaust temperature becomes higher as the ratio of TDF blends in diesel fuel increasing. Furthermore, as the engine speed increase, more fuel is injected and combusted in the combustion chamber thus cause exhaust gas temperature increase when engine speed increase.
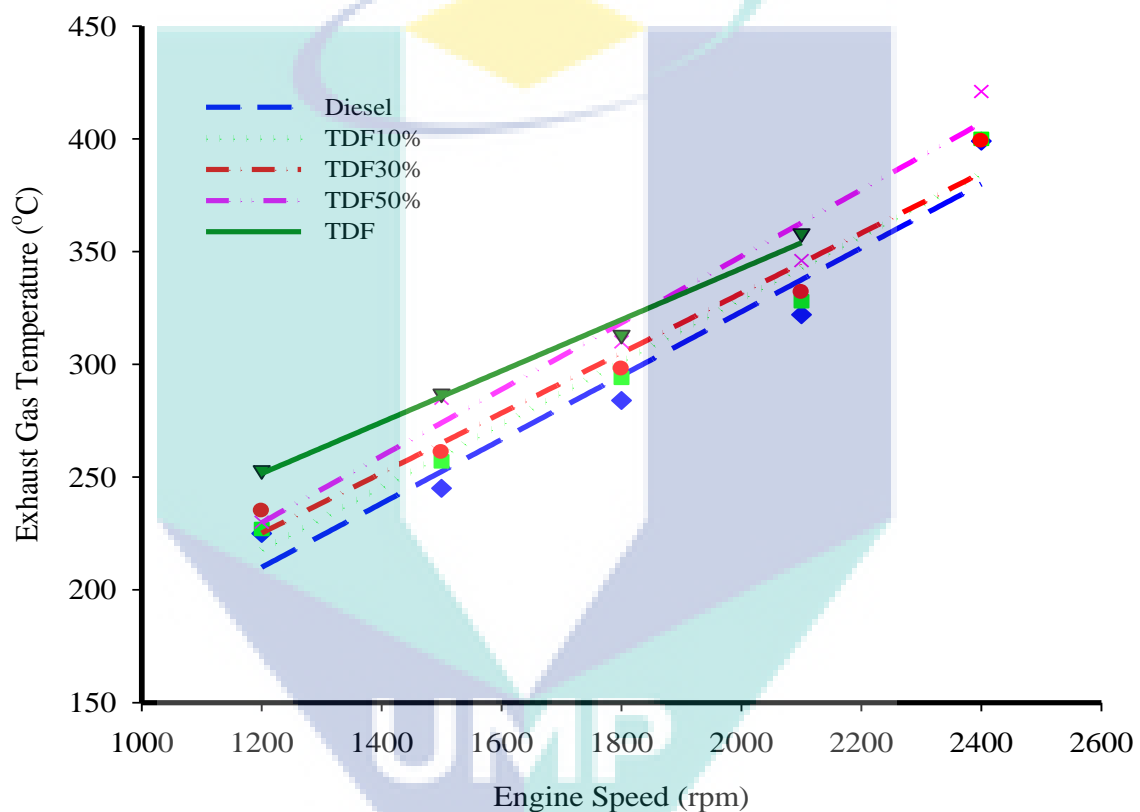
Figure 4.22: Exhaust gas temperature

4.7.2   Carbon Monoxide (CO) Emission

Figure 4.23 shows the carbon monoxide (CO) emission versus engine speed for all test fuel. From the figure, it can be observed that TDF produce the highest CO emission compared to the other fuel. This can be related to high kinematic viscosity of TDF. High kinematic viscosity cause poor fuel atomization hence causes poor mixing rate and poor fuel penetration through the combustion chamber (Adam et al., 2011).

Poor fuel atomization process lead to the incomplete combustion reaction thus causes large formation of carbon monoxide (CO).

In addition, from the figure, it can be seen that diesel fuel produce lowest CO emission. This is followed by TDF10% which is 130% higher compared to diesel fuel in average. Next, TDF30% produce 177% higher compared to diesel fuel and TDF50% produce 233% higher than diesel fuel in average. TDF produces highest CO emission among the test fuels by 265% compared to diesel fuel in average. From the graph, it can be seen that all fuel produce higher CO emission as the engine speed increase. This can be related to the higher carbon content in the TDF blends as the TDF ratio in diesel fuel is increase.
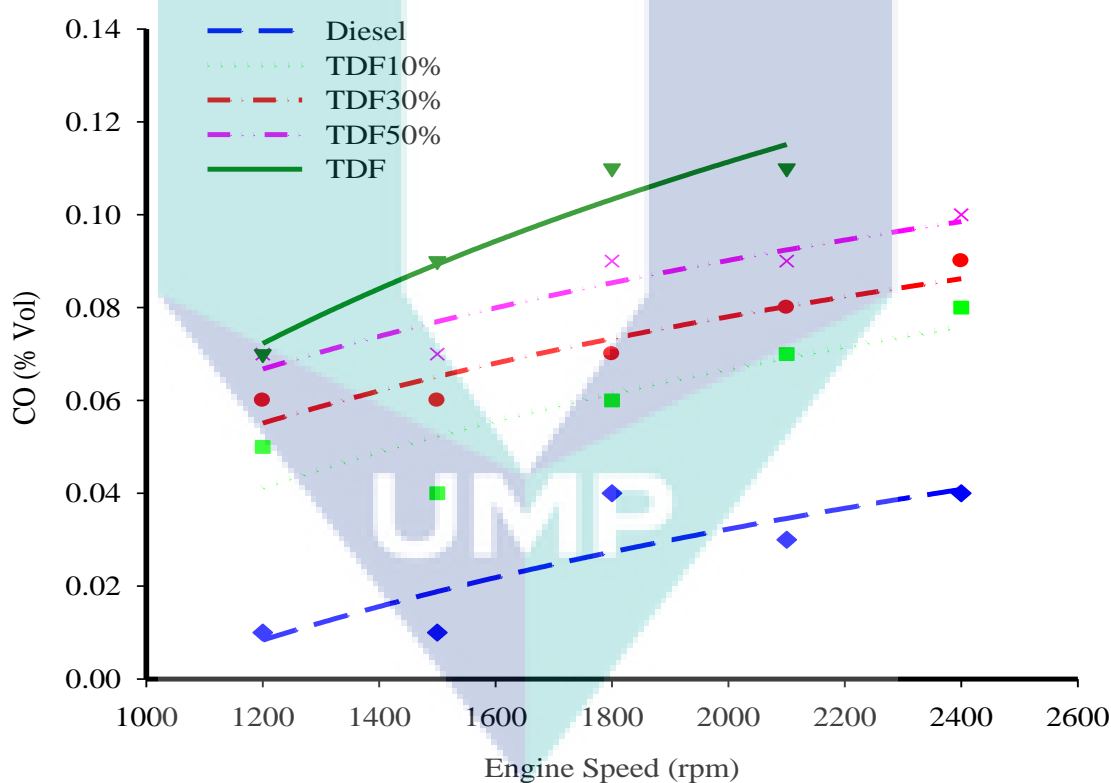
Figure 4.23: Carbon monoxide (CO) emission

Moreover, high formation of CO also cause by the high density of fuel as the ratio of TDF in diesel fuel is increase. The reason is when more carbon molecules exist in a higher density fuel for the same volume compared to the lower density fuel. High carbon content fuel forms higher CO emission during combustion. Incomplete

combustion also may cause the production of CO. As the density of fuel increase, the fuel droplets becomes bigger, hence cause poor mixing between air and fuel thus cause incomplete combustion of fuel.

4.7.3   Carbon Dioxide (CO_2) Emission
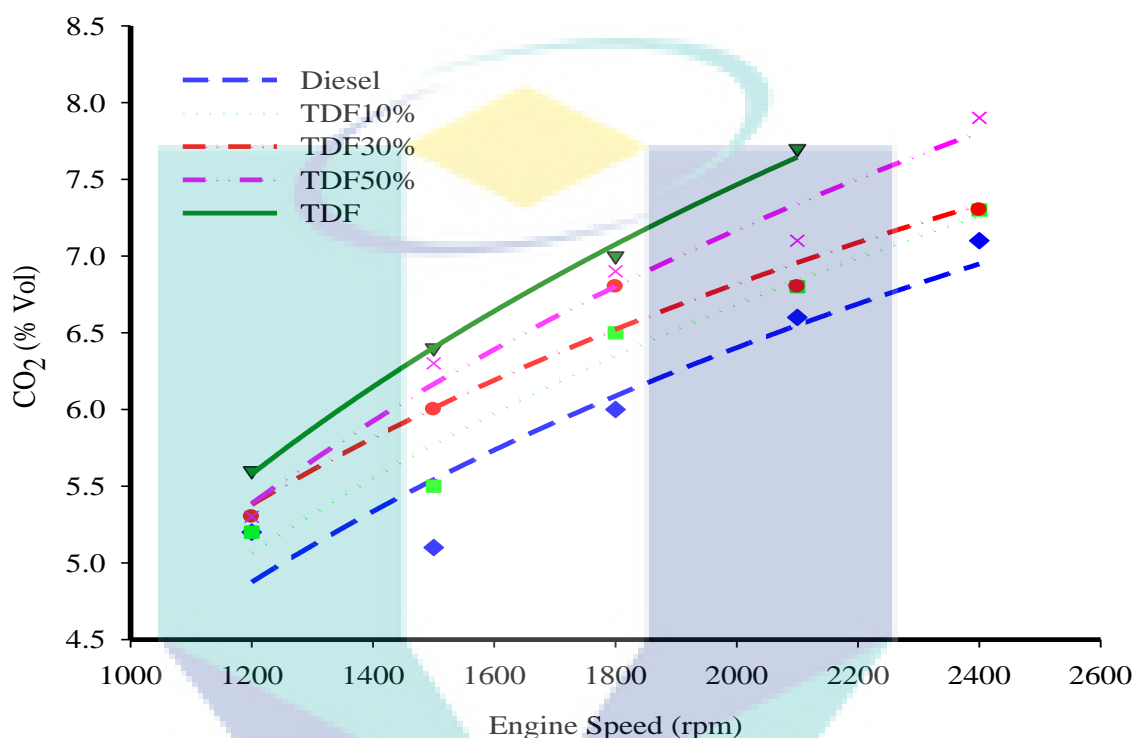
Figure 4.24: Carbon dioxide (CO_2) emission

Figure 4.24 shows the CO_2 emissions versus engine speed. From the figure, it can be observed that diesel fuel produce lowest CO_2 emission, followed by TDF10% which is 4.33% higher compared to diesel fuel in average. Then, TDF30% produce 7.33% higher CO_2 emission compared to diesel fuel while TDF50% yield 11.67% higher CO_2 compared to diesel fuel. TDF produces 11.33% higher CO_2 emission compared to diesel fuel. From the figure, it can be observed that the CO_2 emission increase as the TDF ratio in diesel fuel increase. The reason of this condition is, when the ratio of TDF increase, the concentration of carbon in the TDF-diesel fuel blends also increases. As a result, the emission of CO_2 increases as the ratio of TDF in diesel fuel increase.

From the figure, it also can be observed that the CO_2 emission increases as the engine speed increases. This is caused by the higher amount of fuel that consumed for combustion as the engine speed increases. Due to the properties of TDF that consist of high carbon content, high TDF ratio combustion will emits higher carbon molecules where it react with oxygen (O_2) thus produce higher CO_2 as the engine speed increase.

4.7.4   Nitrogen Monoxide (NO) Emission

Figure 4.25 shows the nitrogen monoxide (NO) emission for all test fuels versus engine speed. From the figure, it can be observed that diesel fuel produce lowest level of NO, followed by TDF10% which is 10% higher compared to diesel fuel and then TDF30% which is 22% higher compared to diesel fuel in average. TDF50% produce 30% higher NO compared to diesel fuel and TDF produce highest level of NO compared to other fuel at is 83% higher compared to diesel fuel in average. The formation of NO is influenced by the combustion temperature and also ignition delay.
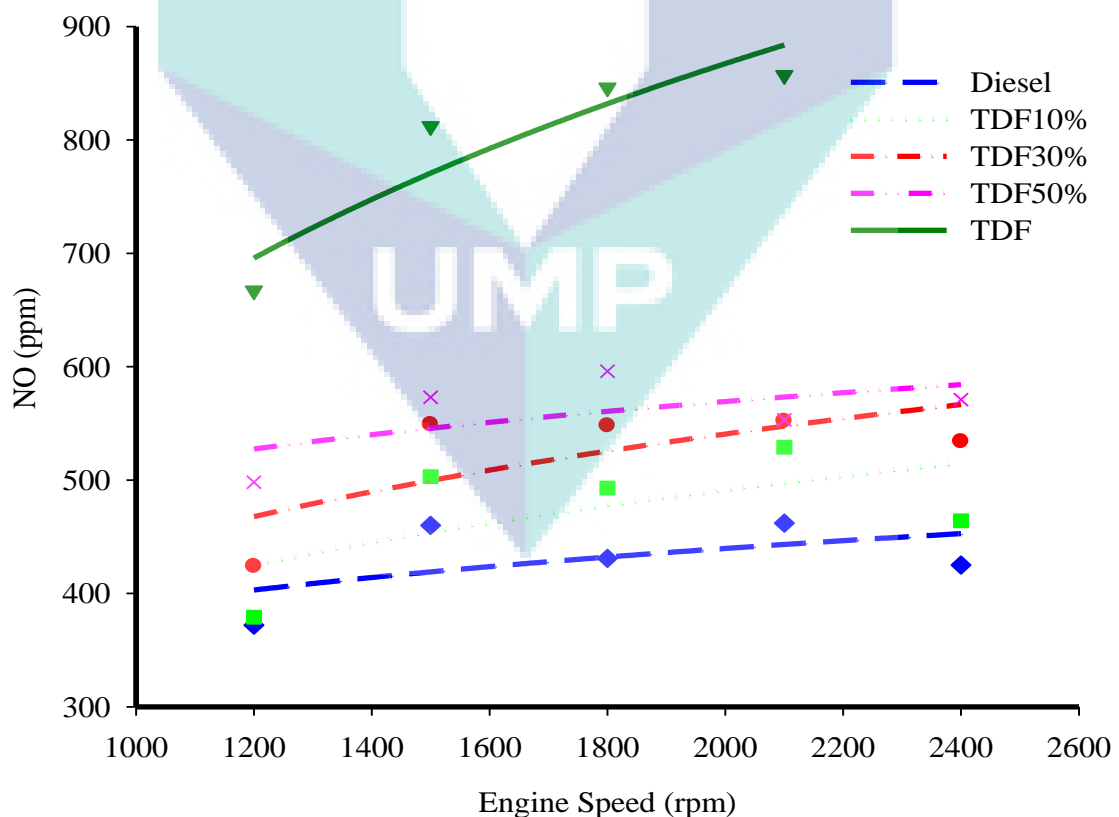
Figure 4.25: Nitrogen monoxide (NO) emission

Long ignition delay contributes to high formation of NO. As shown in Figure 4.13, Figure 4.16 and Figure 4.19, ignition delay period is increased with the increment of the ratio of TDF in diesel fuel. Longer ignition delay will cause more fuel entering the combustion chamber during the delay period, causing a rapid burning when the combustion starts. Long ignition delay combustion will produce high combustion temperature hence cause high formation of NO. Furthermore, according to Borman (1998), naturally aspirated engine with long ignition delay and sufficient time available for premixing between fuel and air will strongly affect on NO formation.

The higher exhaust gas temperature indicates the formation of NO. When high combustion temperature occurs, the exhaust temperature is also high thus causing high formation of NO. Comparing between Figure 4.22 and Figure 4.25, same trends occur for both graphs. For exhaust gas temperature, diesel fuel produces the lowest exhaust gas temperature, followed by TDF10%, TDF30%, TDF50% and TDF. Same trend is shown by Figure 4.25 as diesel fuel produce the lowest NO, followed by TDF10%, TDF30% and TDF50%. TDF produces the highest level of NO.

4.7.5 Nitrogen Oxides (NO_x) Emission

Figure 4.26 shows the nitrogen oxides (NO_x) emission versus engine speed. It can be seen from the figure that diesel fuel produce lowest amount of NO_x compared to other fuel. The second lowest is TDF10% which is 11% higher compared to diesel fuel in average, followed by TDF30% which is 22% higher compared to diesel fuel and TDF50% which is 30 higher compared to diesel fuel in average. TDF produce highest amount of NO_x which is 83% compared to diesel fuel in average. From Figure 4.25 and 4.26, it can be seen that the trend for NO emission and NO_x emission is almost the same. NO_x consist of NO and NO_2. NO_2 contain up to 10% to 30% of total NO_x emission while the 70% to 90% is NO.
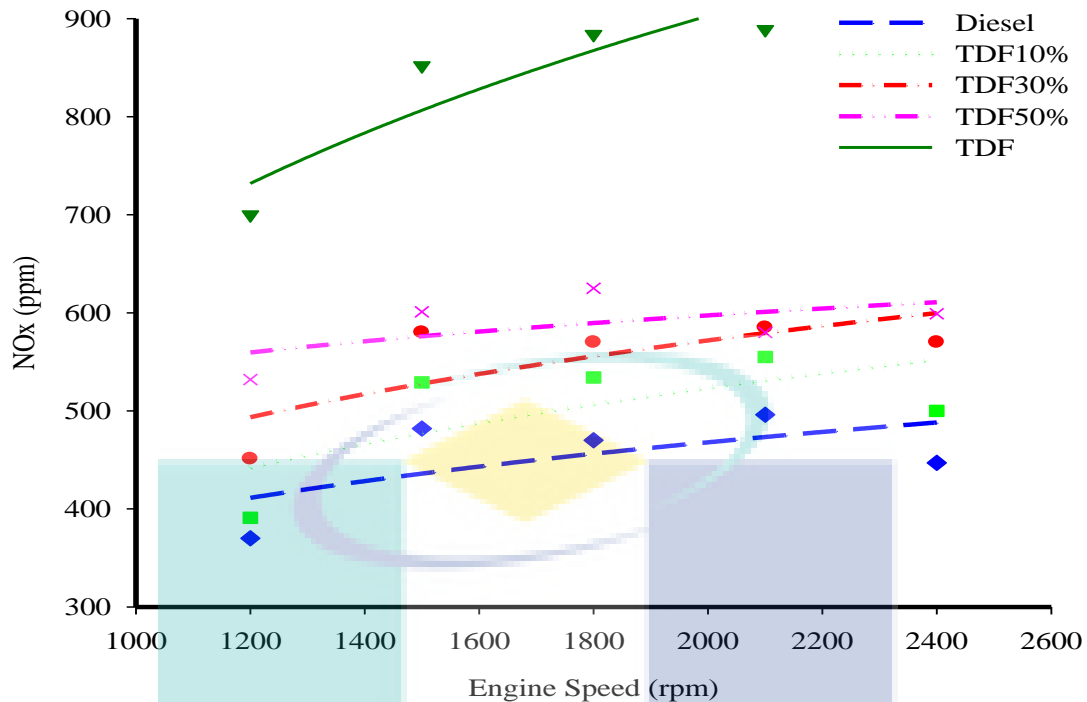
Figure 4.26: Nitrogen oxides (NO$_x$) emission

TDF produce highest level of NO$_x$ as it can be related to its high kinematic viscosity value. This physical property cause poor fuel atomization thus producing bigger fuel droplets when injected in the combustion chamber. Bigger fuel droplets cause reduction of the surface area of the fuel droplets resulting rich equivalence ratio since less air molecules can react with the fuel during combustion. Therefore, high level of NO$_x$ produce by high kinematic viscosity of TDF causes high formation of NO$_x$.

Increasing TDF ratio in diesel fuel causes the ignition delay become longer. Longer ignition delay also contributes to high formation of NO$_x$. As shown in Figure 4.13, Figure 4.16 and Figure 4.19, the ignition delay becomes longer with the increment of the ratio of TDF. Longer ignition delay cause more fuel entering the combustion chamber during the delay period. When the combustion starts, a rapid combustion will occur as a result of more fuel existence in the combustion chamber. This condition will produce higher combustion temperature hence causing higher formation of NO$_x$. From Figure 4.26, it can be concluded that higher TDF blend ratio will cause higher formation of NO$_x$. This is because higher TDF blend ratio cause longer ignition delay, caused rapid pressure rise when the combustion started hence higher combustion pressure.

Higher combustion pressure produce higher combustion temperature thus contributes to higher NO_x emission.

4.8   Engine Performance when PDF is used as Fuel

4.8.1   Engine Torque

Figure 4.27 shows the engine torque of the test fuels. From the figure, it can be observed that the amount of torque increases as the engine speed increases for all test fuels. It can also be seen from the figure that PDF produce lowest amount of torque compared to diesel fuel and TDF. PDF produce 10.4% lower average torque compared to diesel fuel and 7% lower average torque compared to TDF.
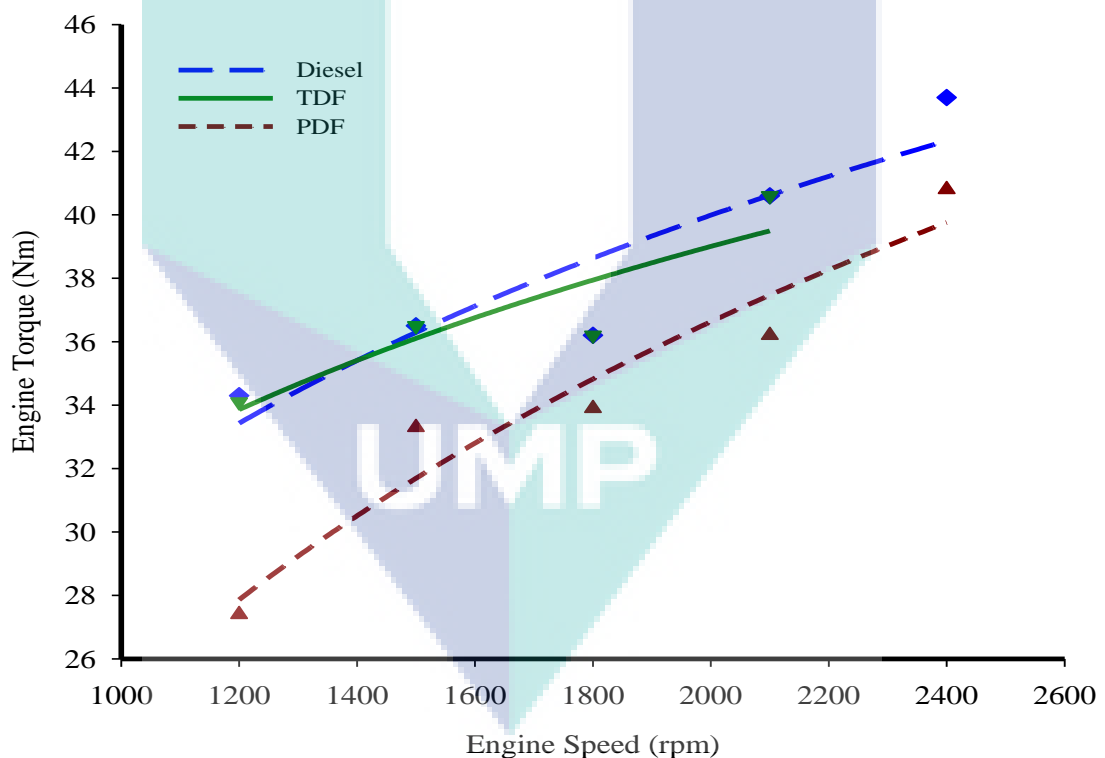
Figure 4.27: Engine torque

One of the possible cause that make PDF to produce lower torque output is PDF has lower gross calorific value compared to diesel fuel and TDF. Low amount of gross

calorific value produce low energy output during combustion hence give low torque output for PDF compared to diesel fuel and TDF.

The density of the fuel also contributes to this phenomenon. The density of the PDF is lower compared to diesel fuel and TDF. Lower density of PDF cause lower amount of mass that is injected into the combustion chamber for the same volume compared to other fuels. This aspect may also cause the combustion of PDF produce lower amount of torque compared to other fuels.

4.8.2 Engine Power
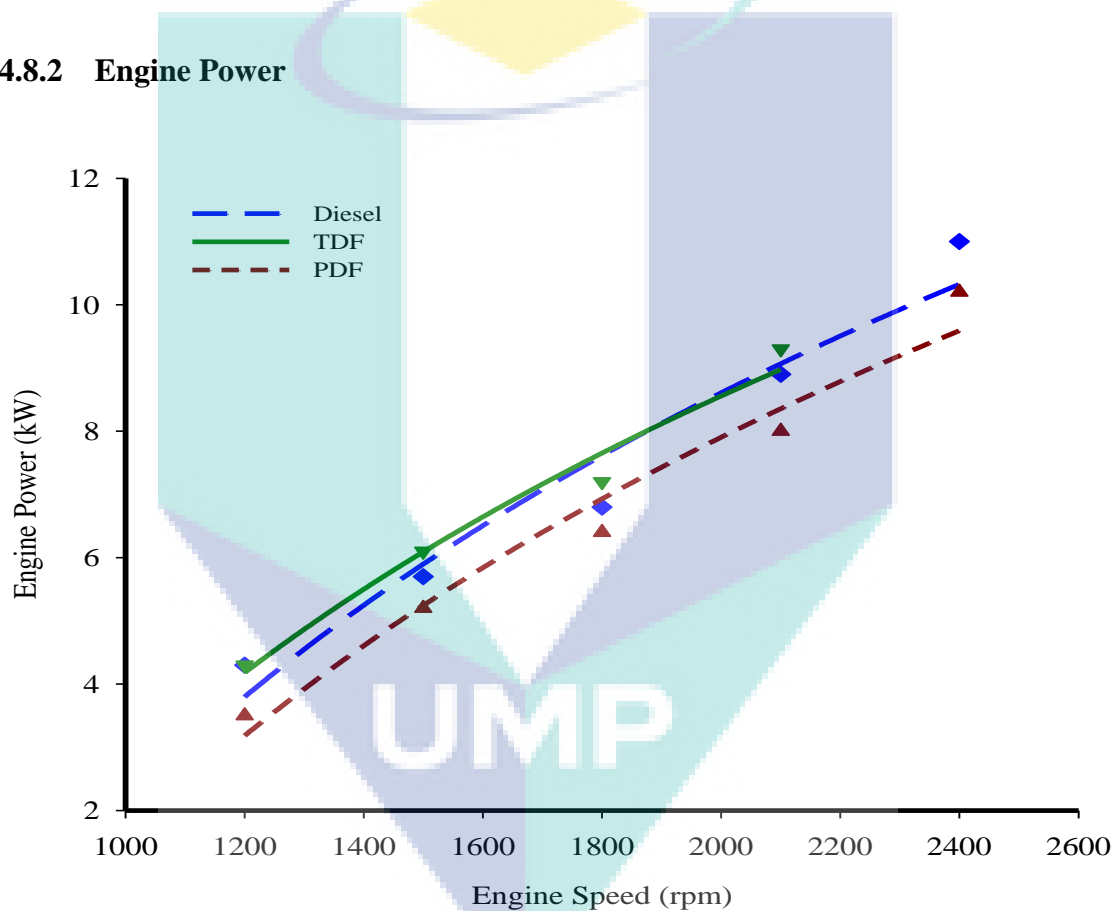
Figure 4.28: Engine power

Figure 4.28 shows the power produced by the engine when all the fuels are tested. From the curve, it can be seen that the power output when all the fuels are tested is increasing as the engine speed increasing. It also can be observed from the graph that PDF produce lowest average power output compared to diesel fuel and TDF. PDF

produce 9.3% lower average power output compared to diesel fuel and 1% lower compared to TDF.

PDF produce low power output because of the lower gross calorific value. Low amount of gross calorific value will cause the fuel combustion to produce less power output compared to the fuel that has high gross calorific value. Lower amount of power produced by PDF compared to diesel fuel and TDF also caused by lower density of PDF compared to the other fuels. Low fuel density causes less mass injected into the combustion chamber. This situation causes less amount of power produced by PDF compared to the other fuels.

4.9 Combustion Characteristics of PDF

4.9.1 Cylinder Pressure at 1200 rpm
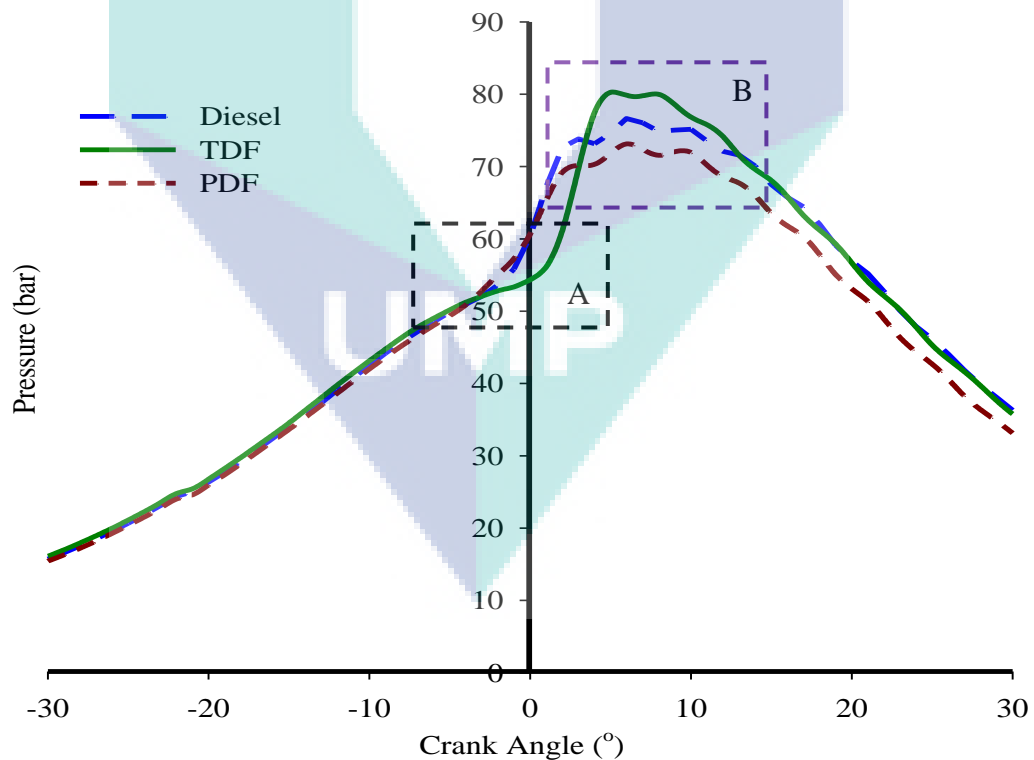
Figure 4.29: Cylinder pressure at 1200 rpm

Figure 4.29 shows the cylinder pressure curve for fuel combustion at low speed which is 1200 rpm. From the curve, it can be observed the ignition delay for diesel fuel, TDF and PDF in area 'A'. Further than that, the peak pressure of the combustion for every fuel can be determined where the peak pressure is shown in area 'B'.

Figure 4.30 shows the ignition delay of all test fuels at 1200 rpm. Referring to Figure 4.29, ignition delay during this engine speed refers to region 'A' where Figure 4.30 shows the ignition delay in separated axis. From the figure, it can be observed that the ignition delay for PDF is comparable to diesel fuel. However, TDF shows longer ignition delay compared to PDF and diesel fuel.
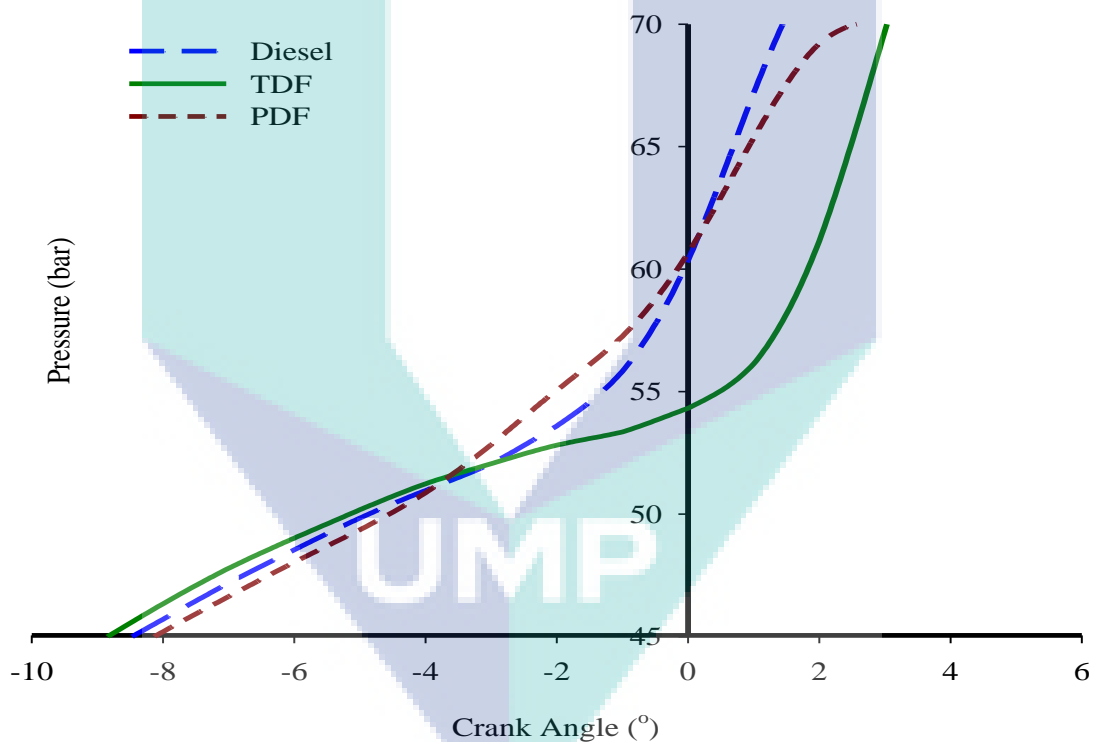
Figure 4.30: Ignition delay at 1200 rpm

The difference in ignition delay between the fuels may be related to several causes. The first reason that may be related to this is the cetane number of the fuels. TDF has lower cetane number compared to diesel fuel and PDF. This property cause longer ignition delay of TDF compared to diesel fuel and PDF. Moreover, TDF has higher kinematic viscosity compared to other fuel. Higher kinematic viscosity will

cause bigger fuel droplets. Bigger fuel droplets will have smaller surface area thus causing poor mixing rate between the fuel and air. This condition will cause the time for combustible air-fuel mixture to be formed is longer thus prolong the ignition delay.

For PDF, its cetane number is lower compared to diesel fuel as stated by Mani (Mani et al., 2011) hence supposedly produce longer ignition delay compared to diesel fuel. However, PDF has almost the same ignition delay compared to diesel fuel. The reason for this condition may relate to the second factor that related to the spray quality of PDF. The factor that gives effect to the spray quality of PDF is the kinematic viscosity. Referring to Figure 4.6, kinematic viscosity of PDF is lower compared to diesel fuel by 46.3%. Lower kinematic viscosity will produce finer fuel droplets thus providing larger surface area of the fuel. This condition provides larger surface area of the fuel and improves the mixing rate between the fuel and air. Faster mixing rate between fuel and air will produce ignitable air-fuel mixture at a faster rate thus shortened the ignition delay of the fuel. This is the possible reason why PDF has almost the same ignition delay compared to diesel fuel even though it has lower cetane number.

Figure 4.31 shows the peak pressure of all test fuels at 1200 rpm. Referring to the Figure 4.29, peak pressure refers to region 'B'. From the figure, it can be observed that the peak pressure of TDF is the highest which is 80.2 bar at 5° aTDC while diesel fuel produce second lowest peak pressure which is 76.6 bar at 6° aTDC. PDF produces lowest peak pressure which is 73.1 bar at 6° aTDC. TDF produces highest peak pressure which can be related to the ignition delay of the fuel. TDF has longest ignition delay compared to diesel fuel and PDF where longer ignition delay contribute to higher peak pressure. This is because more fuel entering the combustion chamber during ignition delay period. This condition cause more rapid and higher pressure rise when the combustion occur. The other factor that can be related to this condition is the density of the fuels. The density of TDF is the highest compared to diesel fuel and PDF. Higher density of fuel cause more fuel entering the combustion chamber for the same volume hence cause more fuel can be combusted at a cycle. More fuel that has been combusted causes higher peak pressure of the fuel.
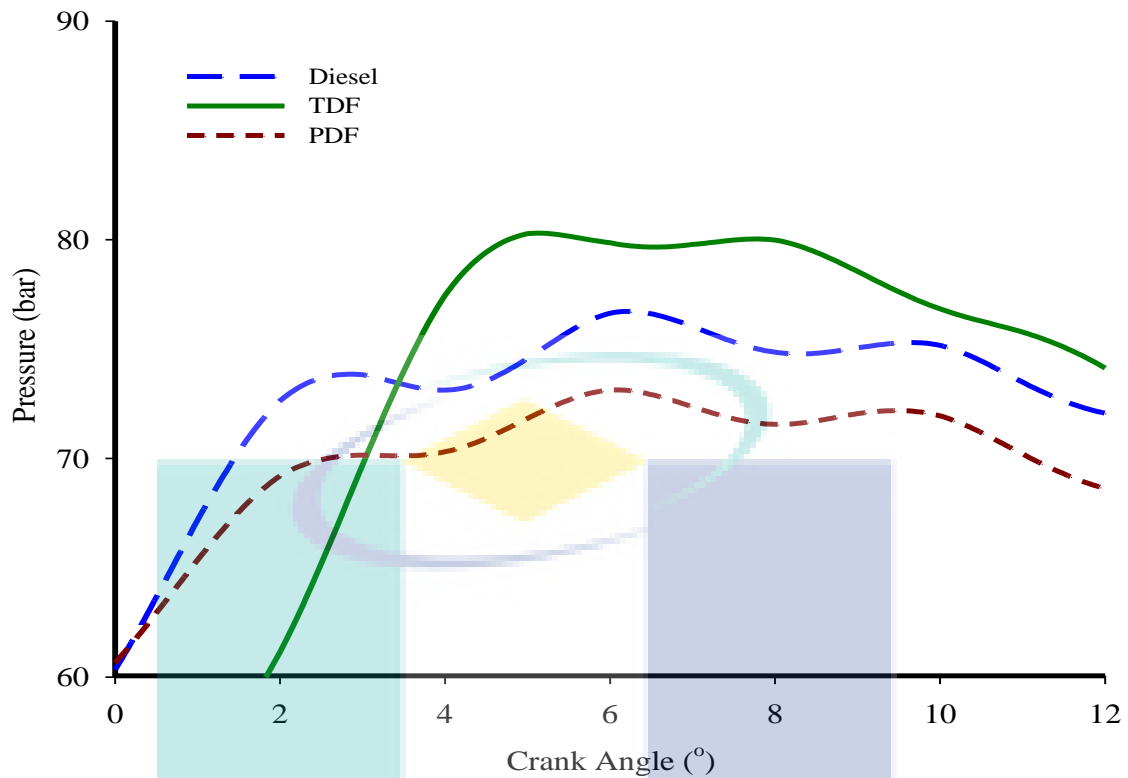
Figure 4.31: Peak pressure at 1200 rpm

The peak pressure of PDF is lower compared to diesel fuel and TDF. This can be related to the gross calorific value of PDF which is lower compared to diesel fuel and TDF. This factor cause PDF produce lower peak pressure when combusted in the combustion chamber since less energy released as the energy content in the fuel is lower compared to diesel fuel and TDF. Moreover, PDF has lower density compared to diesel fuel and TDF. This condition causes less mass of PDF that combusted in the combustion chamber at the same volume, thus resulting lower peak pressure.

4.9.2 Combustion Characteristics at 1800 rpm

Figure 4.32 shows the cylinder pressure of test fuels at moderate engine speed which is 1800 rpm. From the figure, two main region are focused which are ignition delay and peak pressure of the test fuels. Ignition delay for all test fuels is shown in area labelled as 'A' while the peak pressure for test fuels are shown in area labelled as 'B'.
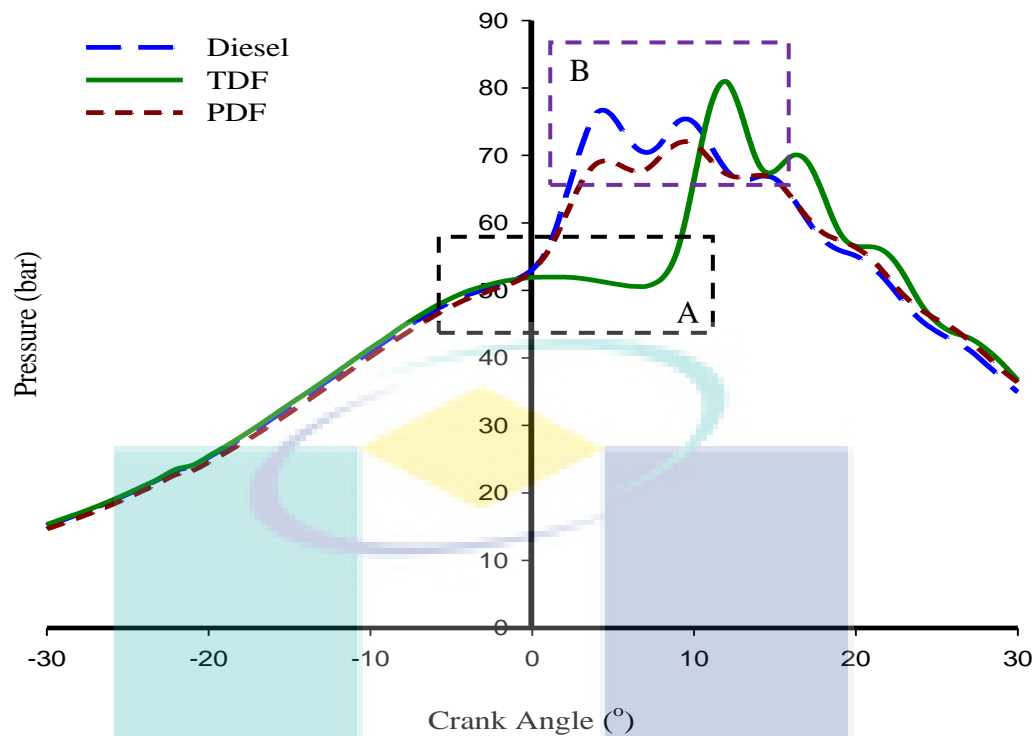
Figure 4.32: Cylinder pressure at 1800 rpm

Figure 4.33 shows the ignition delay at 1800 rpm for every test fuel. Referring to Figure 4.32, ignition delay refers to the region 'A'. From Figure 4.33, it can be observed that the ignition delay of diesel fuel is the shortest, followed by PDF while TDF shows the longest ignition delay. The trend can be related to the cetane number of the fuels. PDF has lower cetane number compared to diesel thus cause it to have longer ignition delay compared to diesel fuel. Even though PDF has lower kinematic viscosity where it will produce finer fuel droplets, the time for the fuel droplets can react with air to produce combustible air-fuel mixture is less as the engine speed increase. TDF has longest ignition delay because it has lowest cetane number compared to diesel fuel and TDF.
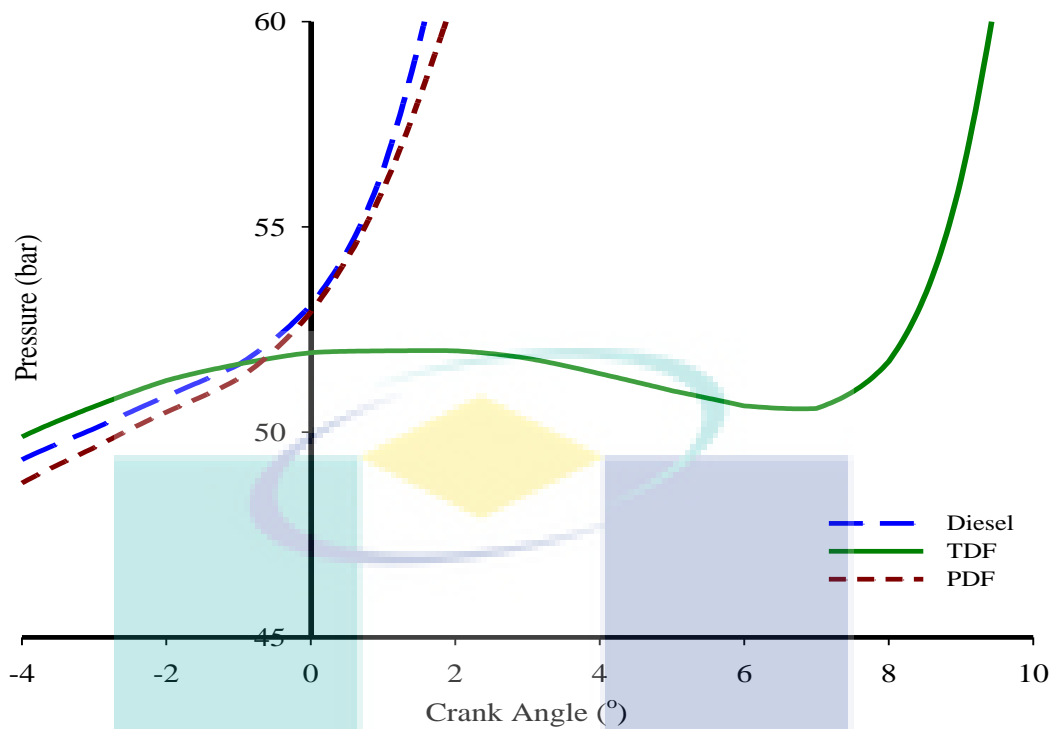
Figure 4.33: Ignition delay at 1800 rpm

Figure 4.34 shows the peak pressure for all test fuels at 1800 rpm. From the figure, it can be observed that TDF has the highest peak pressure which is 80.9 bar at 12° aTDC while diesel fuel is the second highest which is 75 bar at 9° aTDC. PDF produces lowest combustion pressure which is 71.8 bar at 9° aTDC. This trend can be related to the ignition delay of TDF which is the longest among the fuel. As described in section 4.9.1, prolong ignition delay because more fuel entering the combustion chamber, thus cause more rapid and higher pressure rise when the combustion occurs. This cause the peak pressure of TDF is higher compared to other test fuels.

PDF produces lowest peak pressure compared to other test fuels. This phenomenon can be related to the gross calorific value of PDF which is lower compared to TDF and diesel fuel. Lower gross calorific value will cause less energy released as the fuel is combusted in the combustion chamber hence produce lower peak pressure compared to the fuel that has higher gross calorific value. Moreover, PDF has lower density compared to TDF and diesel fuel thus cause lower peak pressure when PDF is combusted. This is because less mass of PDF is combusted in the combustion chamber

for the same volume compared to diesel fuel and TDF, thus cause the peak pressure of PDF is lower compared to TDF and diesel fuel.
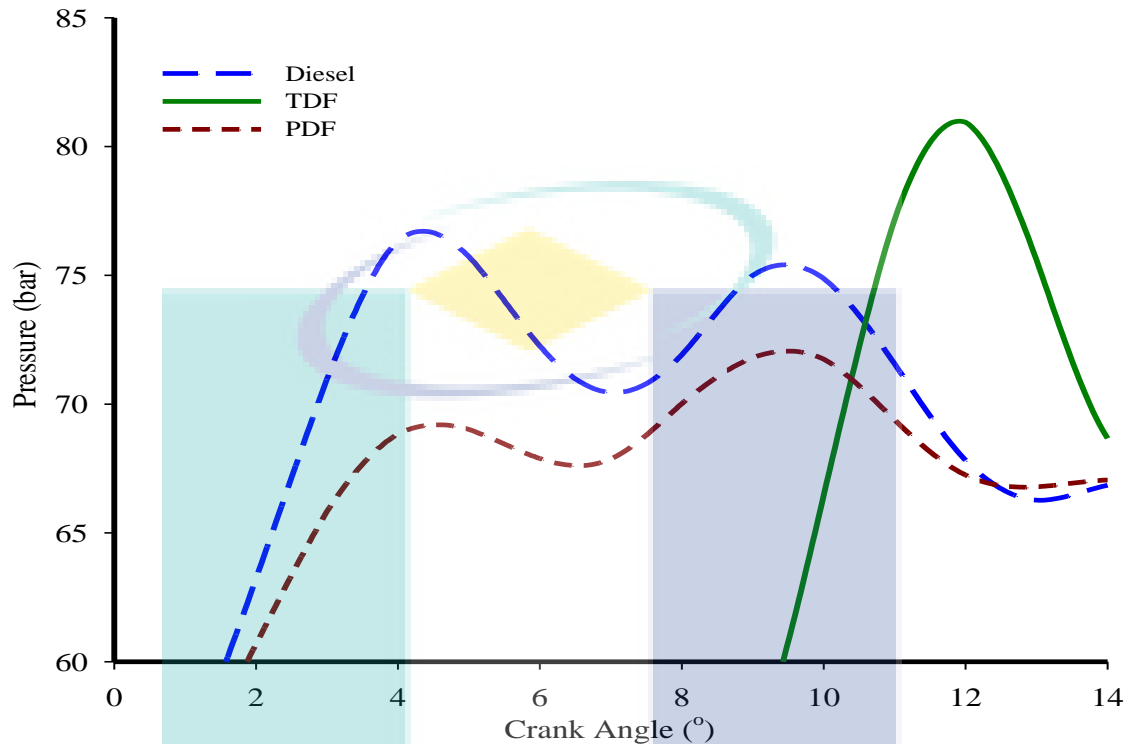
Figure 4.34: Peak pressure at 1800 rpm

4.9.3 Combustion Characteristics at 2100 rpm

Figure 4.35 shows the cylinder pressure versus crank angle of test fuels at high speed which is 2100 rpm. The figure shows three different fuels which are diesel fuel, TDF and PDF. There are two regions that mainly discussed in the figure. The first region is the ignition delay where it is shown in area labelled as 'A'. The second region is the peak pressure which shown in area labelled as 'B'.

Figure 4.36 shows the ignition delay of the test fuels at 2100 rpm. Referring to Figure 4.35, ignition delay is the region labelled as 'A'. From the figure, it can be observed that the ignition delay of TDF is the longest while diesel fuel and PDF have comparable ignition delay.
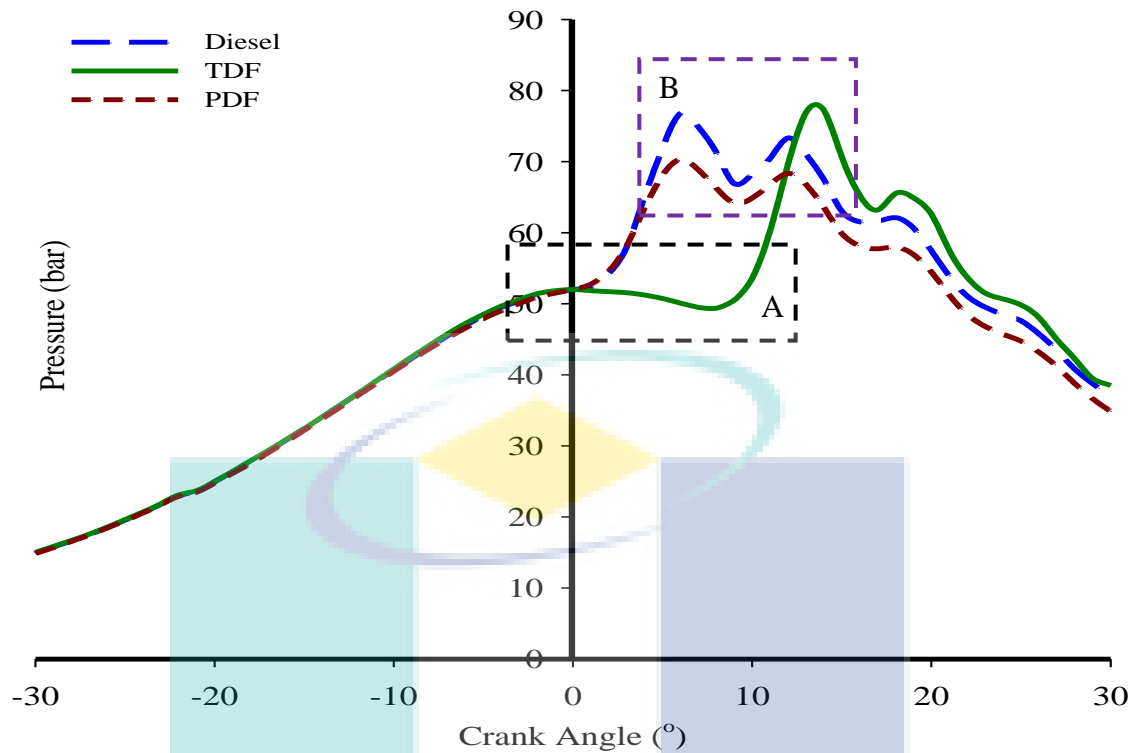
Figure 4.35: Cylinder pressure at 2100 rpm

TDF has the longest ignition delay because of its lowest cetane number. Since it has lowest cetane number, its ignition delay is the longest compared to diesel fuel and PDF. Moreover, it has higher kinematic viscosity compared to diesel fuel and PDF. Higher kinematic viscosity will cause larger fuel droplets, thus reduces the fuel surface area. This condition lowers the mixing rate between fuel and air and cause longer time for combustible mixture to be formed. This cause longer ignition delay as the engine speed increase.
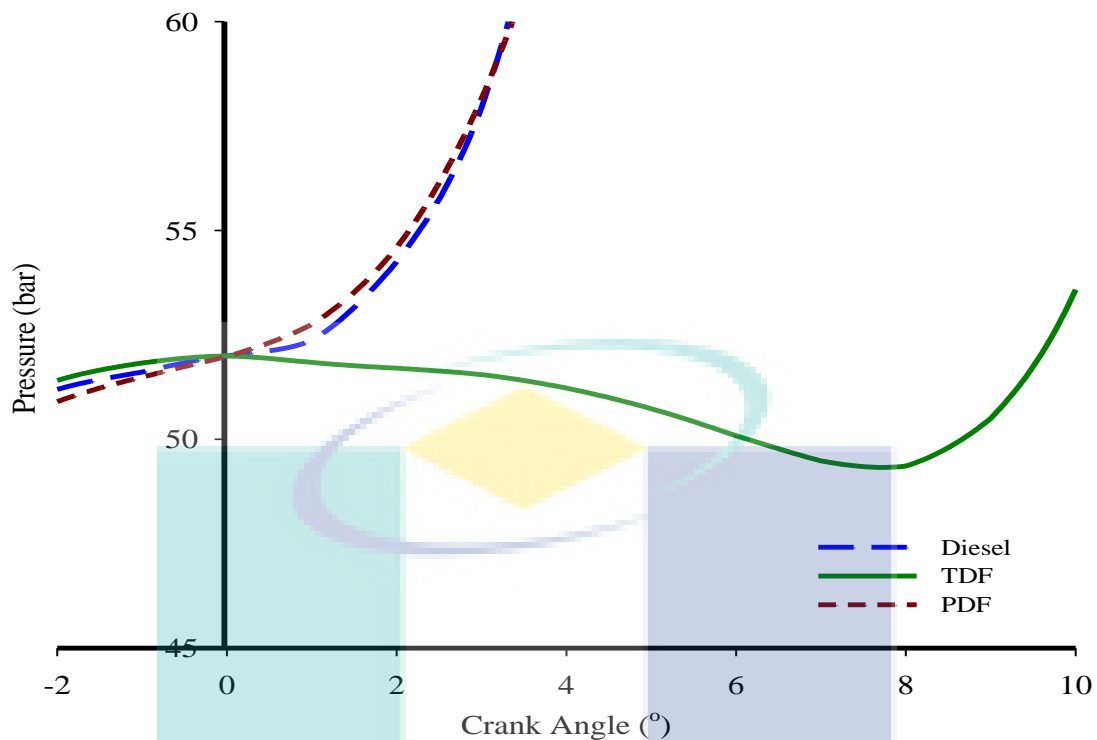
Figure 4.36: Ignition delay at 2100 rpm

The ignition delay for diesel fuel and PDF have comparable timing that is possibly related to higher cetane number for diesel fuel and shorter time for combustible air-fuel mixture to be formed for PDF. Diesel fuel has higher cetane number compared to PDF. Higher cetane number will cause shorter ignition delay thus produce higher combustion quality of the diesel fuel. Compared to diesel fuel, PDF has lower cetane number where it supposedly has longer ignition delay compared to diesel fuel. However, it has comparable ignition delay because of its lower kinematic viscosity compared to diesel fuel. Lower kinematic viscosity cause finer fuel droplets when PDF is injected into the combustion chamber. Finer fuel droplets will improve the mixing rate between the fuel and air, thus shorten the time for combustible air-fuel mixture to be formed. This condition possibly causes PDF has comparable ignition delay compared to diesel fuel even it has lower cetane number.
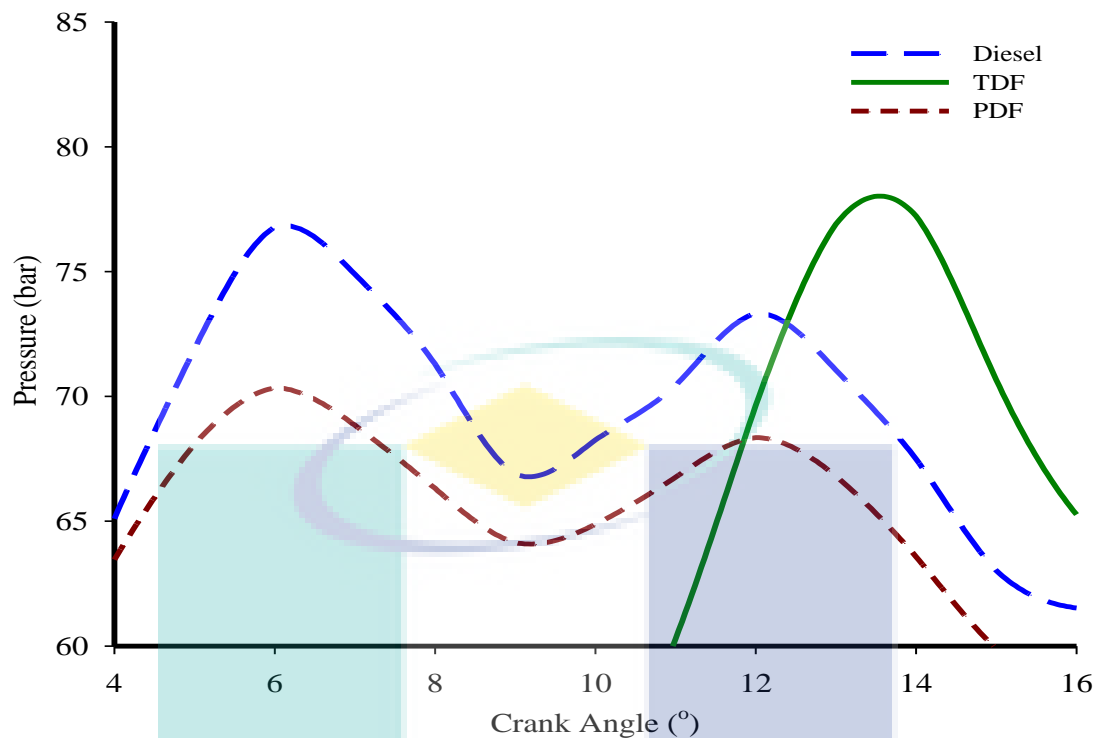
Figure 4.37: Peak pressure at 2100 rpm

Figure 4.37 shows the peak pressure of test fuels at 2100 rpm. Referring to Figure 4.35, peak pressure refers to the region in the box labelled as 'B'. From the figure, it can be observed that TDF has the highest peak pressure which is 77.2 bar at 14° aTDC while diesel fuel has the second highest peak pressure which is 76.7 bar at 6° aTDC. PDF has the lowest peak pressure among the test fuels which is 70.3 bar at 6° aTDC.

TDF has the highest peak pressure compared to other fuels where it can be related to its longest ignition delay. Longer ignition delay cause more fuel presence in the combustion chamber between the fuel injection phase and start of combustion. When the combustion starts, a rapid, uncontrolled combustion phase will take place at the beginning where rapid and higher pressure rise will occur as a result of more fuel available in the combustion chamber. However, the peak pressure at 2100 rpm is lower compared to peak pressure at 1800 rpm. This is because the combustion of TDF occurs when the compression pressure in the combustion chamber starts to decrease as the

piston starts to move downward. As the engine speed is increasing, the ignition delay is prolonged thus causing the peak pressure to decrease at higher engine speed.

PDF produces the lowest peak pressure compared to TDF and diesel fuel probably because of its lower gross calorific value and density compared to the other fuels. Fuel that has lower gross calorific value will produce less energy when it is combusted. This will result on lower peak pressure compared to the fuel that has higher gross calorific value. Moreover, fuel that has lower density will combust less mass for the same volume compared to more dense fuel thus producing lower peak pressure.

4.10   Exhaust Gas Emission of PDF

4.10.1 Exhaust Gas Temperature
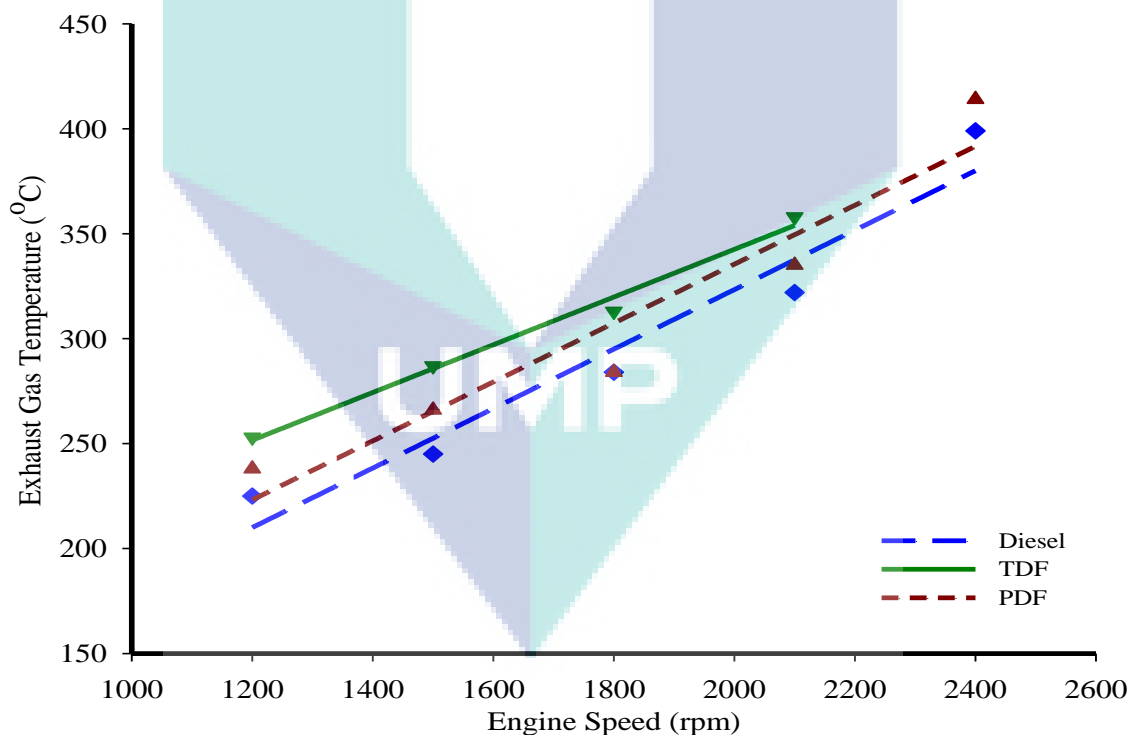
Figure 4.38: Exhaust gas temperature

Figure 4.38 shows the variations of exhaust gas temperature versus engine speed for diesel fuel, TDF and PDF. From the figure, it can be observed that PDF produces

higher exhaust gas temperature compared to diesel fuel by 4% in average. However, PDF produce lower exhaust gas temperature compared to TDF by 1.3% in average. The exhaust gas temperature for all fuels increases as the engine speed increases. This is because more fuel is combusted as the engine speed increases. The PDF produce higher exhaust gas temperature compared to diesel fuel because PDF has lower kinematic viscosity compared to diesel fuel. Lower kinematic viscosity produces finer fuel droplets, hence improve the PDF combustion. This factor cause higher exhaust gas temperature for PDF compared to diesel fuel. TDF produce higher exhaust gas temperature compared to PDF because TDF has longer ignition delay compared to PDF. Longer ignition delay cause higher rate of heat release when the combustion starts, hence producing higher exhaust gas temperature.

4.10.2 Carbon Monoxide (CO) Emission
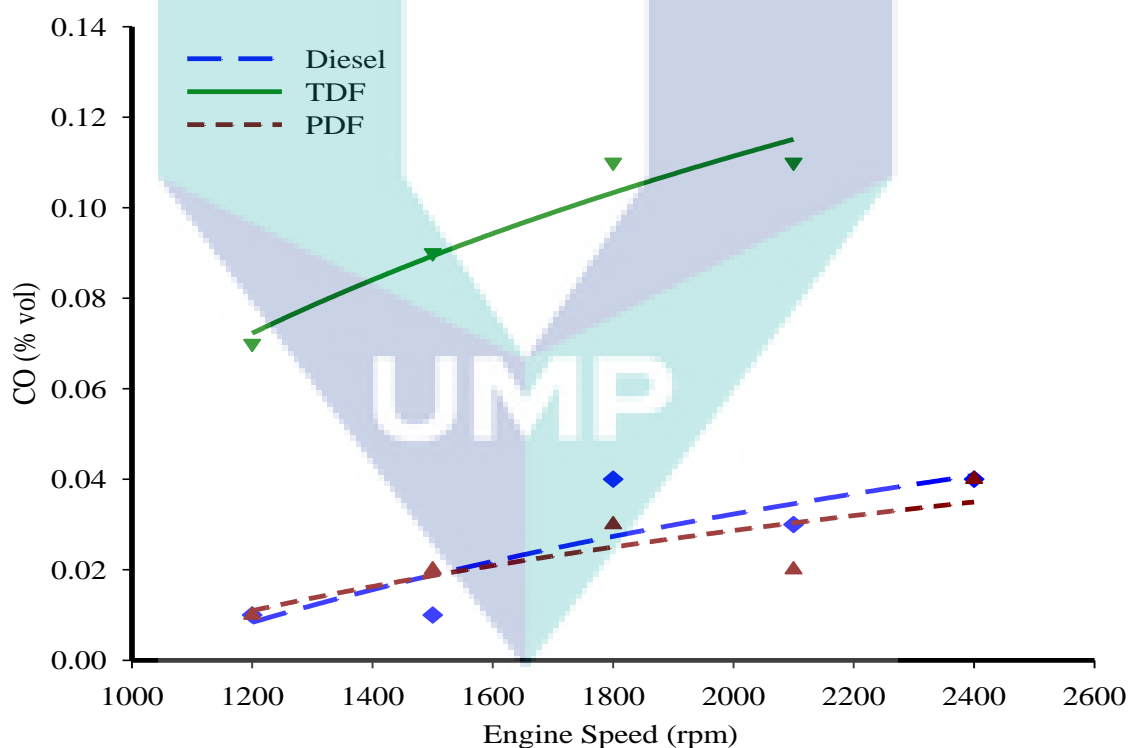
Figure 4.39: Carbon monoxide (CO) emission

Figure 4.39 shows the carbon monoxide (CO) emission versus engine speed for the test fuels. From the figure, it is shown that PDF produce lower CO emission

compared to diesel fuel by 33.3% in average. PDF also produces lower amount of CO compared to TDF by 92% in average. The formation of CO is caused by incomplete combustion of the fuel. This is influenced by the mixture preparation and local rich regions. Since PDF has lower kinematic viscosity, the fuel droplets that are formed during fuel atomization are finer. Finer fuel droplets cause better mixing between fuel and air hence producing more complete combustion. This causes the CO produced when PDF is used as fuel is lower compared to TDF and diesel fuel. TDF produces highest level of CO because of its highest kinematic viscosity. High kinematic viscosity causes larger fuel droplets produced during fuel atomization. This cause poor mixing between air and fuel hence cause incomplete combustion. This condition causes high level of CO emission produced by TDF combustion.

4.10.3 Carbon Dioxide (CO$_2$) Emission
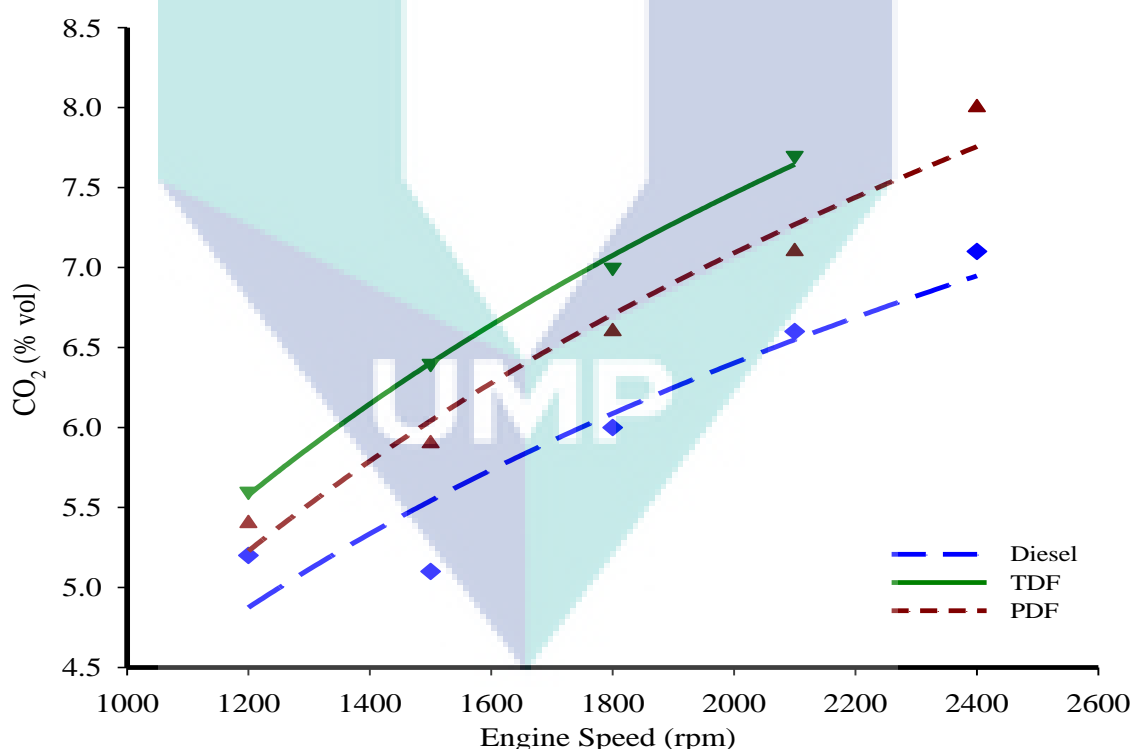
Figure 4.40: Carbon dioxide (CO$_2$) emission

Figure 4.40 shows the carbon dioxide (CO$_2$) emission versus engine speed for test fuels. From the figure, it can be seen that PDF produces higher level of CO$_2$

compared to diesel fuel by 10% in average. Then, the CO_2 emission level when PDF test is lower compared to TDF by 1.5% in average. CO_2 is a product of complete fuel combustion. Since PDF has better air-fuel mixing due to finer fuel droplets compared to diesel fuel, the combustion of PDF produce more CO_2 due to more complete combustion. TDF produce highest level of CO_2 because of high carbon content in TDF compared to diesel fuel and PDF.

4.10.4 Nitrogen Monoxide (NO) Emission
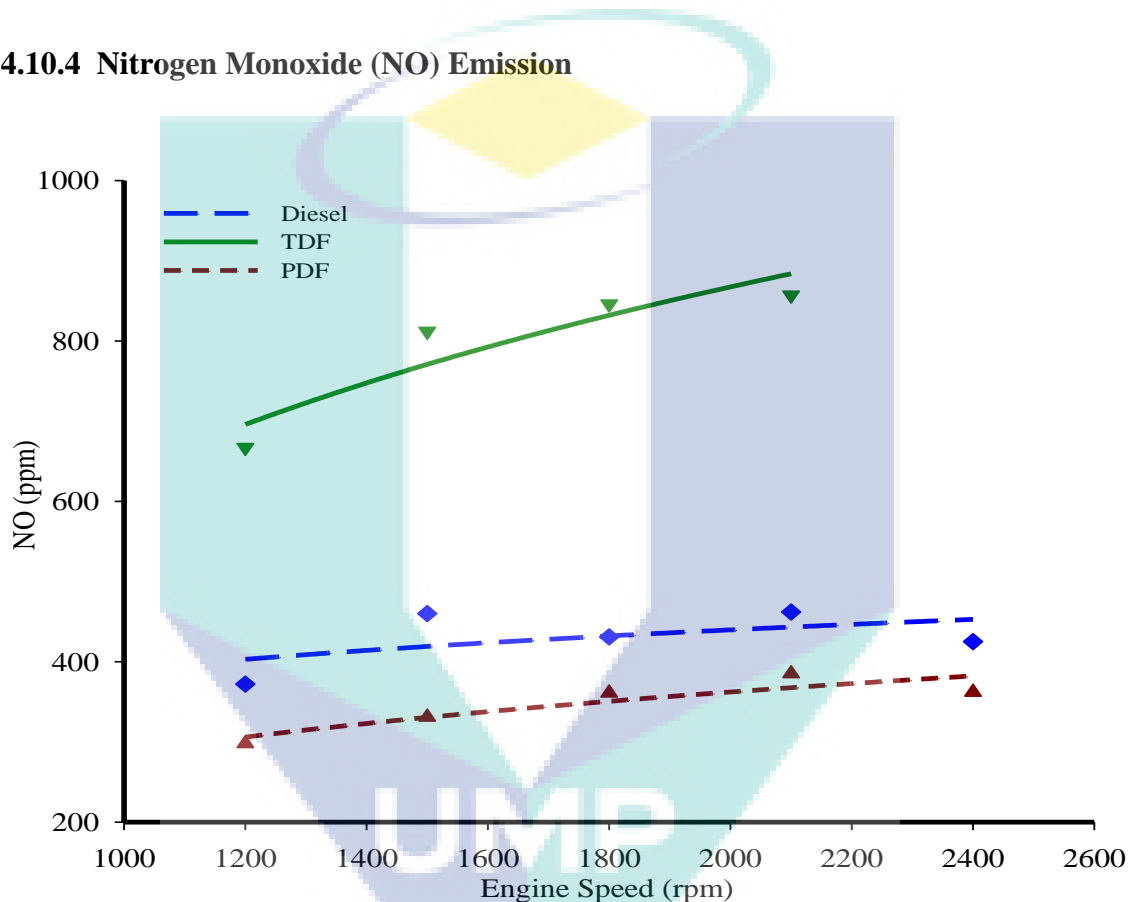
Figure 4.41: Nitrogen monoxide (NO) emission

Figure 4.41 shows the nitrogen monoxide (NO) emission versus engine speed. Form the figure, it can be observed that PDF produces lower NO emission compared to diesel fuel by 19.3% and 56.4% lower compared to TDF in average. PDF produce the lowest amount of NO compared to diesel and TDF because PDF has lowest heat release rate compared to the other fuel. This can be seen from the peak pressure of PDF. Compared to the other fuel, PDF produce lowest peak pressure hence cause lowest amount of NO. TDF produce highest level of NO because TDF has the longest ignition

delay. Longer ignition delay cause more fuel exist in the combustion chamber during delay period, cause rapid pressure rise and high heat release rate. This condition cause high level of NO when TDF is used.

4.10.5 Nitrogen Oxides (NO$_x$) Emission
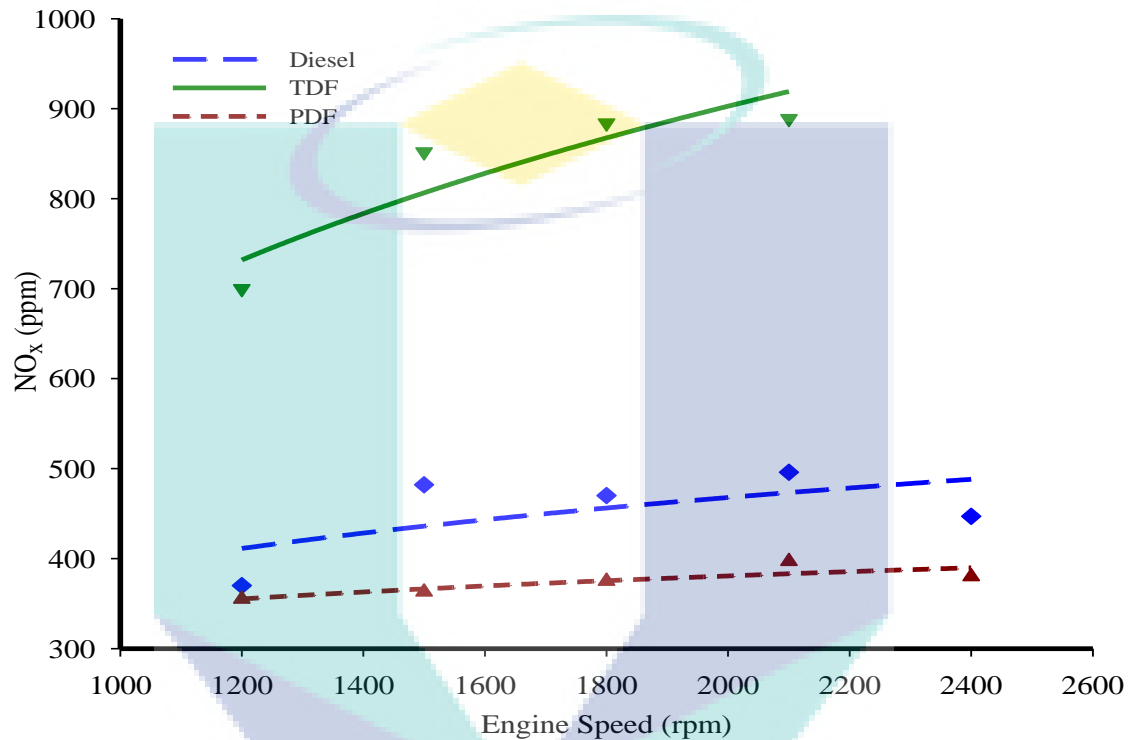
Figure 4.42: Nitrogen oxides (NO$_x$) emission

Figure 4.42 shows the nitrogen oxides (NO$_x$) emission versus engine speed for diesel fuel, PDF and TDF. From the figure, it can be observed that PDF produce lower NO$_x$ emission compared to diesel fuel by 17.4% in average and lower compared to TDF by 55% in average. The trend shown in Figure 4.42 is same with the trend in Figure 4.41. This is because NO$_x$ may consist of NO or NO$_2$. PDF produces lowest level of NO$_x$ because PDF produce lowest combustion temperature compared to other fuels. This can be observed through the lowest level of peak pressure produced by PDF compared to diesel fuel and TDF. Lower combustion temperature causes lower amount of NO$_x$.

CHAPTER 5

CONCLUSIONS AND RECOMMENDATIONS

5.1   Introduction

This chapter mainly will conclude the results obtained from the Chapter 4. The suitability of TDF and PDF that were studied in this thesis to be used as alternative fuel for diesel engine is concluded. This chapter also includes the conclusion about the objectives for this experiment either has been achieved or not. Next, the recommendations about the future research were also being made. The recommendations are made upon the problem and also findings that were obtained during the research conducted.

5.2   Conclusions

Based on the problem statement that stated in section 1.2, there are three objectives that being made. The first objective is to determine the fuel properties of TDF, TDF-diesel fuel blends and PDF. The tested fuels are undergoes chemical lab testing to determine the fuel properties. From the results obtained, the gross calorific value and flash point of TDF-diesel fuel blends are higher compared to diesel fuel and TDF. However, the value decreases when the TDF ratio is increases. Other than that, the fuel density is decreases as the TDF ratio is decreases. While for PDF, the kinematic viscosity, density and gross calorific value are the lowest compared to diesel fuel and TDF.

The second objective for this experiment is to evaluate the performance of TDF and PDF when used as fuel in diesel engine. From the results obtained, diesel engine is able to run with pure, unblended TDF and PDF. Compared to diesel fuel, both TDF and

PDF gives lower performance output. For TDF, it is known that TDF is not suitable for high speed application since it will cause backfires. TDF also emits higher emission level compared to diesel. However, PDF emits lower CO and NOx emission level compared to diesel fuel and TDF.

The third objective that achieved in this thesis is to evaluate the effect when several blend ratio of TDF-diesel fuel are used in diesel engine. There are three different blend ratios that tested which are TDF10%, TDF30% and TDF50%. Each of the fuel undergoes engine testing to measure the effect of different blend ratio to engine performance. All of the tested fuel which is diesel, TDF, PDF, TDF10%, TDF30% and TDF50% also undergoes lab testing to determine the fuel properties for each fuel. From the results obtained, it can be observed that when TDF blend ratio is increases, the engine performance output is decreases. The emissions level are also increases with the increment of TDF blend ratio.

5.3   Recommendations

From this research, there are several recommendations that are suggested. These recommendations are made based from the results obtained. After analysis and discussions that being made in Chapter 4, recommendations for improvement is made for future work in order to gain more understanding of the engine performance when TDF and PDF are used as alternative fuel. The recommendations for further area of research are also being made to expand the possibility for TDF and PDF to be used in diesel engine as alternative fuel.

5.3.1   Validating experimental results using simulation software

Engine testing results can be influenced by many uncontrolled parameters such as loss (mechanical loss, heat loss, etc), humidity, ambient temperature and many more. These aspects will results on inconsistent performance output. By simulating the performance output using software such as GT-Power, the engine performance when any fuel used can be determined at controlled parameters. Comparisons between the

data obtained through simulation and experiment will gain more understanding about the results.

5.3.2 Spray pattern analysis

Spray pattern also influence the performance output of an engine. Parameters such as droplet size, fuel atomization, cone angle, fuel penetration, mixing rate and others gives significant impact to engine performance output. Study on spray pattern of tested fuels will give more understanding on its combustion characteristics. Methods such as shadowgraph technique and Schlieren photographs can be used to analyze the spray pattern when fuel is injected from the injector.

5.3.3 Use distillate TDF instead of crude TDF as test fuel.

TDF that used in this experiment has high kinematic viscosity hence will cause poor fuel atomization. Distillation of the TDF will improve the kinematic viscosity hence produce better fuel properties and also better performance when used in diesel engine.

REFERENCES

(SAE), S. O. A. E. 2011. Engine Power Test Code - Spark Ignition and Compression Ignition - As Installed Net Power Rating.

Abdul-Raouf, M. E., Maysour, N. E., Abdul-Azim, A.-A. A. & Amin, M. S. 2010. Thermochemical recycling of mixture of scrap tyres and waste lubricating oil into high caloric value products. *Energy Conversion and Management,* **51,** 1304–1310.

Adam, A., Rizalman, M., Kidoguchi, Y. & Yatsufusa, T. 2011. Analysis of Straight Vegetable Oil (SVO) Spray Characteristics and Droplets Distribution by Using Nano-Spark Shadowgraph Photography Technique. *The Third International Renewable Energy Congress.* Hammamet Tunisia.

Amari, T., Themelis, N. J. & Wernick, I. K. 1999. Resource recovery from used rubber tires. *Resources Policy,* **25,** 179-188.

Association, M. A. 2012. Market Review 1st Half 2012 Compared to 1st Half 2011.

Aydın, H. & İlkılıç, C. 2012. Optimization of fuel production from waste vehicle tires by pyrolysis and resembling to diesel fuel by various desulfurization methods. *Fuel,* **102,** 605-612.

Banar, M., Akyıldız, V., Özkan, A., Çokaygil, Z. & Onay, Ö. 2012. Characterization of pyrolytic oil obtained from pyrolysis of TDF (Tire Derived Fuel). *Energy Conversion and Management,* **62,** 22-30.

Baranescu, R. & Challen, B. J. 1999. *Diesel Engine Reference Book.*

Bhatt, M. P. & Patel, D. P. 2012. Suitability of Tyre Pyrolysis Oil (TPO) as an Alternative Fuel for Internal Combustion Engine. *International Journal of Advanced Engineering Research and Studies,* **1,** 61-65.

Borman, G. L. & Ragland, K. W. 1998. *Combustion engineering*, McGraw-Hill New York.

Brain, M. 2000. *How Diesel Two-Stroke Engines Work* [Online]. Available: http://auto.howstuffworks.com/diesel-two-stroke1.htm [Accessed 22 November 2014].

Budhiarta, I., Siwar, C. & Basri, H. 2012. Current Status of Municipal Solid Waste Generation in Malaysia. *International Journal on Advanced Science Engineering Information Technology,* **2,** 16-21.

Cataluna, R. & Silva, R. D. 2012. Effect of Cetane Number on Specific Fuel Consumption and Particulate Matter and Unburned Hydrocarbon Emission from Diesel Engines. *Journal of Combustion*.

Chong, T. L. 2006. Waste to Wealth: How it works in Malaysia. *IMPAK.* Department of Environment, Ministry of Natural Resources and Environment.

Doğan, O., Çelik, M. B. & Özdalyan, B. 2012. The effect of tire derived fuel/diesel fuel blends utilization on diesel engine performance and emissions. *Fuel,* **95,** 340-346.

El-Kasaby, M. & A.Nemit-Allah, M. 2013. Experimental Investigations of Ignition Delay Period and Performance of a Diesel Engine Operated with Jatropha Oil Biodiesel. *Alexandria Engineering Journal,* **52,** 141–149.

Enweremadu, C. C. & Rutto, H. L. 2010. Combustion, emission and engine performance characteristics of used cooking oil biodiesel—A review. *Renewable and Sustainable Energy Reviews,* **14,** 2863–2873.

Fauziah, S. & Agamuthu, P. 2012. Trends in sustainable landfilling in Malaysia, a developing country. *Waste Management & Research,* 30**,** 656-663.

Flagan, R. C. & Seinfeld, J. H. 2012. *Fundamentals of air pollution engineering,* Courier Dover Publications.

Frigo, S., Seggiani, M., Puccini, M. & Vitolo, S. 2014. Liquid fuel production from waste tyre pyrolysis and its utilisation in a Diesel engine. *Fuel,* **116,** 399-408.

Ganesan, V. 2012. *Internal Combustion Engines*, McGraw Hill.

Hariharan, S., Murugan, S. & Nagarajan, G. 2013. Effect of diethyl ether on Tyre pyrolysis oil fueled diesel engine. *Fuel,* **104,** 109-115.

Harshal, R. P. & Shailendra, M. L. 2013. Waste plastic Pyrolysis oil Alternative Fuel for CI Engine - A Review. *Research Journal of Engineering Sciences,* 2.

Heywood, J. B. 1988. *Internal Combustion Engine Fundamental*, McGraw-Hill.

Hossain, A. K. & Davies, P. A. 2013. Pyrolysis liquids and gases as alternative fuels in internal combustion engines – A review. *Renewable and Sustainable Energy Reviews,* **21,** 165-189.

İlkılıç, C. & Aydın, H. 2011. Fuel production from waste vehicle tires by catalytic pyrolysis and its application in a diesel engine. *Fuel Processing Technology,* **92,** 1129–1135.

Islam, M. R., Tushar, M. S. H. K. & Haniu, H. 2008. Production of liquid fuels and chemicals from pyrolysis of Bangladeshi bicycle/rickshaw tire wastes. *Journal of Analytical and Applied Pyrolysis,* **82,** 96-109.

Jääskeläinen, H. 2013. *Early History of the Diesel Engine* [Online]. Available: https://www.dieselnet.com/tech/diesel_history.php [Accessed 1 April 2015]

Janès, A. & Chaineaux, J. 2013. Experimental Determination Of Flash Points Of Flammable Liquid Aqueous Solutions. *Chemical Engineering Transactions,* 31.

Kumar, S., Prakash, R., Murugan, S. & Singh, R. K. 2013. Performance and emission analysis of blends of waste plastic oil obtained by catalytic pyrolysis of waste HDPE with diesel in a CI engine. *Energy Conversion and Management,* **74,** 323-331.

Lefebvre, A. H. 1989. *Atomization and Sprays.*

Mani, M. & Nagarajan, G. 2009. Influence of injection timing on performance, emission and combustion characteristics of a DI diesel engine running on waste plastic oil. *Energy,* **34,** 1617–1623.

Mani, M., Nagarajan, G. & Sampath, S. 2010. An experimental investigation on a DI diesel engine using waste plastic oil with exhaust gas recirculation. *Fuel,* **89,** 1826–1832.

Mani, M., Nagarajan, G. & Sampath, S. 2011. Characterisation and effect of using waste plastic oil and diesel fuel blends in compression ignition engine. *Energy,* **36,** 212-219.

Mani, M., Subash, C. & Nagarajan, G. 2009. Performance, emission and combustion characteristics of a DI diesel engine using waste plastic oil. *Applied Thermal Engineering,* **29,** 2738–2744.

Martyr, A. J. & Plint, M. A. 2007. *Engine Testing Theory and Practice*, Elsevier Ltd.

Mcallister, S., Chen, J.-Y. & Fernandez-Pello, A. C. 2011. Diesel Engines. *Fundamentals of Combustion Processes.* Springer.

Mcnamee, R., Monk, I., Page, T. & Taglieri, M. 2010. *Hydraulic Dynamometer.* Degree of Bachelor of Science, Worcester Polytechnic Institute.

Murphy, F., Mcdonnell, K., Butler, E. & Devlin, G. 2012. The evaluation of viscosity and density of blends of Cyn-diesel pyrolysis fuel with conventional diesel fuel in relation to compliance with fuel specifications EN 590:2009. *Fuel,* **91,** 112–118.

Murugan, S., Ramaswamy, C. & Nagarajan, G. 2008a. Influence of distillation on performance, emission, and combustion of a DI diesel engine, using tyre pyrolysis oil diesel blends. *Thermal Science,* **12,** 157-167.

Murugan, S., Ramaswamy, M. C. & Nagarajan, G. 2008. The use of tyre pyrolysis oil in diesel engines. *Waste Management,* **28,** 2743-2749.

Murugan, S., Ramaswamy, M. C. & Nagarajan, G. 2008b. A comparative study on the performance, emission and combustion studies of a DI diesel engine using distilled tyre pyrolysis oil–diesel blends. *Fuel,* **87,** 2111-2121.

Murugan, S., Ramaswamy, M. C. & Nagarajan, G. 2008c. Running a Diesel Engine with Tire Pyrolysis Oil Diesel Blends at Different Injection Pressures. *Thammasat Int. J. Sc. Tech,* **13,** 56-65.

Murugan, S., Ramaswamy, M. C. & Nagarajan, G. 2008d. The use of tyre pyrolysis oil in diesel engines. *Waste Management,* **28,** 2743-2749.

Naima, K. & Liazid, A. 2013. Waste oils as alternative fuel for diesel engine: A review. *Journal of Petroleum Technology and Alternative Fuels,* **4,** 30-43.

Nicolas, R. 2013. *Introduction to engine fuelling systems* [Online]. Available: http://www.car-engineer.com/introduction-to-engine-fuelling-systems/#prettyPhoto [Accessed 11 September 2014].

Panda, A. K., Singh, R. K. & Mishra, D. K. 2010. Thermolysis of waste plastics to liquid fuel; A suitable method for plastic waste management and manufacture of value added products—A world prospective. *Renewable and Sustainable Energy Reviews,* **14,** 233–248.

Patel, N. S. & Desai, K. D. 2013. Waste Plastic Oil As A Diesel Fuel In The Diesel Engine: A Review. *International Journal of Engineering Research & Technology,* **2**, 1-6.

Pratoomyod, J. & Laohalidanond, K. 2013. Performance and Emission Evaluation of Blends of Diesel fuel with Waste Plastic Oil in a Diesel Engine. *International Journal of Engineering Science and Innovative Technology,* **2**, 57-63.

Pulkrabek, W. W. 2004. *Engineering fundamentals of the internal combustion engine*, Pearson Prentice Hall New Jersey.

Pundir, B. P. 2010. *IC Engines Combustion and Emissions*, Alpha Science.

Rodríguez, R. P., Sierens, R. & Verhelst, S. 2011. Ignition delay in a palm oil and rapeseed oil biodiesel fuelled engine and predictive correlations for the ignition delay period. *Fuel,* **90,** 766-772.

S.A.Shahir, H.H.Masjuki, M.A.Kalam, A.Imran, I.M.Rizwanulfattah & A.Sanjid. 2014. Feasibility of diesel–biodiesel–ethanol / bioethanol blend as existing CI engine fuel:An assessment of properties,material compatibility,safety and combustion. *Renewable and Sustainable Energy Reviews,* **32,** 379–395.

Saiyasitpanich, P., Lu, M., Keener, T. C., Liang, F. & Khang, S.-J. 2005. The Effect of Diesel Fuel Sulfur Content on Particulate Matter Emissions for a Nonroad Diesel Generator. *Journal of the Air & Waste Management Association,* **55,** 1-7.

Sebola, R., Pilusa, J. & Muzenda, E. 2013. Characteristics of Tyre Derived Fuel-Diesel Blends. *3rd International Conference on Medical Sciences and Chemical Engineering (ICMSCE'2013).* Bangkok (Thailand).

Sharma, A. & Murugan, S. 2013. Investigation on the behaviour of a DI diesel engine fueled with Jatropha Methyl Ester (JME) and Tyre Pyrolysis Oil (TPO) blends. *Fuel,* **108,** 699-708.

Tan, P.-Q., Hu, Z.-Y. & Lou, D.-M. 2009. Regulated and unregulated emissions from a light-duty diesel engine with different sulfur content fuels. *Fuel,* **88,** 1086-1091.

Tillman, D. & Harding, N. S. 2004. Tire-Derived Fuel as an Alternative Fuel *Fuels of Opportunity: Characteristics and Uses In Combustion Systems: Characteristics and Uses In Combustion Systems.* Elsevier.

Valencia, F. A. & Armas, I. P. 2005. Ignition Quality of Residual Fuel Oils. *Journal of Maritime Research,* **2,** 77-96.

Williams, P. T. 2013. Pyrolysis of waste tyres: A review. *Waste Management,* **33,** 1714-1728.

Youn, I. M., Park, S. H., Roh, H. G. & Lee, C. S. 2011. Investigation on the fuel spray and emission reduction characteristics for dimethyl ether (DME) fueled multi-cylinder diesel engine with common-rail injection system. *Fuel Processing Technology,* **92,** 1280–1287.

Younus, S. M., Kumar, V. R. & Rao, Y. V. H. 2013. Performance and Emissions Characteristics of Diesel Engine Fueled With Tyre Pyrolysis Oil & Diesel Blends with Additives. *International Journal of Engineering Science Invention,* **2,** 32-37.

APPENDIX 1

Diesel Engine Specifications

	Specs
Engine Model	YANMAR TF120M
Type	Horizontal, Diesel 4 Stroke cycle
Combustion System	Direct Injection
Number of Cylinder	1
Injection Timing	17° BTDC
Bore x Stroke (mm)	92 x 96
Displacement (cc)	638
Compression Ratio	17.7
Fuel Injection Pump	Bosch
Injection Pressure (kg/cm^2)	200
Cooling Water System	Radiator Type
Cooling Water Capacity (L)	2.3
Connecting Rod Length (mm)	149.5

APPENDIX 2

YANMAR TF120M Technical Drawing

APPENDIX 3

Hydraulic Specification for Gear Pump

		Specs
Model		HGP-3A-F23
Flow	cc/rev	23.0
Speed Drive	rpm	3000 (max)
		400 (min)
Inlet & outlet size	inch	3/4" (inlet)
		1/2" (outlet)
Maximum Pressure	kg/cm^2	250
Working Pressure	kg/cm^2	210
Weight	kg	3.35

APPENDIX 4a

Dynamometer Bracket Drawing (front bracket)
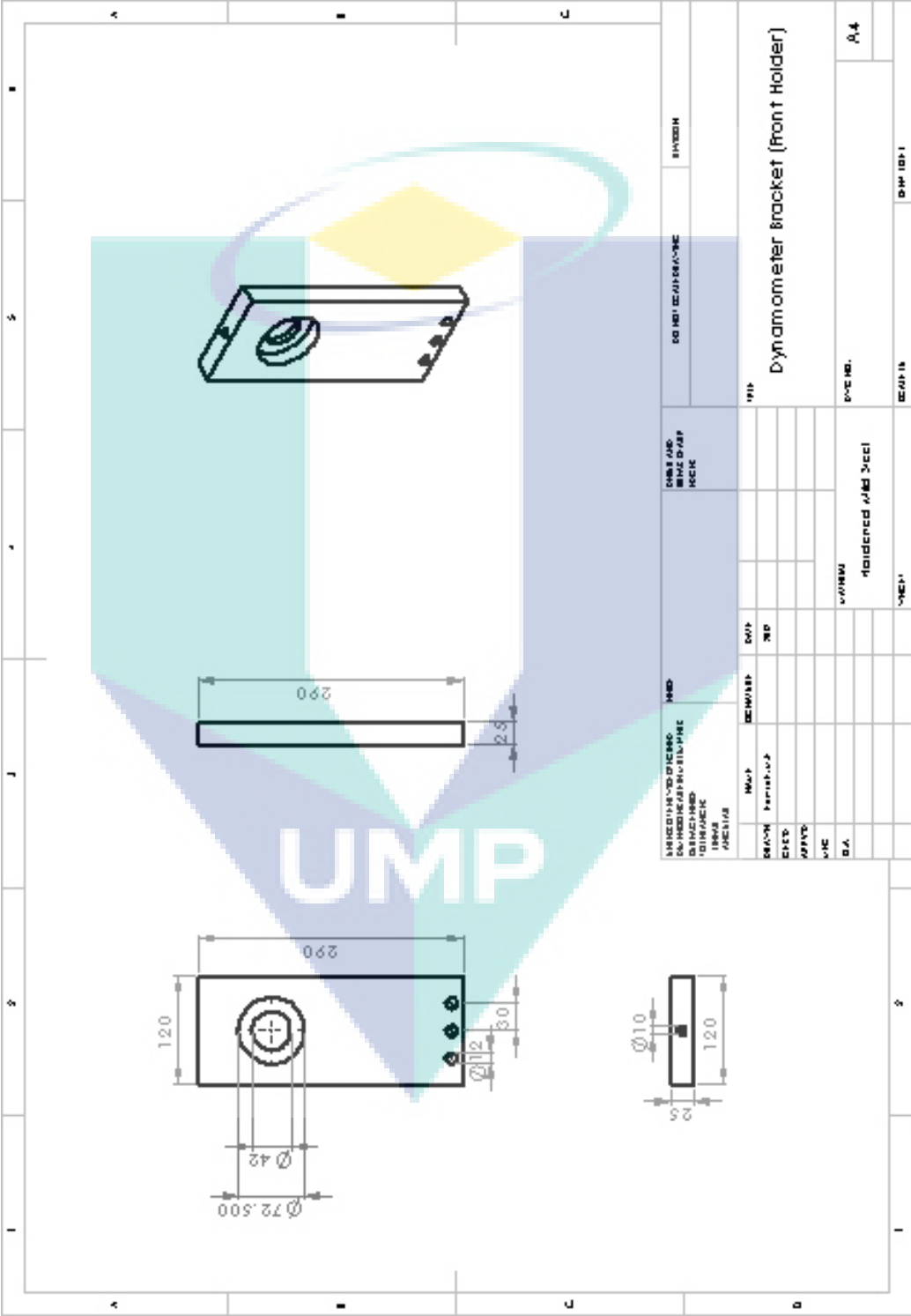
APPENDIX 4b

Dynamometer Bracket Drawing (rear bracket)

APPENDIX 4c

Dynamometer Bracket Drawing (base)

APPENDIX 4d

Dynamometer Bracket Drawing (torque arm)
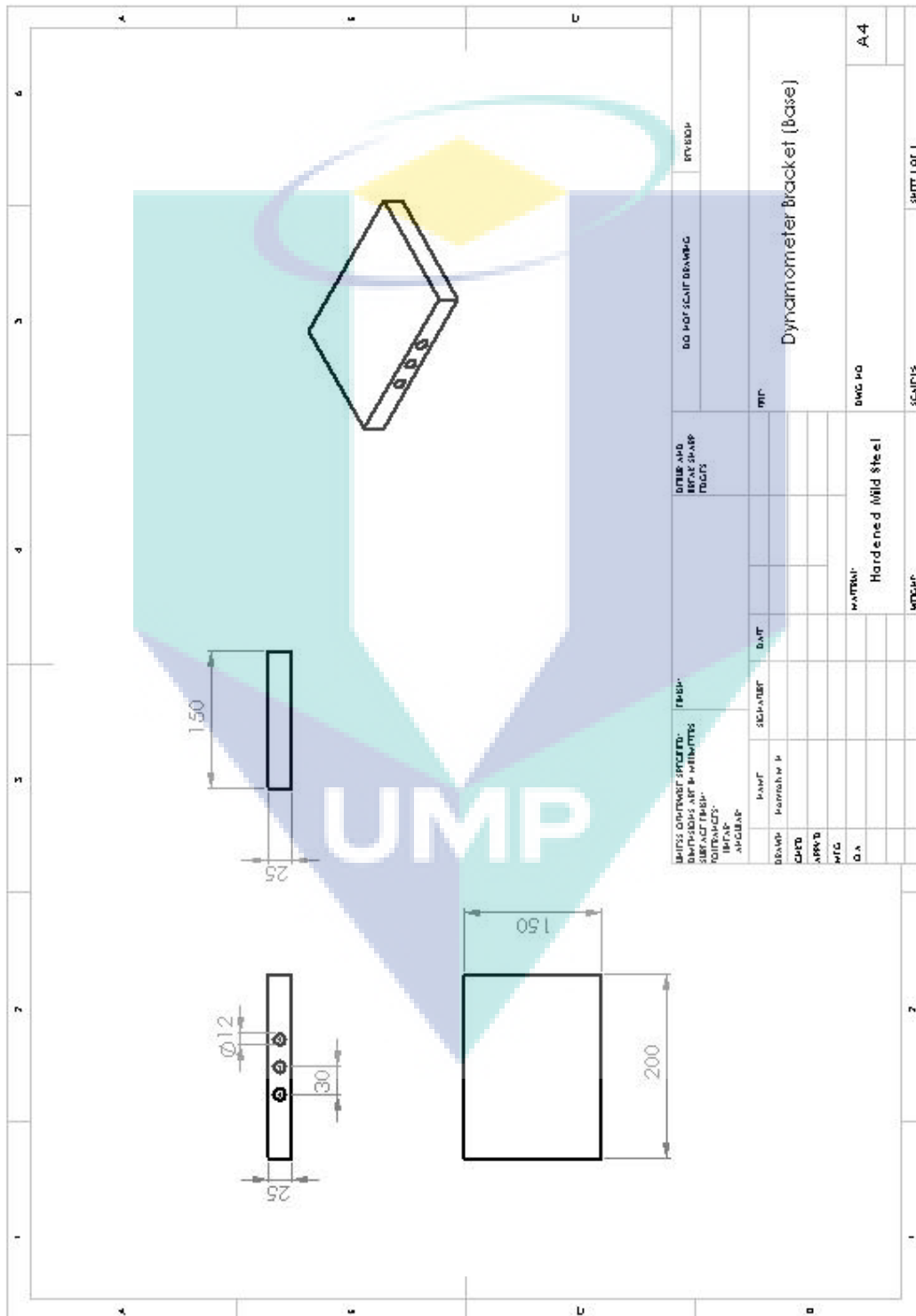
APPENDIX 4e

Dynamometer Bracket Drawing (upper holder)
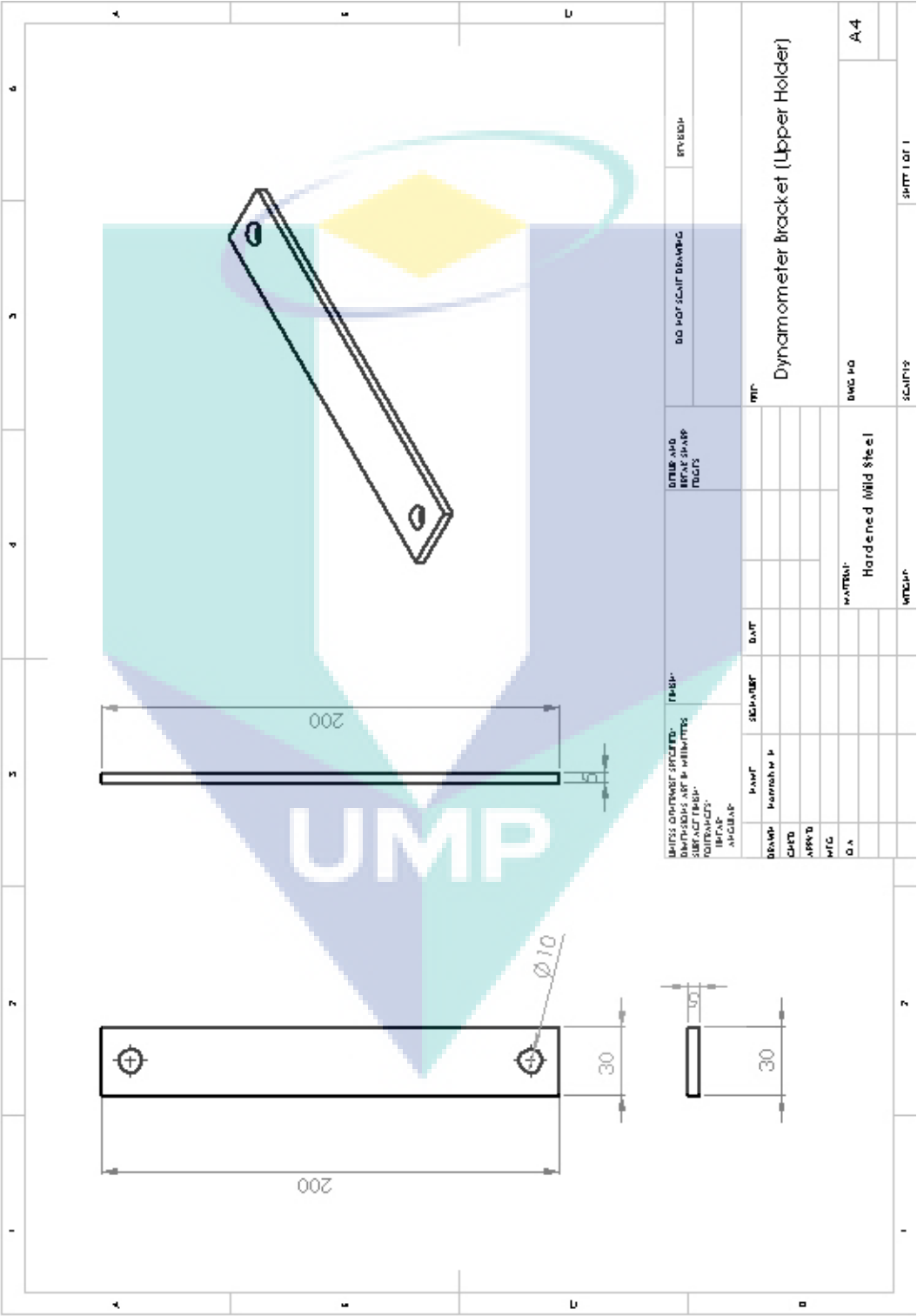
APPENDIX 5

NBK Flexible Coupling Specifications
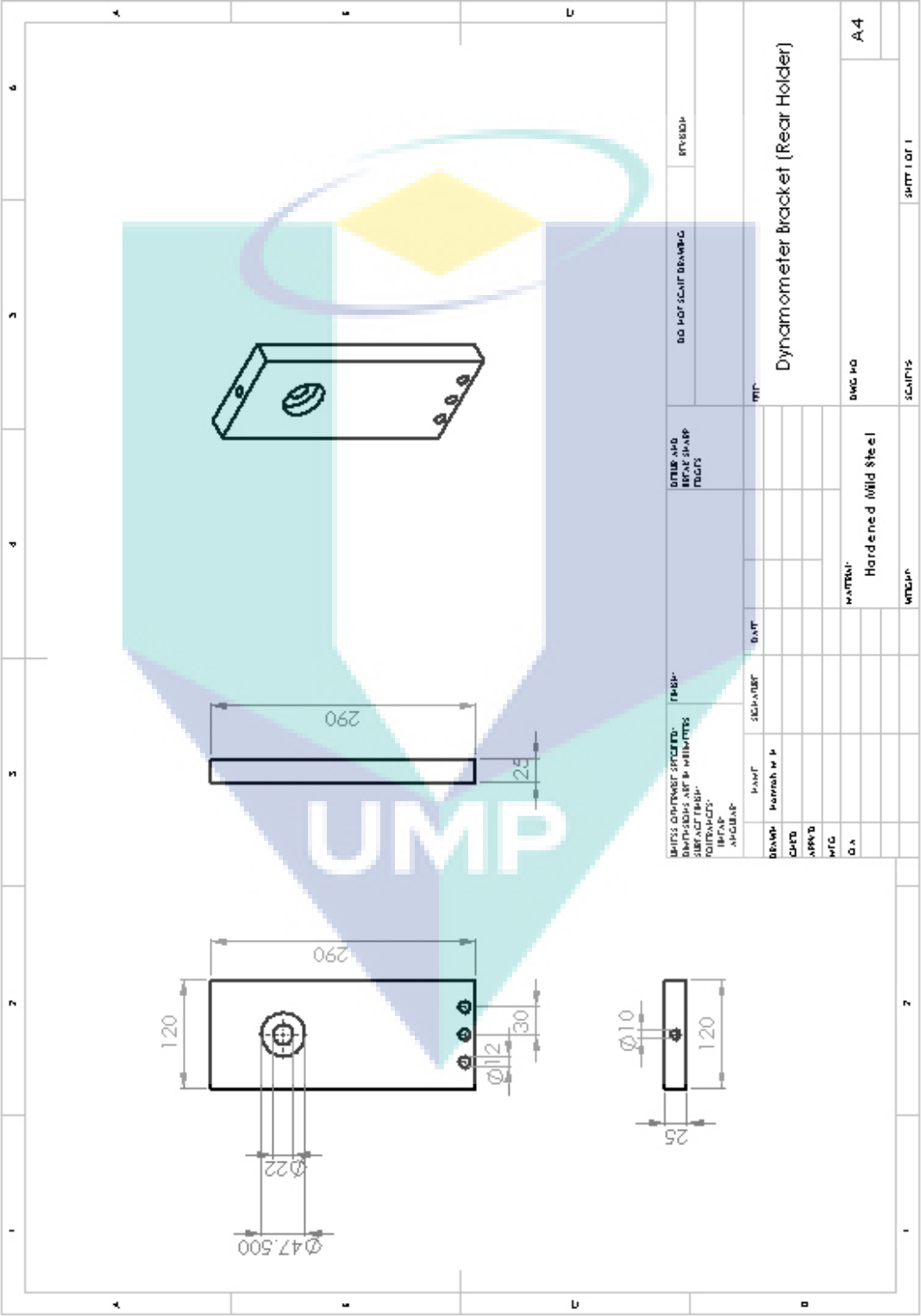
Description	Unit	Specification	
Catalogue Number		FCL 140	
Maximum Bore	mm	D_1	32
		D_2	38
Maximum Torque	kgf/m	13	
Maximum Revolution	min^{-1}	4000	
Moment of Inertia	kg/m^2	1.1×10^{-2}	
Errors of Eccentricity	mm	0.2	
Errors of Angularity		1/6	
Errors of Shaft End-Play	mm	±2.1	
Mass	kg	4.88	

APPENDIX 6

Custom Pulley Drawing
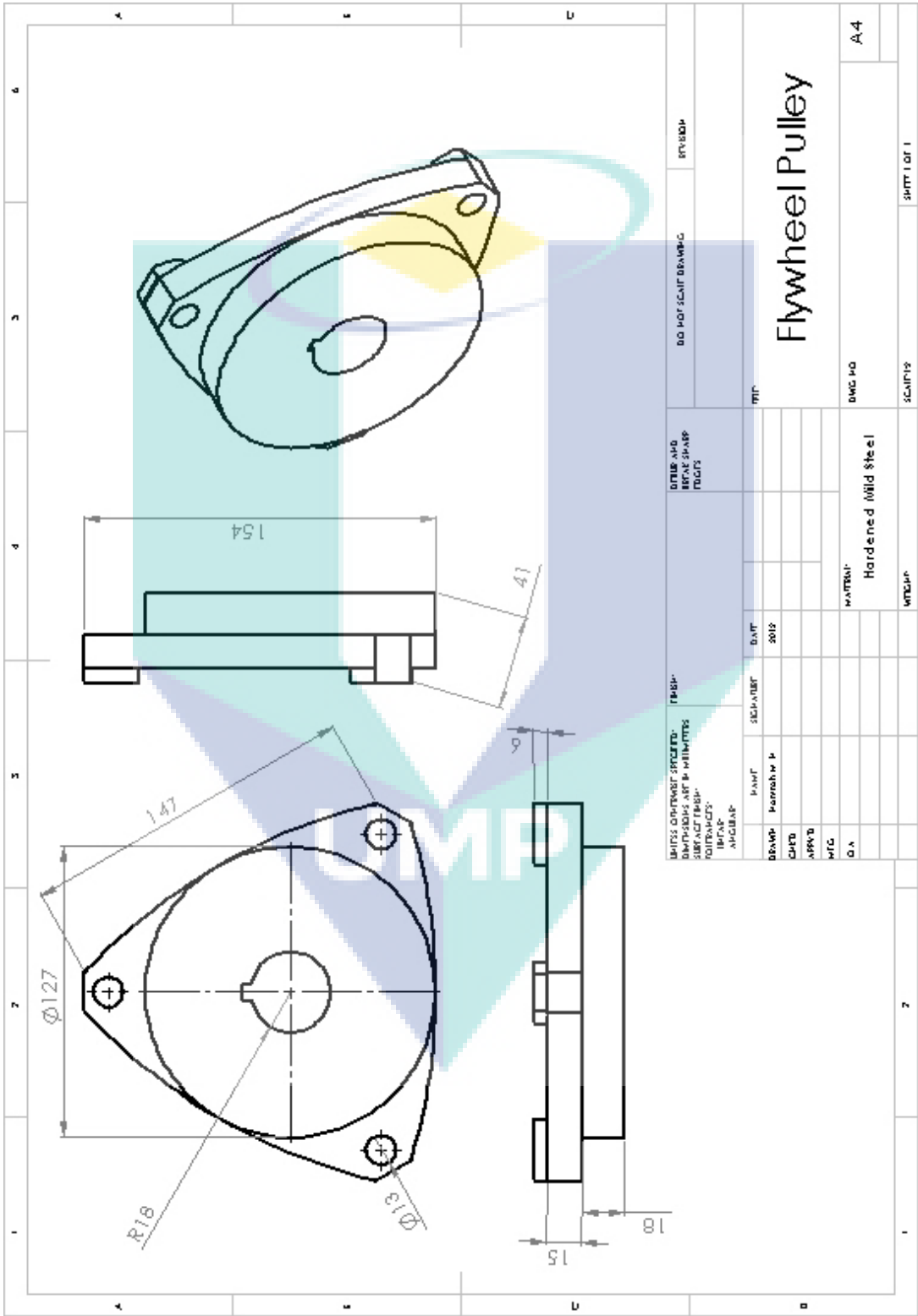
APPENDIX 7

S Type Load Cell Specifications

Parameter	Value				Unit
Rated capacity—R.C. (E_{max})	25, 50, 75, 100, 150, 200, 250, 300, 500, 750, 1k, 1.5k, 2k, 2.5k, 3k, 5k, 10k, 15k, 20k				lbs
	50 kg, 100 kg, 250 kg, 500 kg, 1T, 2.5T, 5T, 10T				kg/metric tons
Rated output—R.O. kg	3.0				mV/V
Rated output tolerance kg	50 kg–1T: +25 / –10 2.5T–3T: ±0.25				%
Zero balance	1.0				±% FSO
Combined error	0.02	0.02	0.03	0.02	±% FSO
Non-repeatability	0.01				±% FSO
Creep error (30 minutes)	0.03	0.025	0.03	0.017	±% FSO
Temperature effect on zero	0.0010	0.0010	0.0015	0.0010	±% FSO/°F
Temperature effect on output	0.0008	0.0008	0.0008	0.0007	±% of load/°F
Compensated temperature range	14 to 104 (–10 to 40)				°F (°C)
Operating temperature range	0 to 150 (–18 to 65)				°F (°C)
Storage temperature range	–60 to 185 (–50 to 85)				°F (°C)
Safe sideload	30				% of R.C.
Maximum safe central overload	150				% of R.C.
Ultimate central overload	300				% of R.C.
Excitation, recommended	10				VDC
Excitation, maximum	15				VDC
Input impedance	343–450				Ω
Output impedance	349–355				Ω
Insulation resistance at 50 VDC	>1000				MΩ
Material	Nickel-plated alloy tool steel				
Environmental protection	IP67				

APPENDIX 8

Calibration Chart of Load Cell

Mass (kg)	Voltage (mV)
1	14.59
2	15.59
3	16.59
4	17.59
5	18.59
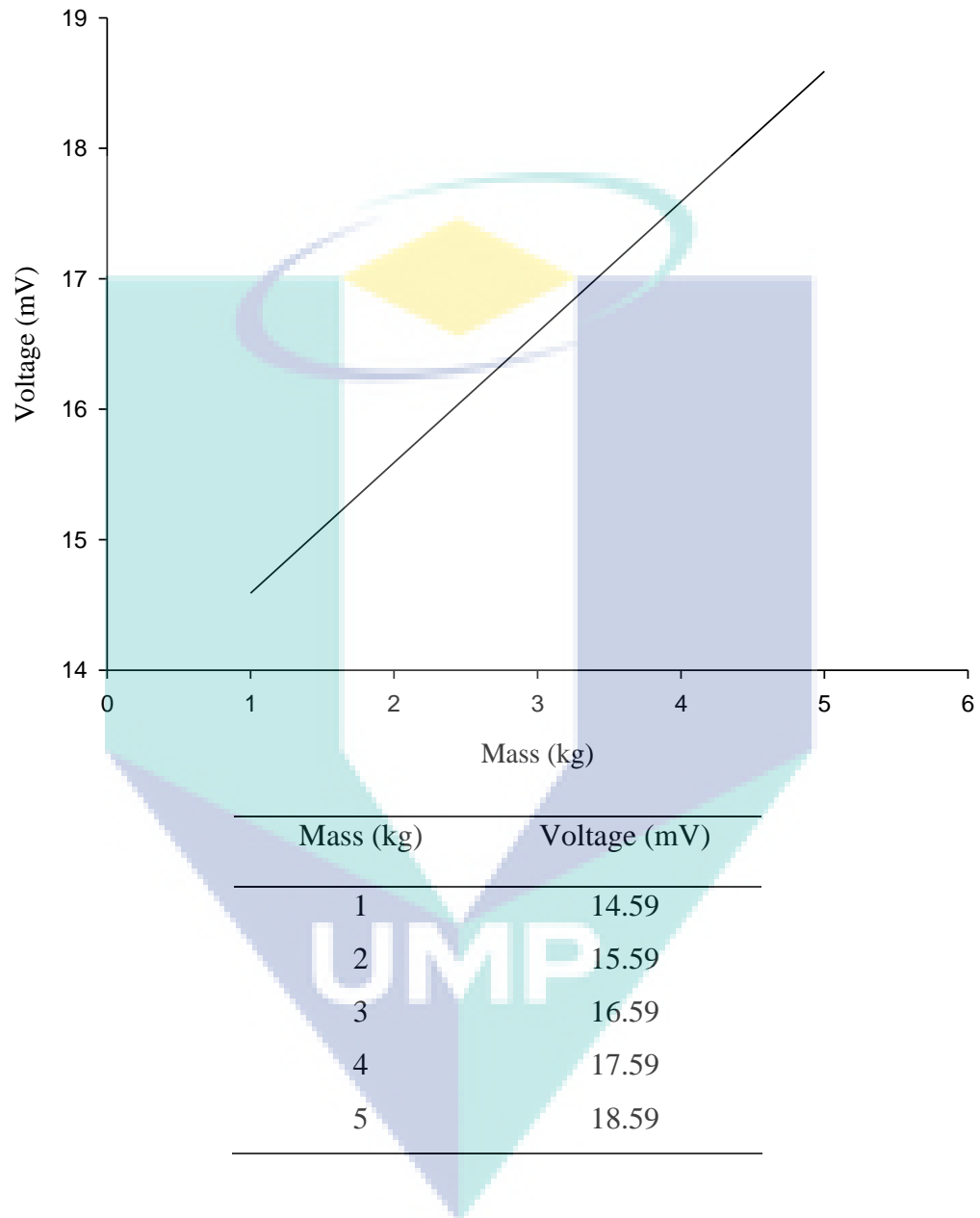
The equation for the graph is:

$$Y = X + 13.59$$

Hence, using the equation, any load that exerted to the load cell can be determined.

APPENDIX 9

Manometer Specifications
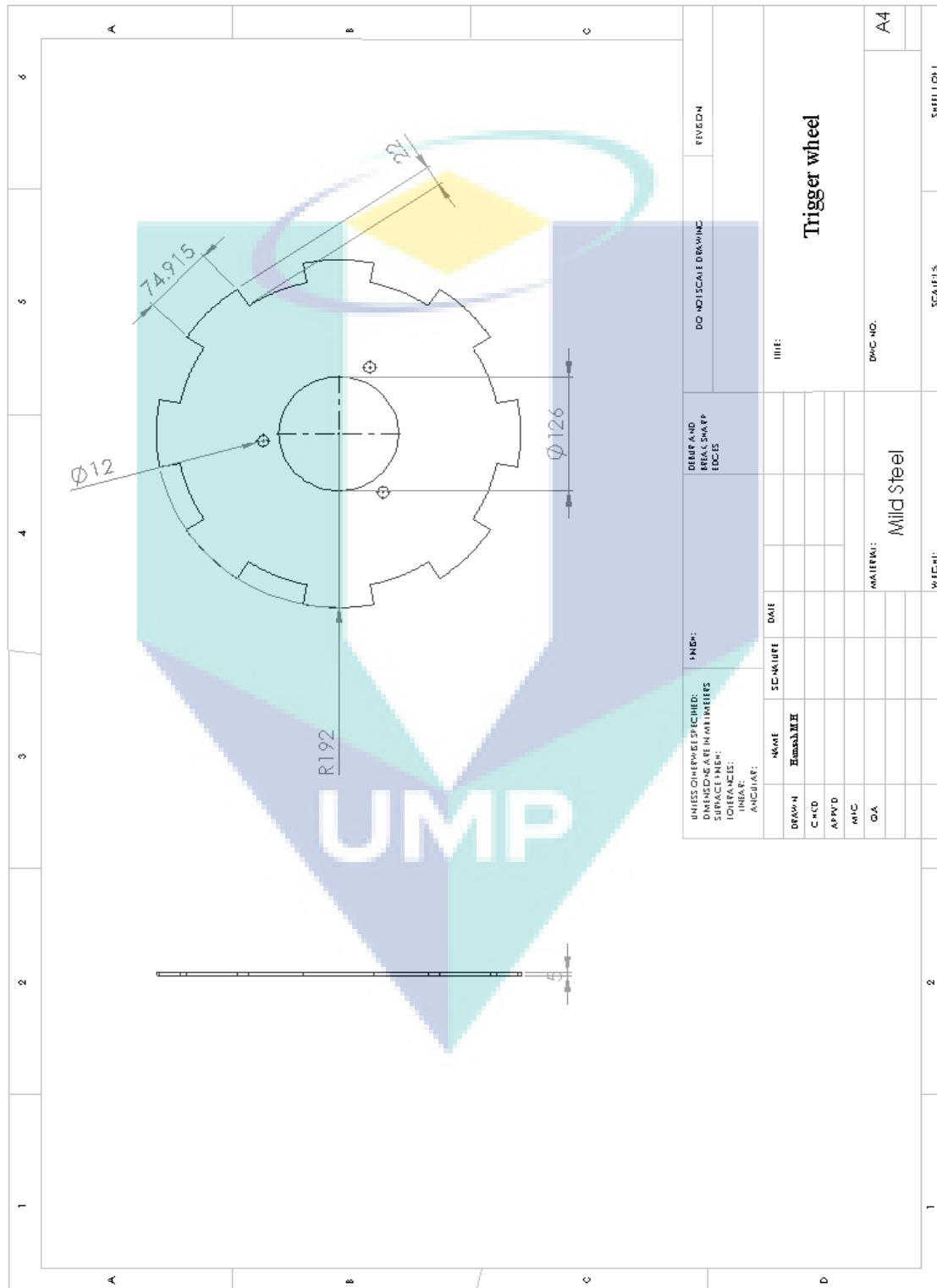
Description		Specifications
Accuracy	%	3
Temperature limits	°C	60
Pressure limits	kPa	70
Scale length	cm	1
Weight	g	472

APPENDIX 10

Technical Drawing of Trigger Wheel

APPENDIX 11

KANE Gas Analyzer Auto 5-3 Specifications

	Specified Range	Over Range	Accuracy Vol	Accuracy	Resolution
CO	0-10%	20%	±0.06%	±5%	0.01
HC	0-2000 PPM	20 000 PPM	±12 PPM	±5%	1
O_2	0-21%	48%	±0.1 %	±5%	0.02
CO_2	0-16%	25%	±0.5 %	±5%	0.1%
NO_x	0-5000 PPM	5000 PPM	25 PPM	±5%	1 PPM
Lambda	0.8-1.2				0.001
AFR	11.76-17.64				0.01
RPM	200-6000 RPM		50 RPM		1 RPM
Oil Temperature	0-150 °C		±0.2 °C	±0.3%	1.0 °C

APPENDIX 12

Engine Stand Drawing
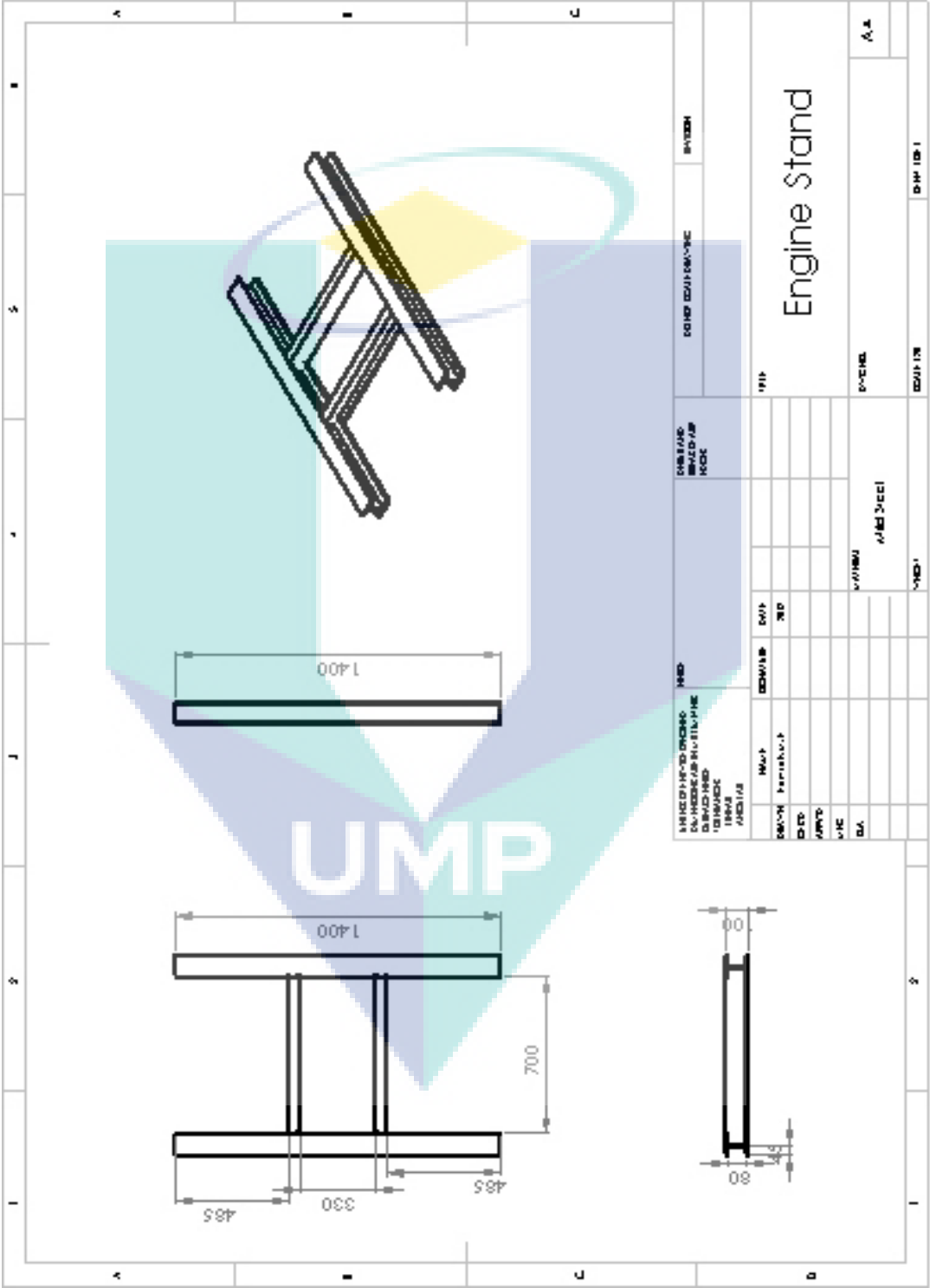
APPENDIX 13

PETRONAS Dynamic Diesel Properties

Properties	Method	Unit	Value
Density @ 15 °C	ASTM D 4052-96	Kg/L	0.87
Colour	ASTM D 1300-98		2.0
Distillation @90% Recovered	ASTM D 86-00a	°C	365.7
Kinematic Viscosity @40°C	ASTM D 445-97	cSt	4.0 (Typical)
Sulphur	ASTM D 4294-03	wt%	0.3
Carbon Residue (10% Residue)	ASTM D 4530-00	wt%	<0.1 (Typical)
Flash Point	ASTM D 93-00	°C	91.0
Total Acid Number	ASTM D 974-97	mgKOH/g	0.1 (Typical)
Water by Distillation	ASTM D 95-99	vol%	<0.05 (Typical)
Ash	ASTM D 482-00a	wt%	0.002 (Typical)
Cetane Index	ASTM D 976-00		55
Pour Point	ASTM D 97-96a	°C	+9
Sediment by Extraction	ASTM D 473-95	wt%	<0.01 (Typical)
Copper Corrotion	ASTM D 130-94		1a

APPENDIX 14

YANMAR TF120M Standard Performance Curve
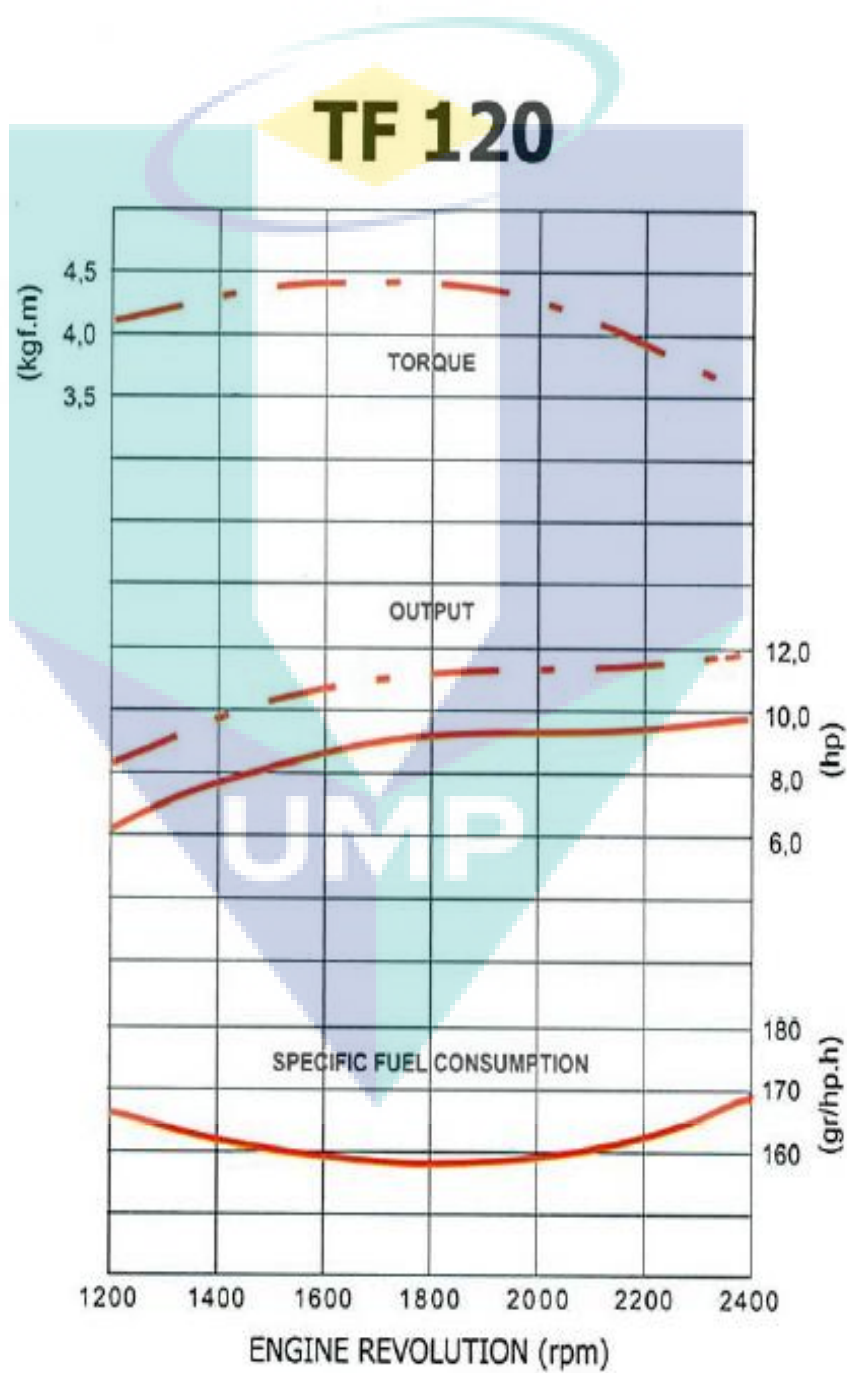
APPENDIX 15

GANTT CHART

Gantt chart/ Project schedule

Project Activities	M 2	M 4	M 6	M 8	M 10	M 12	M 14	M 16	M 18	M 20	M 22	M 24
Example												
1) Literature review												
2) Test rig construction												
3) Experimental testing												
4) Analysis of experimental results												
5) Report writing and complete the project												

○ Milestone
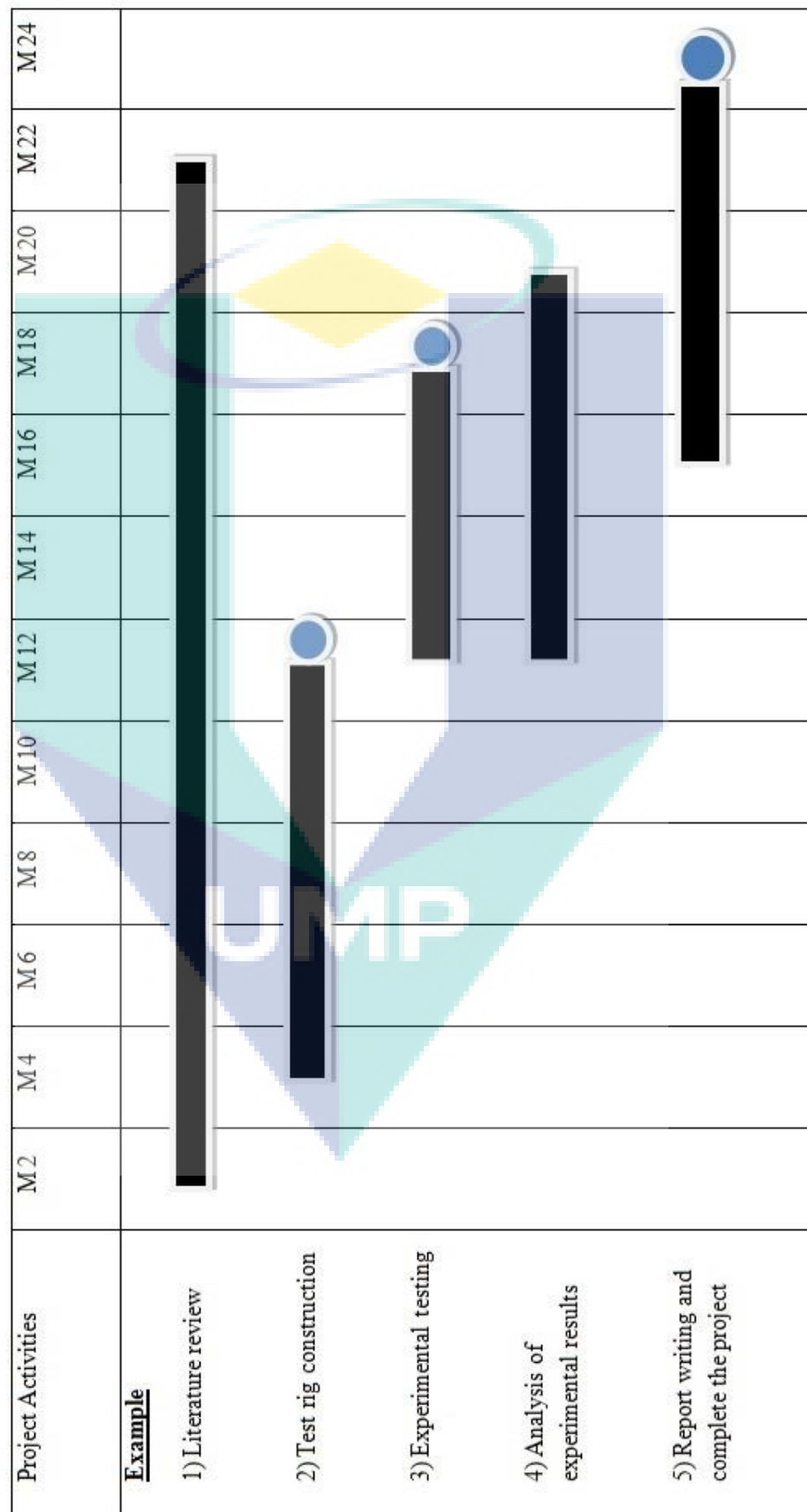
LIST OF PUBLICATIONS

1. **Hamzah, M. H**., Abdullah, A. A., Sudrajad, A., Ramlan, N. A. & Jaharudin, N. F. 2014. Performance of Diesel Engine Operating With Waste Plastic Disposal Fuel. *Applied Mechanics and Materials,* 465-466**,** 423-427.

2. **Hamzah, M. H**., Sudrajad, A., Abdullah, A. A. & Ayob, A. 2012. An Experimental Study of DI Diesel Engine Fuelled With Emulsion Fuel. *3rd International Conference on Engineering and ICT (ICEI2012).* Melaka, Malaysia.

3. Jaharudin, N. F., Abdullah, A. A., Yusop, A. F., Mamat, R., Ramlan, N. A. & **Hamzah, M. H**. 2014. Study on particulate matter (PM) emissions of diesel engine using Palm Oil Methyl Ester. *Applied Mechanics and Materials,* 465-466**,** 433-437.

4. Ramlan, N. A., **Hamzah, M. H**., Jaharudin, N. F., Abdullah, A. A. & Mamat, R. 2014. Analysis of Diesel Engine Performance Fueled With Waste Cooking Oil. *Applied Mechanics and Materials,* 465-466**,** 418-422.

5. **Hamzah, M. H**., Abdullah, A. A., Sudrajad, A., Rasol, M. R. M. & Dewayanto, N. 2012. A Comparison of Fuel Characteristics between Waste Plastic Disposal Fuel (WPDF) and Diesel Fuel For Diesel Engine Testing. *National Conference for Postgraduate Students (NCON-PGR).* Universiti Malaysia Pahang (UMP), Gambang, Pahang.

6. **Hamzah, M. H**., Abdullah, A. A., Sudrajad, A., Ramlan, N. A. & Jaharudin, N. F. 2014. Analysis of Combustion Characteristics of Waste Plastic Disposal Fuel (WPDF) and Tire Derived Fuel (TDF). *Applied Mechanics and Materials* (Under Review)

7. Ramlan, N. A., Abdullah, A. A., **Hamzah, M. H.**, Jaharudin, N. F. & Mamat, R. Evaluation of Diesel Engine Performance and Exhaust Emission Characteristics using Waste Cooking Oil. *Applied Mechanics and Materials*. (Under Review)

8. Jaharudin, N. F., Ramlan, N. A., **Hamzah, M. H.**, Abdullah, A. A., Mamat, R. Study on Particulate Matter of Diesel Engine Using Waste Cooking Oil. *Applied Mechanics and Materials.* (Under Review)